2009

Analysis of Shear Connectors at Regions of Positive and Negative Moment in Composite Beams

Joseph Preston Huie
University of Alabama at Birmingham

ANALYSIS OF SHEAR CONNECTORS AT REGIONS OF POSITIVE AND NEGATIVE MOMENT IN COMPOSITE BEAMS

by

JOSEPH PRESTON HUIE

TALAT SALAMA, COMMITTEE CHAIR
JASON KIRBY
NASIM UDDIN

A THESIS

Submitted to the graduate faculty of The University of Alabama at Birmingham,
In partial fulfillment of the requirements for the degree of
Master of Science in Civil Engineering

BIRMINGHAM, ALABAMA

2009

ANALYSIS OF SHEAR CONNECTORS AT REGIONS OF POSITIVE AND NEGATIVE MOMENT IN COMPOSITE BEAMS

JOSEPH PRESTON HUIE
M.S.C.E.

ABSTRACT

The modern practice of floor design, which uses a concrete floor slab supported by steel beams, is to take advantage of the strengths of both slab and steel beam and design them to act together to resist loads. The term "composite beam" is used to describe the concrete slab and beam as they act together, interactively.

Composite beams are subject to areas of positive or negative moments. Various studies and papers have addressed the problem of moments in composite beams; there are already traditional methods of designing composite beams subject to positive and/or negative moments. This thesis is an attempt to verify current design methods for composite beams under positive and negative moments as well as address the problem of finite element modeling of composite beams. The focus is on the design of the shear connectors, i.e. does the spacing, size, and number of shear connectors have enough of an effect on the strength of the composite beam to merit either their addition or subtraction in regions of positive or negative moment; does it have enough of an effect to merit new design methodologies.

Finite Element (FE) analysis as manifested in modern computer software makes it possible to model the effects of the shear connectors in composite beams. The efficacy in the placement, number, and size of the shear connectors is demonstrated in the load versus deflection curves as well as shear and moment diagrams included in this paper.

Keywords: composite, moment, shear connectors

ACKNOWLEDGEMENTS

I wish to express my gratitude to my advisor and committee chair, Dr. Talat Salama. His enthusiasm, patience, and advice were vital in the completion of this paper; I cannot overstress how grateful I am for his support nor how important that support was.

I also wish to express my gratitude to the rest of my committee, Dr. Nasim Uddin and Dr. Jason Kirby for their time and advice.

I wish to express my gratitude to my family, especially my mother, as they suffered through the emotional ups and downs I manifested during the research and the writing of this paper.

And lastly, I am grateful the University of Alabama at Birmingham for allowing me to pursue this advanced degree, for the opportunity to gain knowledge and experience which will help me in the practice of my chosen profession.

TABLE OF CONTENTS

LIST OF FIGURES

Figure *Page*

LIST OF TABLES

LIST OF ABBREVIATIONS

A_c	area of concrete slab within effective width
A_s	area of structural steel cross section
A_{sc}	cross sectional area of shear stud
C	compression force
E	young's modulus for steel
E_c	modulus of elasticity for concrete
F_u	minimum specified tensile strength of stud steel
F_y	yield stress for steel
F_{yf}	beam flange yield stress
H_s	length of shear stud after welding
M_n	nominal flexural strength
NA	neutral axis
N_r	number of studs in one rib at a beam intersection
PNA	plastic neutral axis
Q	shear
Q_n	stud strength
Q_{nr}	stud strength
Q_u	ultimate strength
R_{pa}	stud strength reduction factor (deck ribs parallel to the beam)

R_{pe}	stud strength reduction factor (deck ribs perpendicular to the beam)
WF	wide flange beam
b	beam spacing
b_E	effective width
f'_c	concrete compressive strength
h	clear distance between the beam flanges less the fillet or corner radius for rolled shapes
ksi	kips per square inch
h_r	nominal rib height
t_w	beam web thickness
w_r	average width of concrete rib
ΣQm	sum of nominal strengths of shear connectors between the point of maximum positive moment and the point of zero moment to either side
φ_b	resistance factor for flexure
σ_{max}	maximum allowable stress in slab
σ_x	stress in slab
ω	concrete unit weight

CHAPTER 1
HISTORY AND PROBLEM STATEMENT

1.1 History

In 1645, in Saugus, Massachusetts, the first blast furnace and iron works were built in America (Viest, et al. 1997); of course any metal from those iron works was too expensive to be used as a beam or column, but it was a beginning of iron and steel production in North America. In 1871 David Saylor applied for a patent on "new and improved cement [portland]," which he produced at a mill in Copley, Pennsylvania.

The first use of steel, (milled) rolled beams embedded in concrete was not commercial or even industrial; it was in a private residence, the Ward House, in 1877, in Port Chester, New York. In 1894, after obtaining an American patent for highway bridge construction, Josef Melan built an arched bridge consisting of several I-beams encased in concrete. Melan submitted calculations to show that the steel and concrete acted together (Šavor and Bleiziffer, 2008). From 1929 to 1931 the Empire State Building was built in New York City; its steel frame was encased in cinder concrete. The strengthening affect of the concrete encasement was not included in load calculations. The stiffening affect of the concrete was included in drift calculations. Engineers assumed the stiffness of individual members would be doubled due to the stiffening affects of the concrete. (Viest, et al. 1997).

The first patent for mechanical (shear) connectors (to be used to connect the steel beam to the concrete slab) was applied for in 1903. In 1954 shear studs were first

tested at the University of Illinois (Nethercot, 2003). In 1956 design formula were published based somewhat on those tests. In December of 1960 a joint committee of ASCE (American Society of Civil Engineers) and ACI (American Concrete Institute), the Joint Committee on Composite Construction (it is still currently in existence), issued "Tentative Recommendations for the Design and Construction of Composite Beams and Girders for Buildings." In 1961, in Detroit, Hall C of Cobo Hall, was completed. It was one of the first buildings to have its steel framing designed with composite action in mind (Viest, et al. 1997). Research on composite beam and composite column still continues; one area of research currently receiving a large amount of attention is composite connections.

1.2 Problem Statement and Objectives

Currently, steel-concrete composite beams are preferred in the construction of buildings and bridges (Fabbrocino, et al. 2000). Although there are standard methods of calculation with which to analyze and design composite beams, experiments and other, more detailed calculations show the behavior of composite beams is complex, even under low loads. The mechanical properties of the three main components of composite beams (reinforced concrete slab, steel beam, and shear connectors) and their arrangement make composite beams able to withstand positive moment loads greater than either slab or steel member might be able by themselves; however, this same arrangement of the components is not much help when the composite beam is under loads which cause negative bending. According to specification I3.2 of The Manual of Steel Construction by AISC (American Institute of Steel Construction), "The negative design flexural

strength…shall be determined for the steel section alone…" Creating a composite beam able to make efficient use of its "compositness" while subject to negative moments is difficult; there seems to be a need for some way to distribute the forces in the composite section such that it may be useful in regions of negative moment.

The reasoning and method of composite beam design for beams under positive moment load, as promulgated by AISC, is well known and reliable. The method described by AISC for the design of composite beams under negative moment load is also well known. And while there are various studies of actual test beams under positive and negative moment loads, there appears to be a dearth of studies using FE (Finite Element) modeling. This not to say there are none, just few, which describe the problems of FE modeling. Three objectives of this thesis are: attempt to verify the current methods of composite beam design under positive moment loads, gain more understanding of composite beams under negative moment loads, and understand the problems associated with FE modeling of composite beams in general.

In the work, which follows, various FE models of composite beams are subjected to positive and negative moments. The results of the loadings are analyzed in order to verify current design methods. The difficulties associated with FE modeling are also discussed.

Under positive bending the steel section is usually subjected to tension and the concrete slab subjected to compression (Figure 1). The shear connection system in a composite section is not perfectly rigid, under load the shear connectors may deform and the concrete may creep until both reach a state where loads are evenly distributed.

Standard methods of composite beam design generally ignore the effects of deformed shear connectors and/or concrete compressing around the shear connector.

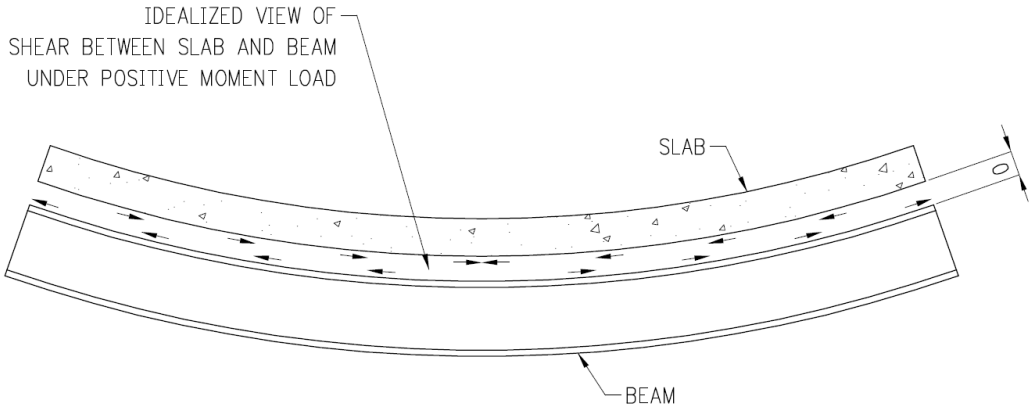

Figure 1 Composite Beam Under Positive Bending

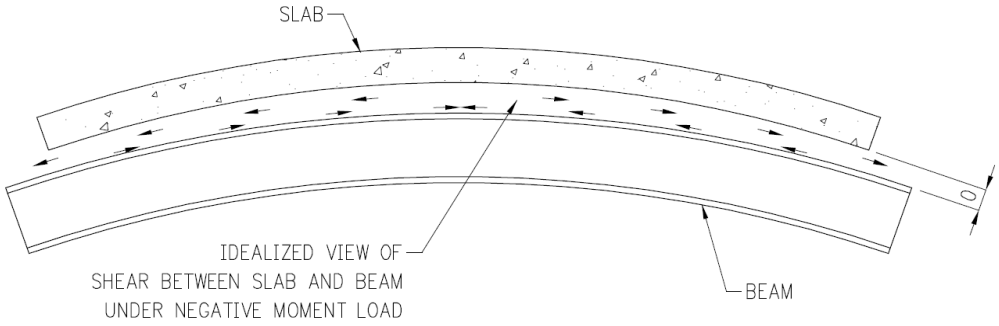

Figure 2 Composite Beams Under Negative Bending

In negative bending tension stresses are imposed on the concrete slab (Figure 2). With negative moment loads, the analysis of the interaction between the concrete slab and the steel profile becomes a bit more complicated. Hogging, or negative, bending place the slab in tension and may cause it to crack at service loads (Gilbert and Bradford, 1995). If the slab should crack any help it may have offered in negative bending

disappears. In addition, the steel section, if under high compression may manifest buckling problems. With the section now loaded in reverse, as it were, the bottom flange becomes prone to lateral buckling.

Under compressive loads (in positive bending) the reinforcement in the slab is not subjected to high tensile strains. Slippage may occur at the slab/steel interface (this slippage has been taken into account in current, conservative design procedures) and a linear strain pattern develops, which applies to each component of the cross section (Figure 3) (NA indicates Neutral Axis). In the composite section it is the interaction between the slab and steel member, the ability of the shear studs to resist the shear between the slab and beam, which control bending and flexural behavior, i.e. deflection, of the composite beam.

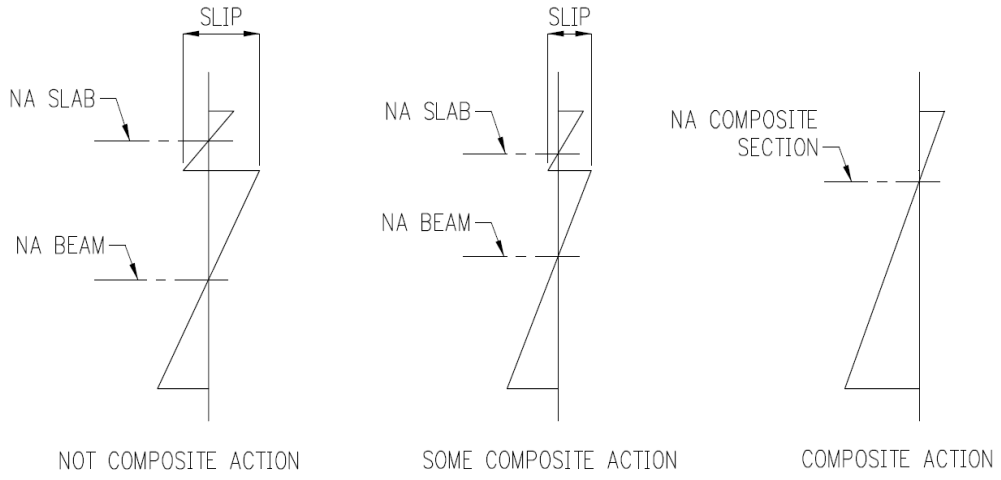

Figure 3 Strain in Composite and Non-composite Sections

As long as concrete and steel remain in the elastic portion of the stress strain curve a linear analysis of composite beams may be used to determine the stresses and strains. Within this thesis there is no analysis of composite beams whose stresses and

strains are outside the elastic range. Inside the elastic range, the FE models are idealized; adhesion and friction between the deck and the beam flange is not taken into account. This thesis is divided into the following sections.

Chapter 1 is a review of the history of composite beams and the current practice in their use.

Chapter 2 is a discussion of traditional testing procedures with the resulting design procedures; this includes a discussion on the merits of concrete and steel as building materials as well as a discussion of shear connectors. There is an overview of the design of composite beams as well as a discussion of composite beam design using classical methods.

Chapter 3 is a discussion of model creation and verification. There is a comparison of the author's FE model results to classical design methods as well as the results of research of others.

Chapter 4 is a discussion of the results of the FE modeling. This section includes a discussion of the parametric study results.

Chapter 5 is the conclusion.

Note, the terms shear connector and shear stud are interchangeable throughout this paper.

CHAPTER 2
COMPOSITE BEAMS IN MODERN CONSTRUCTION

2.1 Standard Construction Techniques

Originally, most composite floors were built with solid concrete cast on removable forms, often with the entire top flange of the beam encased in concrete (Tamboli, 1997). Today, steel beams and metal deck with concrete fill have become the standard type of floor construction favored by many architects and engineers (Figure 4 and Figure 5). Composite floor systems are considered to be high quality because the floors are stiffer and more serviceable (the serviceability issues of deflection and vibration are less of a problem) than open web joists (Allison, 1991). Fire ratings with this type of system are simple to obtain; provided the slab is thick enough all that is required is the application of fireproofing to the underside of the slab and structural shape. A 3¼ inch lightweight concrete slab on a composite metal deck has a two-hour fire resistance rating without the addition of extra fireproofing, the two hour rating being typical of what is required in a standard office building (Allison, 1991).

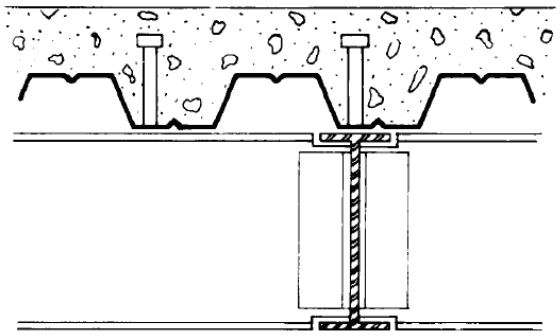

Figure 4 View of the Deck Flutes Perpendicular to the Beams. Adapted from Vulcraft Steel Roof and Floor Deck Catalog, 2001. Used with permission.

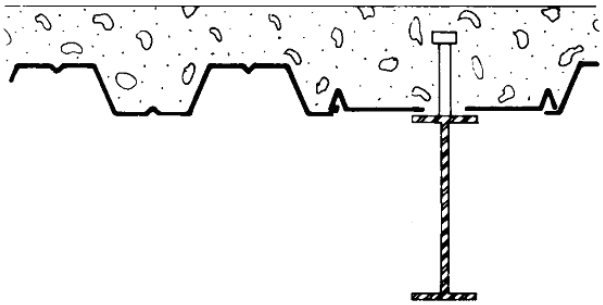

Figure 5 View of the Deck Flutes Parallel to the Beam. Adapted from Vulcraft Steel Roof and Floor Deck Catalog, 2001. Used with permission.

2.2 Advantages of Steel

The interaction between the concrete slab and the supporting steel beam via shear connectors is what defines composite action. The most important characteristics of the beam is its high strength, high Young's Modulus (E), and high ductility; steel also does not take up as much space compared to concrete when looking at the weight-to-building square ft. ratio. Steel beams have the ability to span relatively long distances without the need for additional supports. In current designs the steel shape most commonly used as floor beams is the WF (Wide Flange) shape, usually with a yield strength, F_y, of 50 ksi

(kips per sq. inch). These shapes can be fabricated in a plant with end connections already prepared, which speeds up erection of the structure (Allison, 1991).

2.3 Advantages of Concrete

Structural concrete works well in resisting fire; it has a high mass (important in the area of damping floor vibrations); it is much cheaper than steel; it works well as an insulator; it makes a good structural (horizontal) diaphragm able to distribute wind and seismic shear loads; and it has good compressive strength. In composite construction the criterion for choice of concrete are compressive strength, $f`_c$, Young's modulus (E), and unit weight. Lightweight concrete weighs approximately 110 lbs. per cubic ft; normal weight concrete weighs approximately 145 lbs. per cubic ft. Lightweight concrete is generally a better insulator (due to air entrainment) than normal weight concrete and with its reduced weight shoring requirements may be less than for normal weight concrete (Allison, 1991).

2.4 Deck Profiles

In some cases the steel deck may be designed to act compositely with the concrete slab. In this case the deck may have some sort of deformations, e.g. lugs, ridges, corrugations to help increase the bond between the deck and concrete. Usually the deck has a trapezoidal profile with wide flutes to provide a flat surface through which the stud may be welded to the beam. Composite steel deck slabs help reduce the overall structural depth (this implies increased headroom); increase floor load capacity; and provide a

horizontal, structural diaphragm (Figure 6, Figure 7, Figure 8, Figure 9, Figure 10, Figure 11).

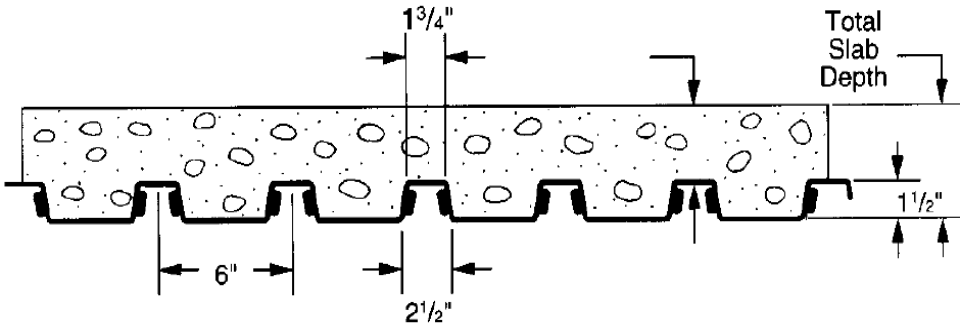

Figure 6 Fluted Deck. Reprinted from Vulcraft Steel Roof and Floor Deck Catalog, 2001. Used with permission.

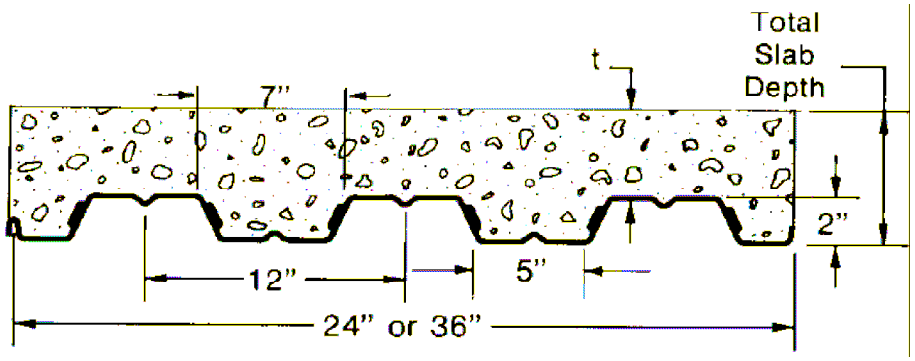

Figure 7 Fluted Deck. Reprinted from Vulcraft Steel Roof and Floor Deck Catalog, 2001. Used with permission.

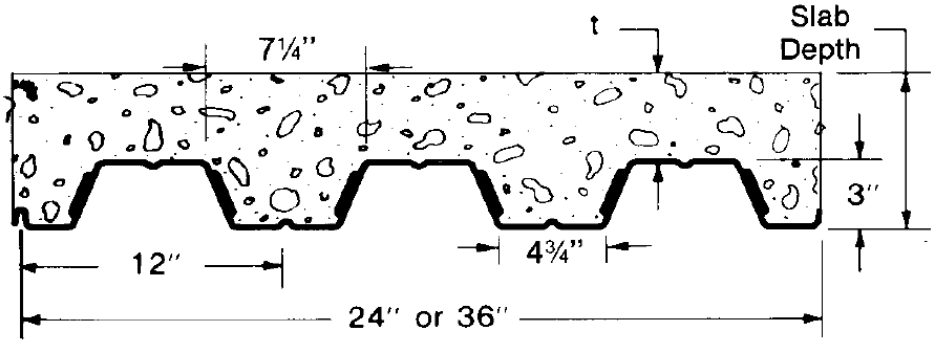

Figure 8 Fluted Deck. Reprinted from Vulcraft Steel Roof and Floor Deck Catalog, 2001. Used with permission.

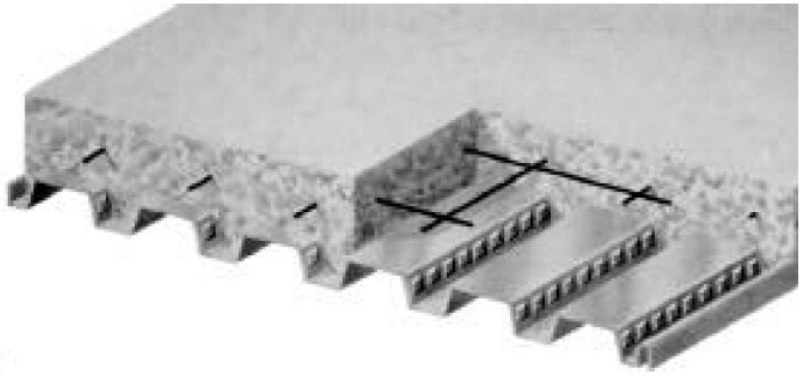

Figure 9 Three Dimensional View of Deck with Lugs. Reprinted from Vulcraft Steel Roof and Floor Deck Catalog, 2001. Used with permission.

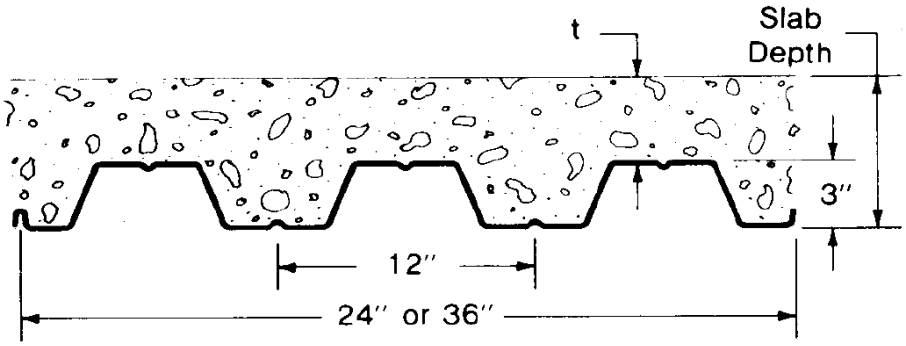

Figure 10 Smooth Fluted Deck. Reprinted from Vulcraft Steel Roof and Floor Deck Catalog, 2001. Used with permission.

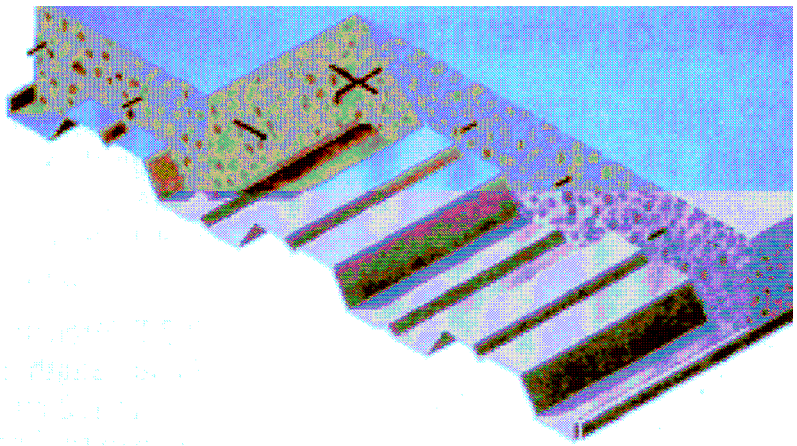

Figure 11 Three Dimensional View of Deck with No Lugs. Reprinted from Vulcraft Steel Roof and Floor Deck Catalog, 2001. Used with permission.

2.5 Stud Welding

Because the connection between the concrete and WF beam is critical, the weld of the shear stud to the beam is also critical. Before the studs are welded to the to the WF beam, the floor is cleared, generally swept clean; the shear connectors, studs, are then welded to the top flange of the supporting beam. Single studs are welded as close as possible to the middle of the beam flange. Unless the stud is placed over the web of the supporting steel beam the stud diameter to flange thickness ratio should not exceed 2.5 (Viest, et al. 1997).

The deck should be dry before welding studs (Figure 12) because excess moisture will affect the weld strength, dramatically. Excess moisture will cause the shear stud weld to cool prematurely and may contaminate the weld as well. Inspection of the stud welds consists of beating on them with a large hammer. If the stud stays upright, the weld is ok; if it doesn't, the weld must be redone.

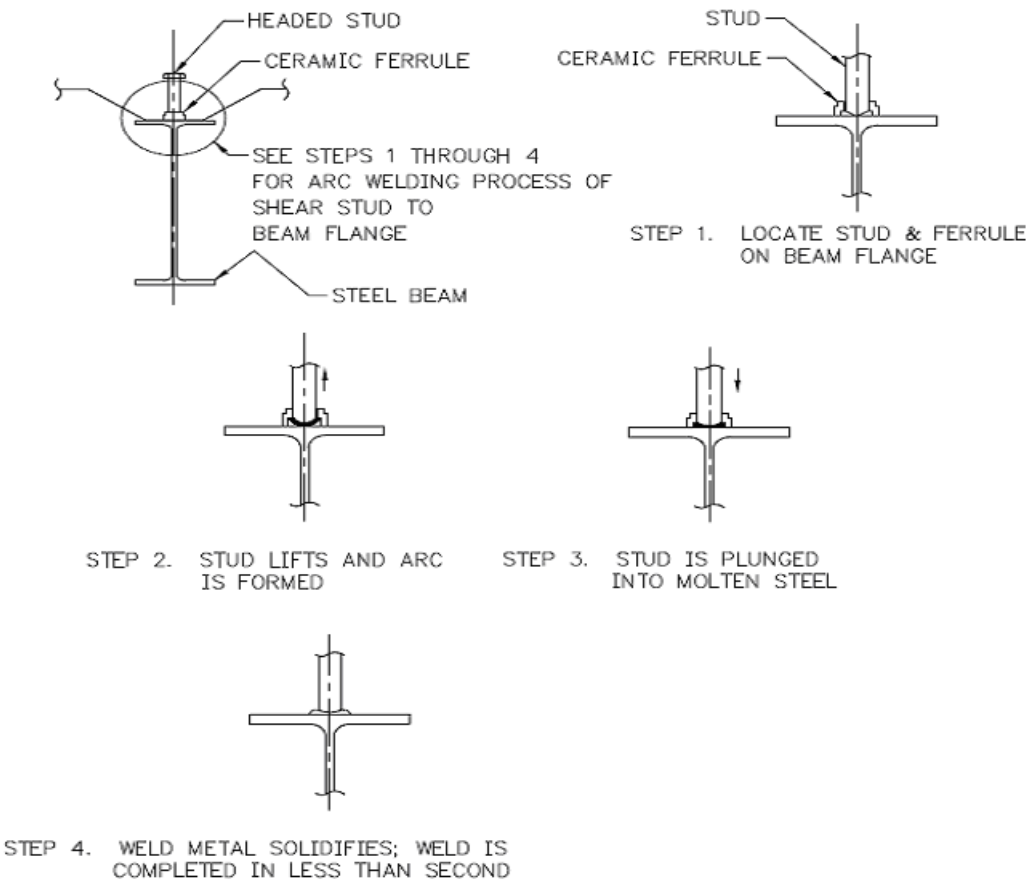

Figure 12 The Welding Process During Stud Welding.

Ironworkers may attempt to overcome the moisture problem by various means. They may choose to dry the deck with blowers of some sort or they may choose to increase the amperage of the electric current coming from the stud-welding machine. This latter choice is not a good idea because the stud, which may be (and often is) off the beam centerline, be welded completely through the beam flange.

From 2000-2005 the author worked for Kline Iron and Steel Company in Columbia, South Carolina. Kline was the fabricator for the steel in the construction of a new parking deck, in Columbia. On several beams the erector welded the studs completely through the beam flanges. On other beams, the location of the stud to the

beam flange was clearly visible due to the deformation on the underside of the beam flanges.

2.6 Shored Construction

When designing composite floor systems the engineer must decide whether the floor will be erected using shored or un-shored construction techniques, and must specify clearly in design drawings which technique is to be used. According to the ASIC Code of Standard Practice the "owner", not the engineer of record (the engineer who is responsible for the design of the structure) is responsible for the "means and methods" of erection. If the engineer responsible for the design of the floor system does not clearly indicate which type of erection procedure is to be used the erector will choose the cheapest method, un-shored. If a steel erector, having bid a project based on un-shored beam erection, is forced to use shored erection procedures mid-project, this might have long-term financial consequences for the erector.

2.7 Un-shored Construction

The un-shored system simplifies the work of the contractor (Allison, 1991). After the studs have been connected and the reinforcement placed in all the specified locations in an area of a pour, the concrete is then placed (or poured) in that area. The floor beams and girders must be designed to support the load of the concrete as non-composite members. In this case it is very likely the main consideration will be one of serviceability and not strength, with the main consideration being one of deflection and how to minimize it. The design engineer may choose to camber the beams in question.

Calculation and engineering judgment are what determine how much to camber a beam. Engineers have been know to specify cambers equal to three-quarters of the theoretical wet load (wet concrete) deflection; some designers allow the floor to be poured flat as long as the floor system has been designed for a slab weight 10% to 15% greater than the theoretical weight (Allison, 1991).

The advantages of shored construction are that the deflections are based on the composite section (a more efficient use of the slab) and a strength check of the structural shape is not required. A disadvantage is that a crack over the girders is almost certain. The designer should specify crack control reinforcement over the girders (Allison, 1991). The use of shored or un-shored construction techniques is also a cost concern; the owner and/or general contractor should be consulted about which is to be used as early as possible in the course of a project.

2.8 The Push-Out Test

The test most often used to determine how well shear forces are transferred between the WF section and the concrete slab via the welded shear stud is the push-out test (Easterling, et al. 1993). There are no standards for push-out tests (Topkaya, et al. 2004).

In the traditional push out test shear connectors are welded to each side of a WF beam. Forms are positioned so that concrete can be poured to create a composite section on each side of the beam making use of both flanges. Usually this means concrete must be poured on one side of the beam, the concrete cured, the beam then flipped and a pour made against the opposite flange (Figure 13).

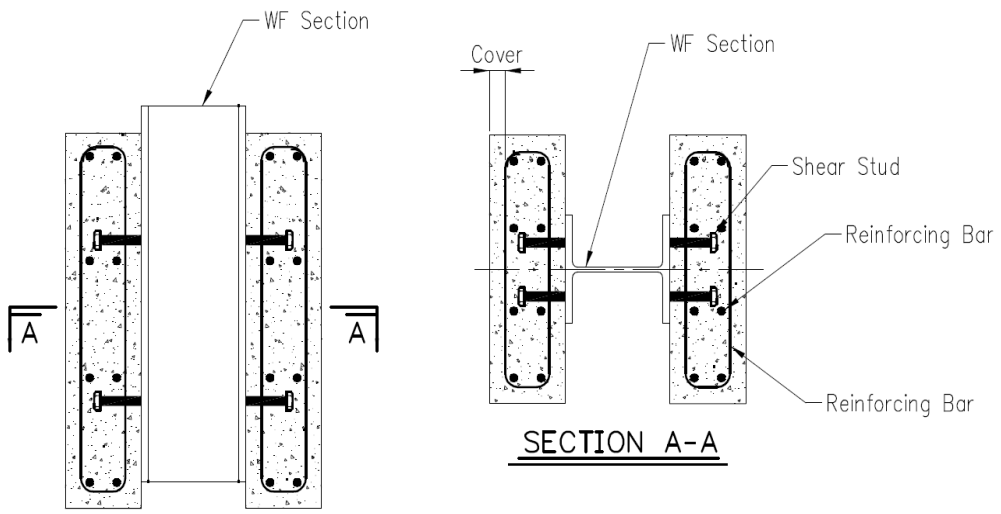

Figure 13 Typical Push-Out Test Specimen

One problem with the creation of the push-out test specimen is the quality control required for the two different concrete pours. The concrete on one side may not match the concrete on the other. A question that could be raised at this point is: Does it really matter; should concrete be considered a precision building material? The short answer is yes. Using modern quality control methods concrete suppliers are able to provide concrete with consistent compressive strengths.

One improvement to the test involves using structural tees (WT). Concrete from the same batch may be poured at the same time on the tees. The WT's are then spliced along the stems to create a WF section with composite action on each flange. After the composite section is created the assembly is placed in a testing machine and tests are run.

2.9 Test Results

As mentioned before, the strength of the shear connector and the compressive strength of the concrete are the main factors affecting the behavior of composite beams

(Lam, et. al 2005). Although the push-out test measures displacement with increasing loads, it is not easy to determine with precision why the test specimen fails. There are generally three failure modes.

1. The first mode of failure is concrete cone failure alone; there is no discernable stud failure. In this failure mode the concrete around the shear stud starts to fail before the shear stud yields.

2. The second mode of failure is shear stud failure alone; the stud yields and there is no discernable concrete failure. This failure mode the yield stress in the shear stud is reached before the maximum concrete stress is reached.

3. The third failure mode is combined failure of the shear stud and concrete slab before the maximum stresses are reached in either one.

Apparently, the failure of the weld of the stud to steel is so rare, at least under lab conditions, it is not be mentioned; or perhaps it may be placed under the second mode of failure where the stud fails before the concrete.

2.10 Strength and Slip

The relationship between strength and slip represented by the equation:

$$Q = Q_{.u}\left(1 - e^{As}\right)^{B} \tag{1}$$

Where Q_u is the ultimate strength; s is slip; A and B are constants, which are derived from test results. This equation is useful when the behavior of the composite beam section must be tracked through the nonlinear range (Viest, et al. 1997).

AISC (American Institute of Steel Construction) uses the following equation to describe the nominal stud strength. This equation is now part of the LRFD specification used in the description of the nominal stud strength:

$$\left(Q_n = .5 \cdot A_{sc} \cdot \sqrt{E_c \cdot f'_c}\right) \leq A_{sc} \cdot F_u \tag{2}$$

Where: A_{sc} = cross sectional area of a stud shear connector

f'_c = specified compressive strength of concrete

E_c = modulus of elasticity of concrete

F_u = minimum specified tensile strength of stud steel

The modulus of elasticity for concrete has been computed per:

$$E_c = \omega^{1.5} \cdot \sqrt{f'_c} \tag{3}$$

Where: ω = the unit weight of concrete in lb/ft^3 (Viest, et al. 1997).

2.11 Stud Strength Based on Concrete Compressive Strength vs. Allowable Tension Strength

If one graphs the equation for Q_n, nominal stud strength, two limit states become apparent. There is the constant value of the stud multiplied by the allowable tensile stress; this value remains constant. The other line shows that as the compressive strength of the concrete increases the stud strength also increases.

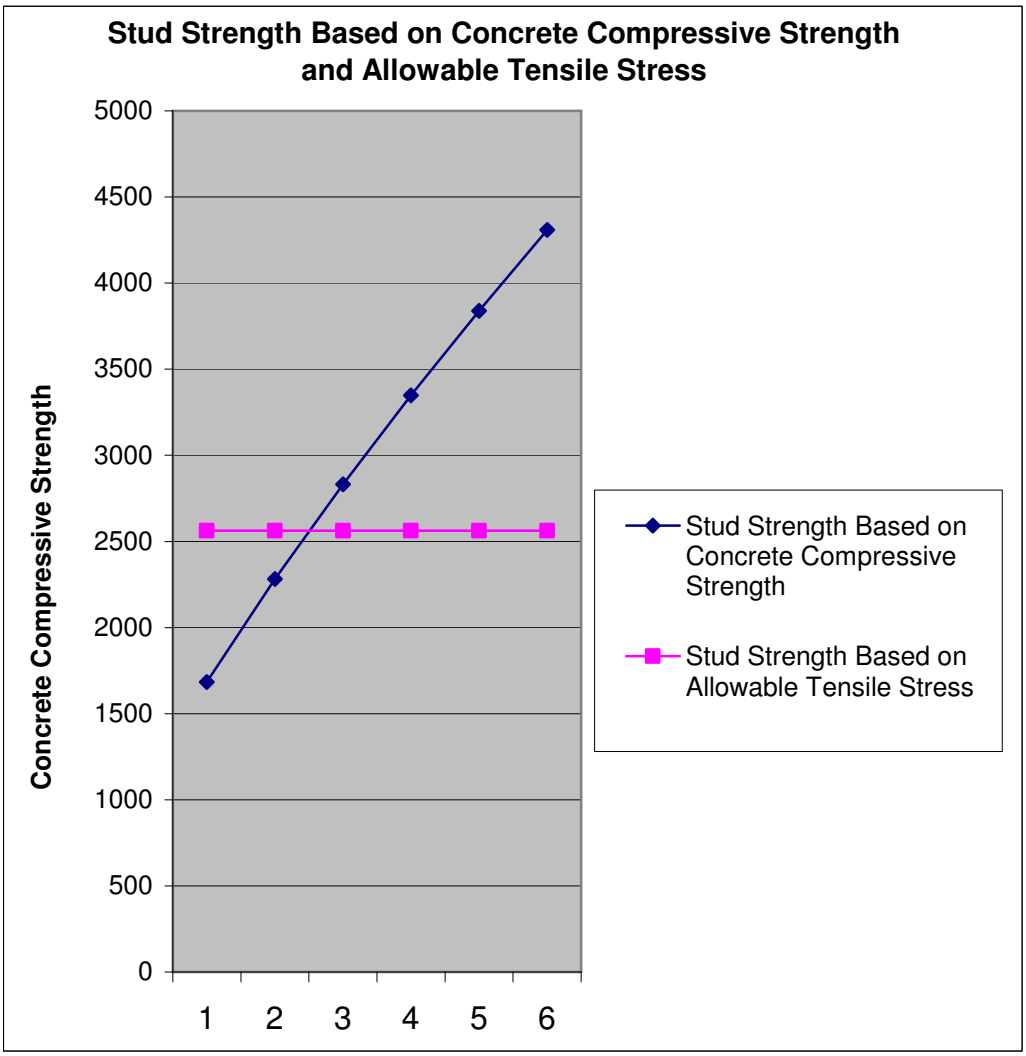

Figure 14 Stud Strength versus Allowable Tensile Stress

According to Ollgard (Viest, et al. 1997), tests on stud strength do not match the graph. His tests showed combined failures of the concrete and steel.

Typically, mechanical shear connections are made with headed shear studs which transfer shear between the steel and concrete; the stud allows the two materials to work as a single element. The effectiveness of this shear transfer is determined by the strength of the shear stud, the strength of the shear stud welds, the resistance to crushing or cracking

around the shear stud, and the slip between the slab and steel section relative to each other. This relative slip is may be characterized by yielding of the shear stud and/or crushing of the concrete. Shear stud capacities are based on static loading of shear studs, not on the type of loading, e.g. wind or seismic loading.

Concrete is not as ductile as steel. As loads are increased concrete becomes inelastic and is permanently deformed as it is being crushed locally around the stud. This creates a void, an area where the stud is able to deform, to be ductile. So, even if calculations indicate the strength of the composite section will be based mostly on the strength of concrete, the real life behavior of ductile steel and brittle concrete will be a failure in combination (see Figure 15). Again, the weld of the stud to the beam is critical because it must resist the shear and moment created when the concrete is forced against the stud.

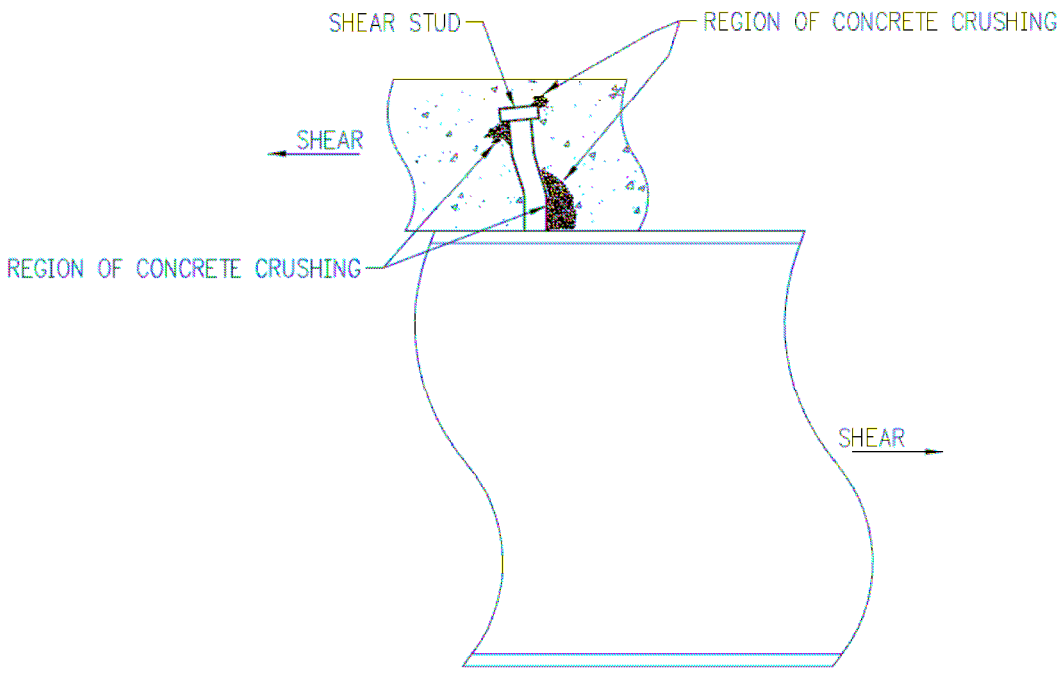

Figure 15 Crushing of Concrete Around Shear Stud

2.12 Reduction Factors

Given the wide spread use of steel deck in construction, calculations have been developed to take into account the influence of the deck's shape or profile. Shear stud strength is based on the equation defining Q_n; this strength value is then reduced according to the deck profile, i.e Q_n is multiplied by a strength reduction factor. When the ribs of the deck are perpendicular to the beam the strength reduction factor is:

$$R_{pe} = \frac{.85}{\sqrt{N_r}} \cdot \frac{\omega_r}{h_r} \cdot \left(\frac{H_s}{h_r} - 1 \right) \leq 1 \tag{4}$$

Where: N_r = number of studs in one rib at beam intersection

ω_r = average width of concrete rib

h_r = nominal rib height

H_s = length of shear stud after welding

When the ribs of the deck are parallel to the beam, the reduction factor, R_{pa}, is calculated per:

(5)

$$R_{pa} = 0.6 \cdot \frac{\omega_r}{h_r} \cdot \left(\frac{H_s}{h_r} - 1 \right) \leq 1$$

These strength reduction equations were developed as part of a Lehigh research program (American Institute of Steel Construction, Inc., 1998)

Some deck profiles have a "stiffener" (a crimped section of deck running the entire length of the deck [see Figure 10]) in the flute. The shear stud is welded to one

side or the other of the stiffener. Tests have shown the placement of the stud on one side or the other of the stiffener makes a difference to the shear stud strength, which raises the question of a possible new reduction factor (Easterling, et al. 1993). The question of the need for new reduction factor will have to be addressed in another paper.

2.13 Design Procedure

Even though a beam is designed as a full composite section, a perfect composite action without any slip is impossible due to the deformation of the shear studs (Nie, et al. 2004). The Load and Resistance Factor Design Specification (LRFD) for Structural Steel Buildings, adopted by AISC is based on the ultimate strength of the composite beam and is the method by which composite beams are currently designed. The design procedure may be summarized (and not necessarily in this order) (Vinnakota, et al. 1988):

1. Design the composite floor deck: decking rib height, h_r, rib width, w_r, and slab thickness, t_s
2. Determine the effective width of the slab, b_E
3. Determine the bending moment, M_r;
4. Determine the beam size
5. Design the shear connector
6. Check Deflection
7. Check strength during construction; specify the use of shored or un-shored construction

2.14 Effective Width

Multiplying the slab thickness times the effective width of the slab produces A; shear lag affects the distribution of strains across a slab. Strains in a slab spanning several equally spaced beams, is not uniform. They're large immediately above the beam and decrease with distance from the beam. The effective width b_E can be defined as the amount of width between beams, i.e. beam spacing, b, that can carry the same total force assuming the stress is uniform and its value is equal to that over the beam, σ_X.

(6)

$$b_{.E} = 2 \cdot \int_0^b \frac{\sigma_{.x}}{\sigma_{.max}} dy$$

Where b = beam spacing

σ_x = stress in slab (Steel Construction Institute, 1988-2002)

The type of loading as well as the ratio of beam spacing to beam length influence the value of b_E. There have been some proposals that the degree of composite action should also influence the value of b_E.

In negative moment regions the question of effective width is problematic because the concrete is subject to tensile stresses making the concrete more prone to cracking; these cracks influence the structural behavior of the composite beam. As cracks form, the longitudinal reinforcement in the slab begins take on tensile stresses; when the concrete is fully cracked the longitudinal reinforcement takes the total tensile load; at this point there is no means by which the tensile stresses may be transferred to the shear connectors. This seems to indicate that at sufficiently high hogging moments, the shear connectors are useless.

An article appearing in the May/June 2007 issue of the Journal of Bridge Engineering, "Effective Slab Width Definition for Negative Moment Regions of Composite Bridges," (Aref, et al. 2007) discusses the problem of effective slab width in hogging moment regions; the authors detail a set of step by step calculations which may be used to define the effective width in negative moment regions. However, in areas of negative moment standard AISC design techniques ignore any contribution, which might be made by the slab and direct the designer to design the beam as though there is no composite action. Because there is no consideration of concrete slab contributions, the question of effective width in regions of negative moments, is, for most designers, moot. The question of effective width in negative moment regions will be ignored and be reserved for later research.

When designing composite beams the current design practice is to determine the value of b_E based primarily on the type of loading (positive or negative moments or shear) and the ratio of beam spacing to beam length. There are tests and analysis, which indicate the slab thickness seldom governs. The AISC-LRFD specification requirements for effective slab width are based only on beam spacing, span length, and the distance to the edge of the slab.

Per AISC-LRFD (specification I3.1) the effective width of the concrete slab is the sum of the effective widths for each side of the beam centerline, each of which will not exceed:

(1) 1/8 of the beam span, center-to-center of supports;

(2) 1/2 the distance to the center-line of the adjacent beam; or

(3) The distance to the edge of the slab.

2.15 Shear Stud Properties

As mentioned before the purpose of the shear connectors in a composite beam is to tie the slab and steel beam together and force them to act as a unit. The shear stud also helps to prevent uplift (due to high wind or seismic loads) and thus to prevent separation between the slab and beam. Common headed shear studs range in diameter from ½ inch to 1inch with common lengths varying from two to eight inches; the ratio of the diameter to the overall length of stud should not be less than 4 (Vinnakota, et al. 1988). The head diameter of the headed shear stud is slightly larger than the body of the stud, creating an anchorage in the concrete slab, which creates the resistance to uplift. The stud material properties are that it is generally made of ASTM-A108 steel, with AISI Grades C1010, C1015, C1017, or C1020 with a minimum tensile stress of 60 ksi. The AWS Structural Welding Code (D1.1-75) also specifies a minimum 20% elongation for a 2 in. gage length. According to LRFD specifications the nominal strength of one shear stud is:

$$Q_n = .5A_{sc}(f`_c\omega)^{3/4} \leq A_{sc}R_{pa} \qquad (7)$$

Where: A_{sc} = cross sectional area of a stud shear connector

$f`_c$ = specified compressive strength of concrete

ω = unit weight of concrete in lbs. per cubic ft.

F_u = minimum specified tensile strength of stud steel

Equations for strength reduction, R_{pa} and R_{pe}, have been presented earlier in this paper. The strength of the shear stud may be represented by:

$$Q_{nr} = R_{pa}Q_n \quad (8)$$

or $$Q_{nr} = R_{pe}Q_n \quad (9)$$

depending on the orientation of the deck.

As the load on the composite beam is increased the shear studs nearest the support will begin to yield and deform. As they deform other studs will take on additional load until all are stressed to the yield point (Vinnakota, et al. 1988). The minimum spacing of shear studs along the length of a beam is the diameter of shear stud times six. That is not to say that shear studs must be located through the high flutes of steel decking if it happens to be perpendicular to the beam; the shear stud spacing should be somewhat compatible with the steel deck. The maximum longitudinal spacing of shear studs should not exceed 32 inches or eight times the total slab thickness (Vinnakota, et al. 1988).

2.16 Composite Beam Design at Areas of Positive Moment

Experiments have indicated the true moment capacity of a composite section subjected to positive bending can be approximated by assuming that either the structural steel section is fully yielded or the concrete slab is stressed to $.85f`_c$ through its full depth. The compression force, C, in the concrete slab is the smallest of:

$$C = A_sF_y \quad (10)$$

$$C = .85f`_cA_c \quad (11)$$

$$C = \Sigma Q_{rn} \quad (12)$$

Where: A_c = area of concrete slab within effective width

A_s = area of structural steel cross section

$f`_c$ = concrete compressive strength

F_y = steel yield stress

ΣQ_{rn} = sum of nominal strengths of shear connectors between the point of maximum positive moment and the point of zero moment to either side (Viest, et al. 1997).

Unless the slab is heavily reinforced and the compression force, C, is controlled by that reinforcement, the effect of longitudinal reinforcement may be ignored. In the case of the heavily reinforced slab the area of the longitudinal reinforcement times the yield stress may be added in determining C. Usually though, composite deck slabs contain only nominal reinforcement; the concrete is bonded to the steel deck.

The design for positive bending (for a fully composite beam) may be summarized as (Viest, et al. 1997):

1. Check compactness criteria.
2. Determine the effective width.
3. Determine C.
4. Determine the distances to the centroids of the forces.
5. Compute ultimate capacity.
6. Determine the design moment.
7. Determine the required number of studs.
8. Determine reduction factors.
9. Determine total required number of shear studs.

Per AISC-LRFD (specification I3.2) the positive design flexural strength $\phi_b M_n$ shall be determined as follows:

(a) For $h/t_w \leq 3.76(E/F_{yf})^{1/2}$ (13)

$\phi_b = .85$:

M_n shall be determined from the plastic stress distribution on the composite section.

(b) For $h/t_w > 3.76(E/F_{yf})^{1/2}$ (14)

$\phi_b = .90$:

M_n shall be determined from the superposition of elastic stresses, considering the effects of shoring.

2.17 Composite Beam Design at Areas of Negative Moment

In beams with negative moments the negative moment usually governs the design of composite beam (versus any positive moments that might be present). It is the strength of WF cross section which governs. The design is now one for a beam, a well-known procedure. The design for composite beams in areas of negative moment is not really a design for a composite beam. Because it is assumed that concrete has minimal tensile strength the design of composite beams under negative moments is reduced to the steel section. The design procedure may be summarized (Viest, et al. 1997):

1. Determine the moment capacity
    - A. Locate centroid of tension force in beam
    - B. Determine force in flange

C. Determine force in web

D. Determine centroid of the compression force in web

2. Determine the moment of inertia and elastic section modulus

A. Determine elastic centroid

The design for serviceability (in the negative moment region) is problematic as well. The concrete may creep or shrink under sustained loads; the slab may crack, which in hogging moment regions, will create non-linear load conditions.

AISC states the negative design flexural strength $\phi_b M_n$ shall be determined for the steel section alone, in accordance with the requirements of Chapter F.

AISC also states that alternatively, the negative design flexural strength $\phi_b M_n$ shall be computed with $\phi_b = .85$ and

M_n determined from the plastic stress distribution on the composite section, provided that:

(1) Steel beam is an adequately braced compact section, as defined in Section B5.

(2) Shear connectors connect the slab to the steel beam in the negative moment region.

(3) Slab reinforcement parallel to the steel beam, within the effective width of slab, is properly developed.

Per AISC-LRFD, Chapter F (F1. DESIGN FOR FLEXURE) the nominal flexural strength M_n is the lowest value obtained according to the limit states of:

(a) Yielding

(b) Lateral Torsional Buckling

(c) Flange Local Buckling

(d) Web Local Buckling.

There have been studies, which indicate as long as the shear connectors are designed and placed per the standard requirements for shear strength, deformations due to time dependent behavior may be ignored (Gilbert and Bradford, 1995).

2.18 Composite Beam Flexural and Shear Strength

Experiments indicate the composite action of the concrete slab with the WF section increases flexural and shear strengths in continuous composite beams (Liang, et al. 2003). Johnson and Williamington reported the, "longitudinal steel reinforcement in the concrete slab increases the vertical shear strength and stiffness of continuous composite beams" (Liang, et al. 2003).

According to Johnson and Williamington, if provisions are made to prevent other modes of failure, continuous composite beams will fail mainly due to crushing of concrete in the sagging (positive) moment regions and local buckling of the bottom steel flange in the hogging moment regions (Liang, et al. 2003).

The concrete slab also helps the vertical shear strength of a simply supported composite beam. The strength of a composite plate girder is higher than that of a steel girder alone when designed with enough shear connectors (Liang, et al. 2003).

2.19 Composite Beam Cracking

When the ultimate tensile stress of the concrete section in a composite section is exceeded due to hogging moments the concrete will crack (Dorey and Cheng, 1997). There are three principal reasons for wanting to limit the cracking in a composite

structure. The reasons are appearance, leakage (through the slab), and corrosion of the reinforcing steel, the deck, and perhaps the supporting steel section. Appearance may not matter from a structural point of view, but there are engineers engaged with other trades to whom appearance would be considered a serviceability issue. The issue of leaks is self-explanatory, which leads to the question of corrosion. Corrosion of the reinforcing steel in a composite beam will severely limit the ability of the reinforcing steel to support tension or compression loads. Given a sufficient amount of time corrosion may occur to such a degree as to create voids in the slab where the reinforcement was located. As far as the shear studs are concerned, in negative bending, the spacing of the shear studs provides little aid in controlling cracks (Dorey and Cheng, 1997).

In regions of positive moment if the bending stresses in the shear studs in a continuous composite section can be reduced, i.e. if the studs are stiff enough to carry the energy released as a composite deck cracks, then this may offer some crack control to the section. There are many ways to increase shear connector stiffness: a larger stud diameter, different cross sections such as angle or channel sections, or tie the studs together in some way. This last alternative would allow the studs to act as a simple beam rather than cantilevers.

CHAPTER 3
MODEL CREATION AND VERIFICATION

3.1 Model Creation

Early attempts at modeling composite beams may be noted for the detail with which the FE models were created; the attention to detail was responsible for the creation of a large number of nodes and elements (Figure 16).

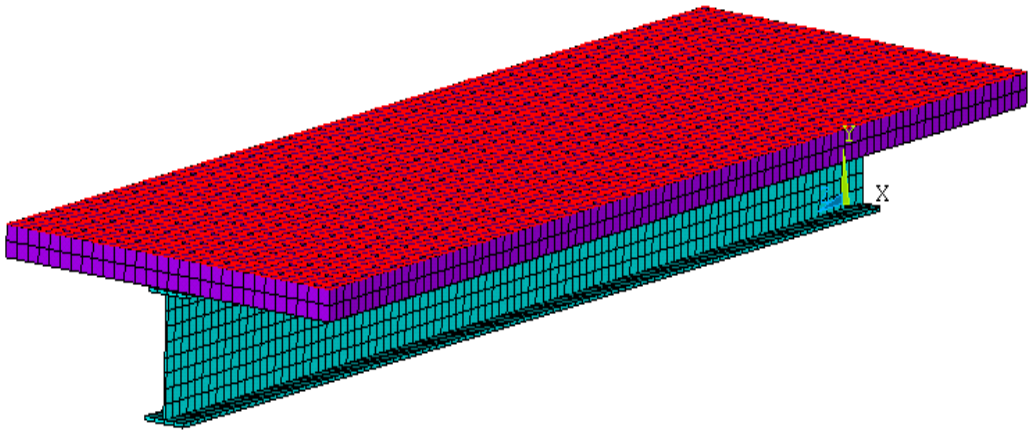

Figure 16 An Early Composite Beam Model

The FE model shown in Figure 16 was created using solid elements. The slab and WF shape were defined using areas and volumes; the connection between the two was accomplished through the use of contact elements. The model calculated but required quite a bit of time. Because of the difficulty associated with using this model, the shear unwieldiness, a different method was chosen to model composite beams. In a paper titled, "Long-term analysis of steel-concrete composite beams: FE modeling for effective

width evaluation", (Macorini, et al. 2006) a method was used, which utilized line elements. The model from the paper used line elements to model the beam, rigid links to model the shear connectors, shell elements to model the slab, and spring elements for long-term analysis of creep and deflection.

The FE models in this paper match, somewhat, that method of composite beam modeling; ANSYS is used to analyze the models. Line elements are utilized for WF beam, slab, and shear connectors. Unmeshed, the models are very simple, a beam line and slab line connected by shear connecter (stud) lines. All the lines are meshed using 3 node beam 189 elements.

There are four models. Three of the models are modeled according to previous research papers, i.e. there has been an attempt to match model parameters, e.g. slabs and WF shapes, in order that preliminary results match those of the previous research. This has been done in order to serve as a means of verifying results. The fourth has no previous research with which it may be compared. For verification of results of the fourth model there is a comparison of results with those rendered by traditional methods of composite beam design.

The four composite beam models are referred to as CBM1, CBM2, CBM3, and CBM4 (CBM stands for Composite Beam Model). There are three loading conditions; they are (I), which represents a single point load in the middle of the span; (II), which represents two point loads located at third points along the span; and (III), which represents a distributed load over the length of the span (Figure 17). There are two boundary conditions; they are A, which represents fixed supports at each of the beam

span and B, which represents pinned supports at each end of the beam span. There are seven stud parameters (Figure 18). They are:

1. Fully composite, entire span length
2. 1/3 reduction in the total amount of studs over the entire span
3. 2/3 reduction in the approximate middle third of the span
4. 2/3 reduction in the approximate end thirds of the span
5. Fully composite, reduced stud area
6. Fully composite, increased stud area
7. Fully composite, original stud diameter, increased slab thickness

(Table 1)

The model names and results are based on these letters and numbers. A model named CBM1(II)A1 translates as Composite Beam Model 1 with the two point load loading condition, fixed ends, and fully composite the entire span length.

The single point load at mid-span was used as means of model verification only except for model CBM2. The two-point load was used to verify that model because that was the manner in which it was loaded in the research paper. A total of 73 models were created (Table 2, Table 3, Table 4).

The purpose of this paper is to analyze shear connectors in regions of positive and negative (hogging) moments. The intent is to stay within the elastic range of beam deflections. Lateral buckling of the bottom flange will not take place in the elastic range. Any desire to look at lateral buckling of the steel beam bottom flange must take place in the plastic range. The means of measuring the effectiveness of the shear connectors is load versus deflection curves and comparison of moment and shear results.

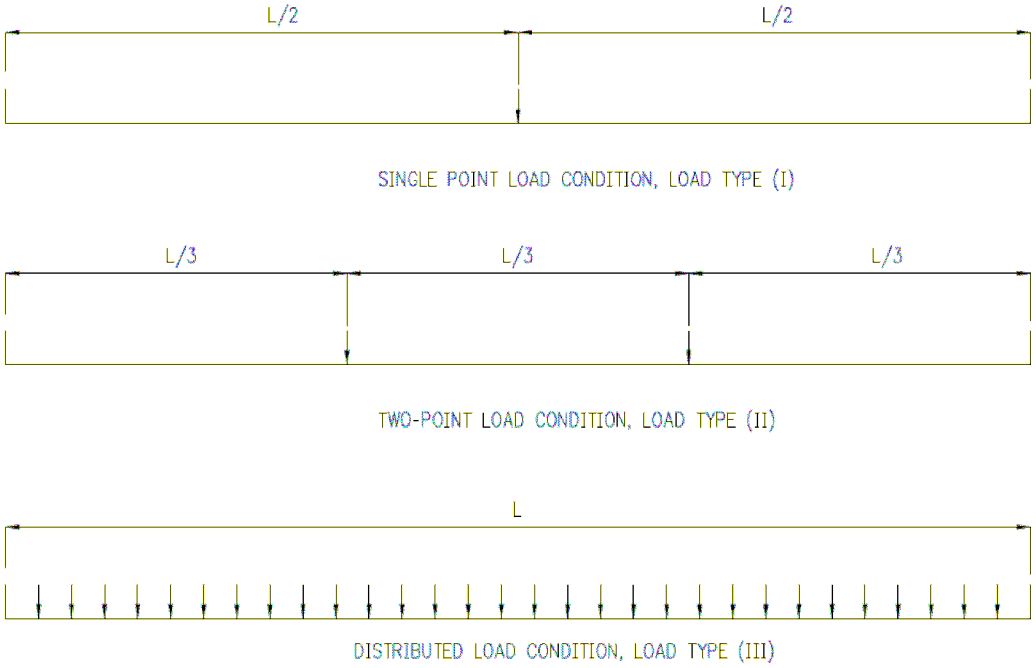

Figure 17 Graphical Representation of Load Types

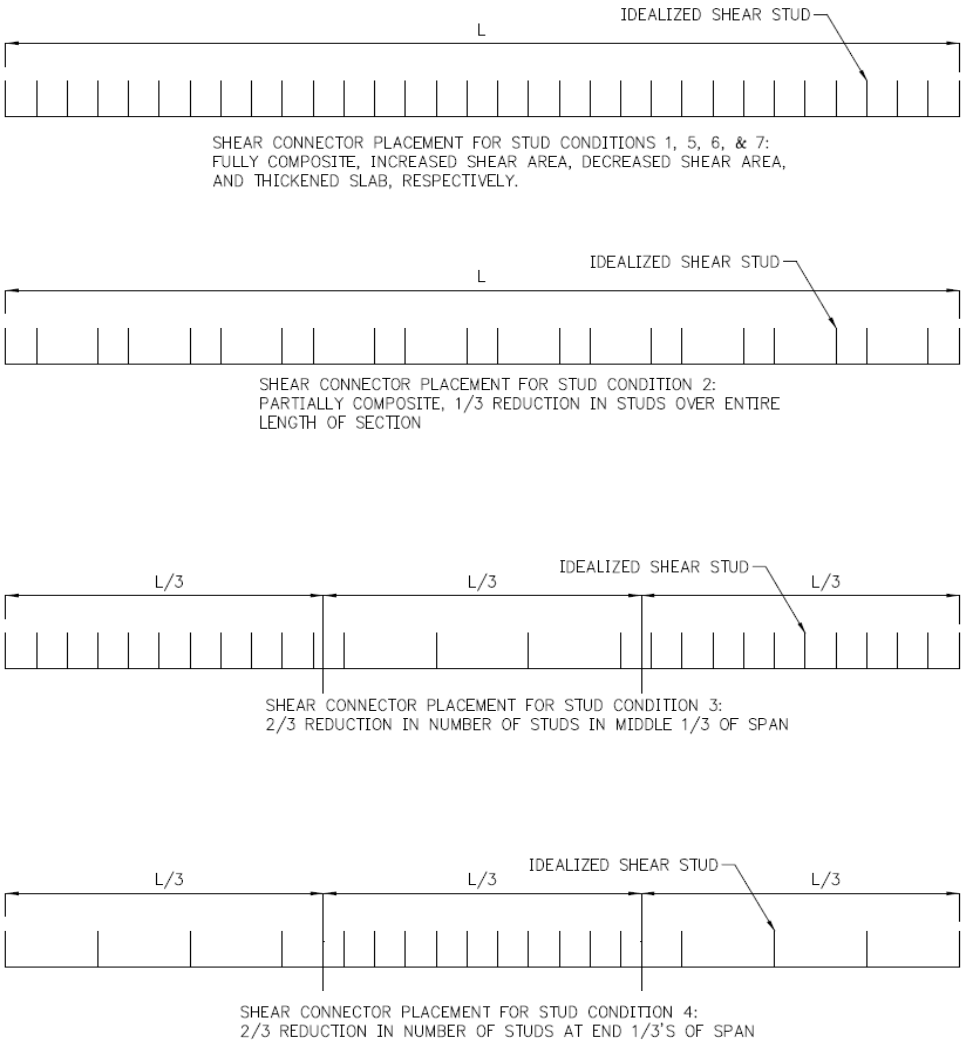

Figure 18 Graphical Representation of Shear Stud Placement

Table 1 Shear Stud Placement Numerical Guide

1	Fully composite, entire span length
2	1/3 reduction in the total amount of studs over the entire span
3	2/3 reduction in the approximate middle third of the span
4	2/3 reduction in the approximate end thirds of the span
5	Fully composite, reduced stud area
6	Fully composite, increased stud area
7	Fully composite, original stud diameter, increased slab thickness

Table 2 List of Model Names

Model Names		Load Condition	End Condition	Shear Stud Placement
CBM1(I)B1		Single Point Load	Pinned	1
CBM1(II)A1		Two-Point Load	Fixed	1
CBM1(II)A2		Two-Point Load	Fixed	2
CBM1(II)A3		Two-Point Load	Fixed	3
CBM1(II)A4		Two-Point Load	Fixed	4
CBM1(II)A5		Two-Point Load	Fixed	5
CBM1(II)A6		Two-Point Load	Fixed	6
CBM1(II)A7		Two-Point Load	Fixed	7
CBM1(II)B1		Two-Point Load	Pinned	1
CBM1(II)B2		Two-Point Load	Pinned	2
CBM1(II)B3		Two-Point Load	Pinned	3
CBM1(II)B4		Two-Point Load	Pinned	4
CBM1(II)B5		Two-Point Load	Pinned	5
CBM1(II)B6		Two-Point Load	Pinned	6
CBM1(II)B7		Two-Point Load	Pinned	7
CBM1(III)A1		Distributed Load	Fixed	1
CBM1(III)A2		Distributed Load	Fixed	2
CBM1(III)A3		Distributed Load	Fixed	3
CBM1(III)A4		Distributed Load	Fixed	4
CBM1(III)A5		Distributed Load	Fixed	5
CBM1(III)A6		Distributed Load	Fixed	6
CBM1(III)A7		Distributed Load	Fixed	7
CBM1(III)B1		Distributed Load	Pinned	1
CBM1(III)B2		Distributed Load	Pinned	2
CBM1(III)B3		Distributed Load	Pinned	3
CBM1(III)B4		Distributed Load	Pinned	4
CBM1(III)B5		Distributed Load	Pinned	5
CBM1(III)B6		Distributed Load	Pinned	6
CBM1(III)B7		Distributed Load	Pinned	7
CBM2(II)B1		Two-Point Load	Pinned	1
CBM2(III)A1		Distributed Load	Fixed	1
CBM2(III)A2		Distributed Load	Fixed	2
CBM2(III)A3		Distributed Load	Fixed	3
CBM2(III)A4		Distributed Load	Fixed	4
CBM2(III)A5		Distributed Load	Fixed	5
CBM2(III)A6		Distributed Load	Fixed	6
CBM2(III)A7		Distributed Load	Fixed	7
CBM2(III)B1		Distributed Load	Pinned	1

Table 3 List of Model Names

Model Names		Load Condition	End Condition	Shear Stud Placement
CBM2(III)B2		Distributed Load	Pinned	2
CBM2(III)B3		Distributed Load	Pinned	3
CBM2(III)B4		Distributed Load	Pinned	4
CBM2(III)B5		Distributed Load	Pinned	5
CBM2(III)B6		Distributed Load	Pinned	6
CBM2(III)B7		Distributed Load	Pinned	7
CBM3(I)B1		Single Point Load	Pinned	1
CBM3(III)A1		Distributed Load	Fixed	1
CBM3(III)A2		Distributed Load	Fixed	2
CBM3(III)A3		Distributed Load	Fixed	3
CBM3(III)A4		Distributed Load	Fixed	4
CBM3(III)A5		Distributed Load	Fixed	5
CBM3(III)A6		Distributed Load	Fixed	6
CBM3(III)A7		Distributed Load	Fixed	7
CBM3(III)B1		Distributed Load	Pinned	1
CBM3(III)B2		Distributed Load	Pinned	2
CBM3(III)B3		Distributed Load	Pinned	3
CBM3(III)B4		Distributed Load	Pinned	4
CBM3(III)B5		Distributed Load	Pinned	5
CBM3(III)B6		Distributed Load	Pinned	6
CBM3(III)B7		Distributed Load	Pinned	7
CBM4(III)A1		Distributed Load	Fixed	1
CBM4(III)A2		Distributed Load	Fixed	2
CBM4(III)A3		Distributed Load	Fixed	3
CBM4(III)A4		Distributed Load	Fixed	4
CBM4(III)A5		Distributed Load	Fixed	5
CBM4(III)A6		Distributed Load	Fixed	6
CBM4(III)A7		Distributed Load	Fixed	7
CBM4(III)B1		Distributed Load	Pinned	1
CBM4(III)B2		Distributed Load	Pinned	2
CBM4(III)B3		Distributed Load	Pinned	3
CBM4(III)B4		Distributed Load	Pinned	4
CBM4(III)B5		Distributed Load	Pinned	5
CBM4(III)B6		Distributed Load	Pinned	6
CBM4(III)B7		Distributed Load	Pinned	7
CBM4(III)A1		Distributed Load	Fixed	1
CBM4(III)A2		Distributed Load	Fixed	2
CBM4(III)A3		Distributed Load	Fixed	3
CBM4(III)A4		Distributed Load	Fixed	4

Table 4 List of Model Names

Model Names		Load Condition	End Condition	Shear Stud Placement
CBM4(III)A5		Distributed Load	Fixed	5
CBM4(III)A6		Distributed Load	Fixed	6
CBM4(III)A7		Distributed Load	Fixed	7
CBM4(III)B1		Distributed Load	Pinned	1
CBM4(III)B2		Distributed Load	Pinned	2
CBM4(III)B3		Distributed Load	Pinned	3
CBM4(III)A1		Distributed Load	Fixed	1
CBM4(III)A2		Distributed Load	Fixed	2
CBM4(III)A3		Distributed Load	Fixed	3
CBM4(III)A4		Distributed Load	Fixed	4
CBM4(III)A5		Distributed Load	Fixed	5
CBM4(III)A6		Distributed Load	Fixed	6
CBM4(III)A7		Distributed Load	Fixed	7
CBM4(III)B1		Distributed Load	Pinned	1
CBM4(III)B2		Distributed Load	Pinned	2
CBM4(III)B3		Distributed Load	Pinned	3
CBM4(III)B4		Distributed Load	Pinned	4
CBM4(III)B5		Distributed Load	Pinned	5
CBM4(III)B6		Distributed Load	Pinned	6
CBM4(III)B7		Distributed Load	Pinned	7

After comparing the two-point load condition with the distributed load condition in the first model (CBM1), the parametric studies were limited to the distributed load condition only in models CBM2, CBM3, and CBM4.

3.2 CBM1 Model Description

The composite beam CBM1 was created according to the parameters of the composite beam model discussed in the paper, "Ultimate Strength of Continuous Composite Beams in Combined Bending and Shear" (Liang, et al. 2003). The slab width and thickness as well as the WF beam properties of CBM1 match those of the model in the research paper (Figure 19). Three shear connectors per composite section were used in the model from the research paper. A single large shear connector was used in the author's model to make up for the discrepancy is shear connector area.

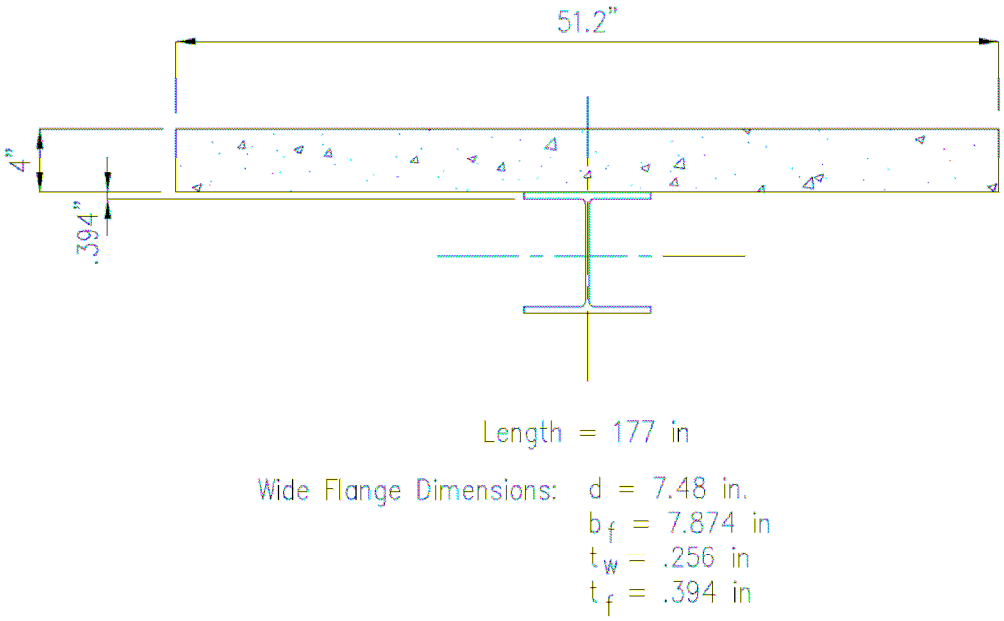

Figure 19 CBM1 Composite Cross Section

In this, as well as the other models, "d" represents the WF beam section depth; "b_f" represents the WF flange width; "t_w" represents the WF web thickness; and "t_f" represents the WF flange thickness. The concrete slab in this model is 4 inches thick.

The material model for the steel beam assumes linear isotropic properties defined by a Young's modulus of 29000 ksi and a poisson ratio of 0.3; multilinear isotropic

properties are defined by the stress/strain curve for steel with a yield stress of 50 ksi. The material model for the slab assumes linear isotropic properties defined by a Young's modulus of 4.287 ksi and a poisson's ratio of .15; concrete properties as calculated below.

1. Open shear transfer coef., 0.15
2. Closed shear transfer coef., 0.85 (The open shear transfer coefficient added to the closed shear transfer coefficient must equal 1.0)
3. Uniaxial Cracking Stress, 638.3 (Approximately 13% of the Uniaxial Crushing Stress)
4. Uniaxial Crushing Stress, 5000 ($f`_c$, the allowable concrete compressive stress)
5. Biaxial Crushing Stress, 6000 (1.2 x $f`_c$)
6. Hydrostatic Pressure, 8660.3 (f'c x $\sqrt{3}$)
7. Hydro Biax Crush Stress, 7250 (1.45 x $f`_c$)
8. Hydro Uniax Crush Stress, 8625 (1.725 x $f`_c$)
9. Tensile Crack Factor, 0.6 (a value < 1.0)

This, as well as the other models, is considered to be that of a composite beam located somewhere in the middle of a floor; it is not an edge beam (effective width calculations for edge beams are not meant to be part of this paper). It is supported at each end with boundary conditions located on the slab centerline to prevent lateral bucking and to prevent rotation along the long axis of the composite beam.

The results of the first loading condition, a simply supported beam with a point load located in the middle of the beam, are indicated in order to verify the accuracy of the model. The difference in the calculated versus ANSYS model results is just a bit over 7%. The difference in the ANSYS model versus research paper results is approximately 15% (Figure 20).

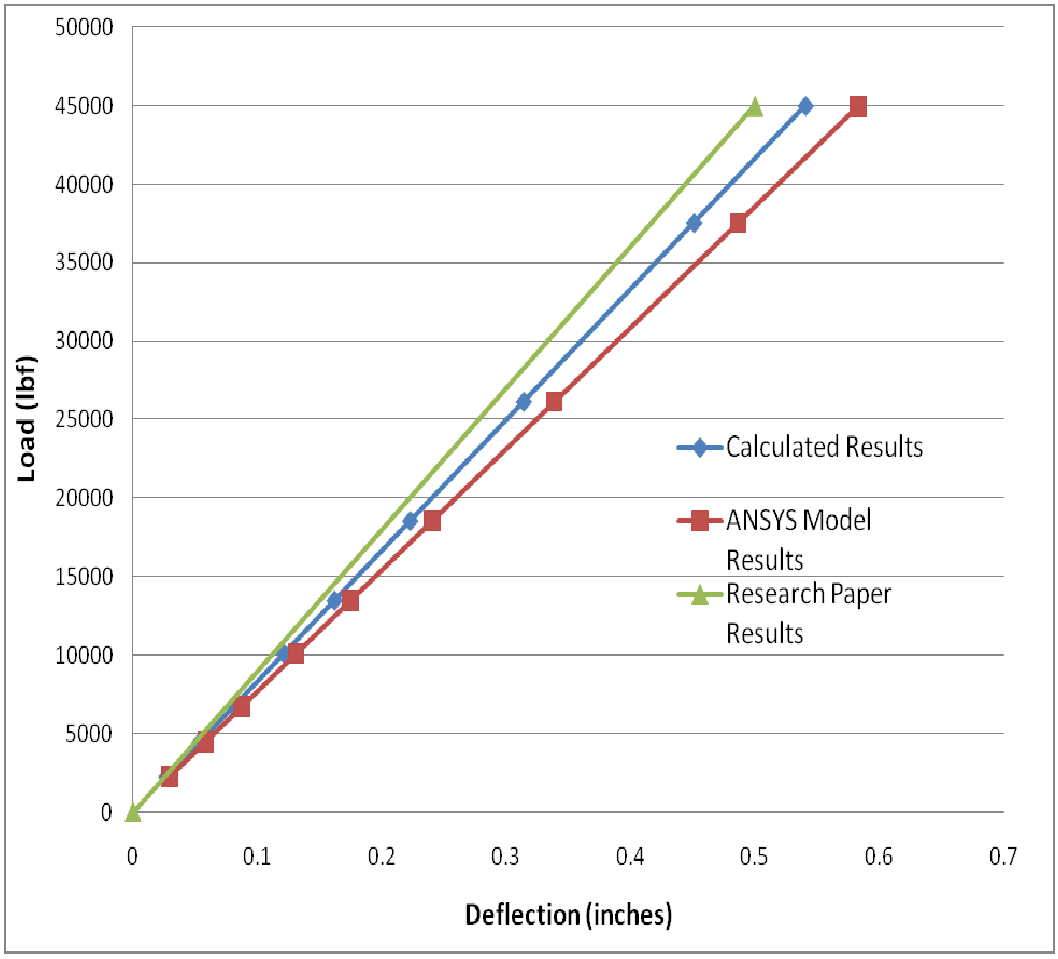

Figure 20 CBM1 Verification Graph

3.3 CBM2 Model Description

The composite beam CBM2 was created according to the parameters of the composite beam model discussed in the paper, "Flexural Strengthening of Composite Steel-Concrete Girders Using Advanced Composite Materials" (Raafat and Ragab, 2003). The slab width and thickness as well as the WF beam properties of CBM2 match those of the model in the research paper (Figure 21). Two shear connectors per composite section were used in the model from the research paper. A single large shear connector was used in the author's model to make up for the discrepancy is shear connector area.

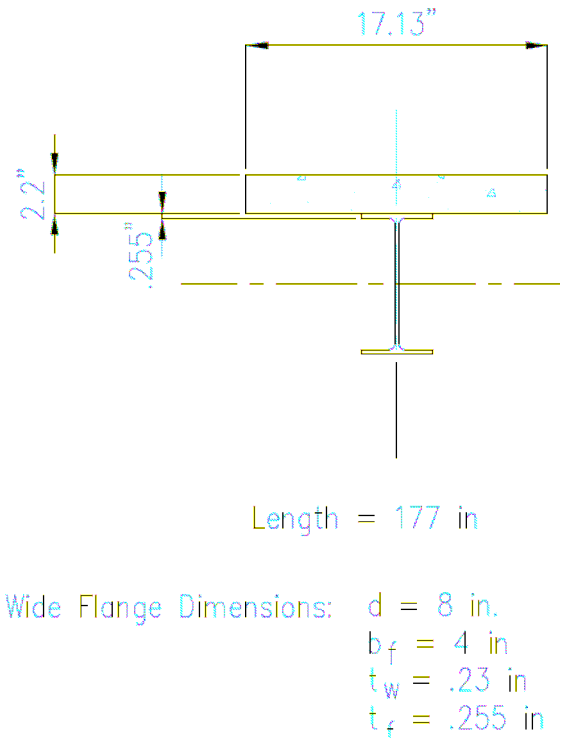

Figure 21 CBM2 Composite Cross Section

The material model for the steel beam assumes linear isotropic properties defined by a Young's modulus of 29000 ksi and a poisson ratio of .3; multilinear isotropic properties are defined by the stress/strain curve for steel with a yield stress of 50 ksi. The material model for the slab assumes linear isotropic properties defined by a Young's

modulus of 4.3881 ksi and a poisson's ratio of .15; concrete properties as calculated below.

1. Open shear transfer coef., 0.15
2. Closed shear transfer coef., 0.85 (The open shear transfer coefficient added to the closed shear transfer coefficient must equal 1.0)
3. Uniaxial Cracking Stress, 740.5 (Approximately 13% of the Uniaxial Crushing Stress)
4. Uniaxial Crushing Stress, 5800 ($f`_c$, the allowable concrete compressive stress)
5. Biaxial Crushing Stress, 6960 (1.2 x $f`_c$)
6. Hydrostatic Pressure, 10046 (f'_c x $\sqrt{3}$)
7. Hydro Biax Crush Stress, 8410 (1.45 x $f`_c$)
8. Hydro Uniax Crush Stress, 10005 (1.725 x $f`_c$)
9. Tensile Crack Factor, 0.6 (a value < 1.0)

The results of the first loading condition, a simply supported beam with a two-point load located in the middle of the beam, are indicated in order to verify the accuracy of the model. The difference in the calculated versus ANSYS model results is just a bit over 10%. The difference in the ANSYS model versus paper results is approximately 11% (Figure 22).

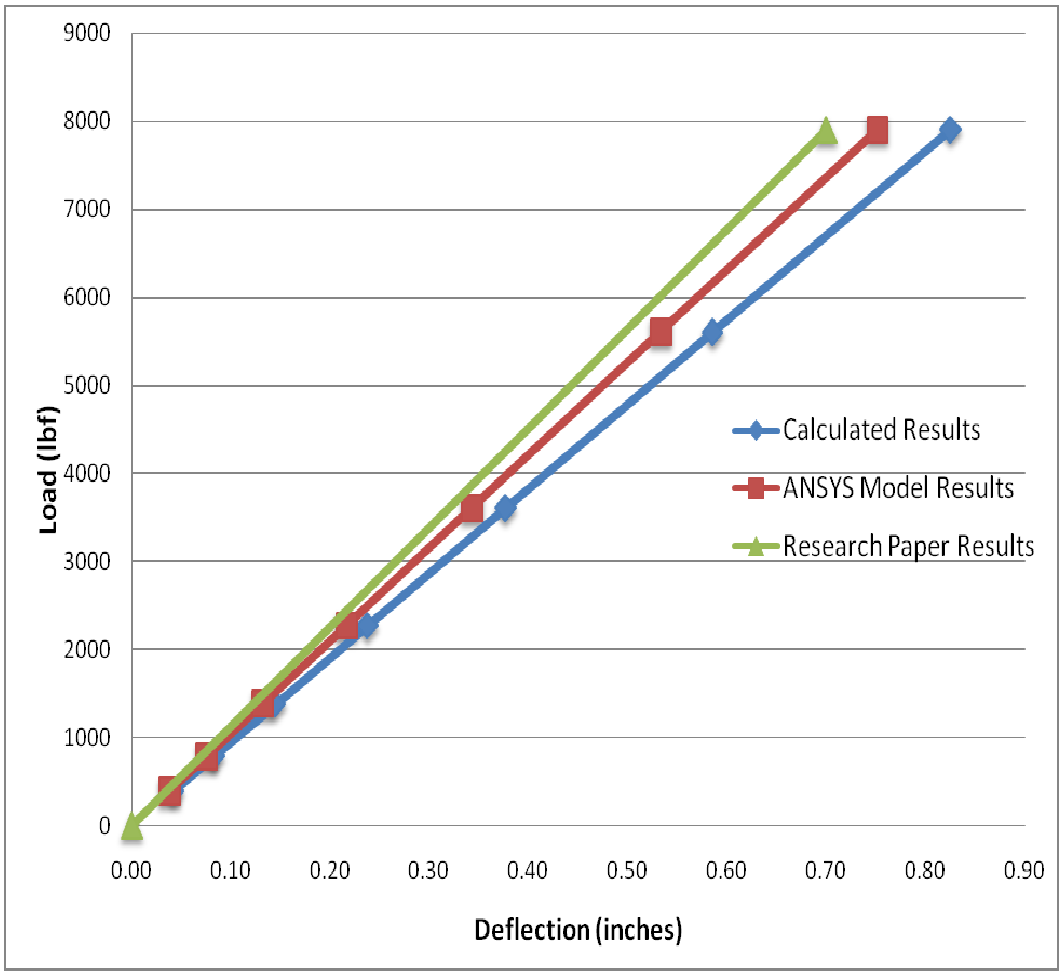

Figure 22 CBM2 Verification Graph

3.4 CBM3 Model Description

The composite beam CBM3 was created according to the parameters of the composite beam model discussed in the paper, "Analysis of Continuous Composite Beams Including Partial Interaction and Bond" (Fabbrocino, et al. 2000). The slab width and thickness as well as the WF beam properties of CBM3 match those of the model in the research paper (Figure 23). A single shear connector was used in the research model as well as that of the author.

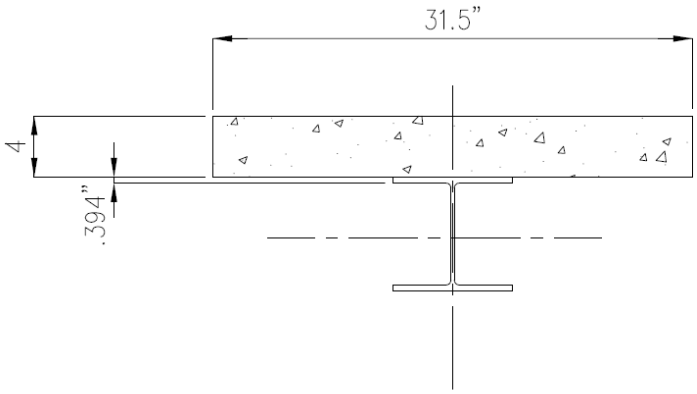

Length = 236 in

Wide Flange Dimensions: d = 7.48 in.
b_f = 7.874 in
t_w = .256 in
t_f = .394 in

Figure 23 CBM3 Composite Cross Section

The paper included an analysis of a continuously supported beam. However the load/deflection curves were supplied for a single span. It is that the single span model CBM3 is patterned after.

The material model for the steel beam assumes linear isotropic properties defined by a Young's modulus of 29000 ksi and a poisson ratio of .3; multilinear isotropic properties are defined by the stress/strain curve for steel with a yield stress of 50 ksi. The

material model for the slab assumes linear isotropic properties defined by a Young's modulus of 3900 ksi and a poisson's ratio of .15; concrete properties as calculated below.

1. Open shear transfer coef., 0.1
2. Closed shear transfer coef., 0.9 (The open shear transfer
3. coefficient added to the closed shear transfer coefficient must equal 1.0)
4. Uniaxial Cracking Stress, 630 (Approximately 13% of the Uniaxial Crushing Stress)
5. Uniaxial Crushing Stress, 4931 ($f`_c$, the allowable concrete compressive stress)
6. Biaxial Crushing Stress, 5917 (1.2 x $f`_c$)
7. Hydrostatic Pressure, 8541 (f'_c x $\sqrt{3}$)
8. Hydro Biax Crush Stress, 7150 (1.45 x $f`_c$)
9. Hydro Uniax Crush Stress, 8506 (1.725 x $f`_c$)
10. Tensile Crack Factor, 0.6 (a value < 1.0)

The results of the first loading condition, a simply supported beam with a point load located in the middle of the beam, are indicated in order to verify the accuracy of the model. The difference in the calculated versus ANSYS model results approximately 5%. The difference in the ANSYS model versus paper results is approximately 16% (Figure 24).

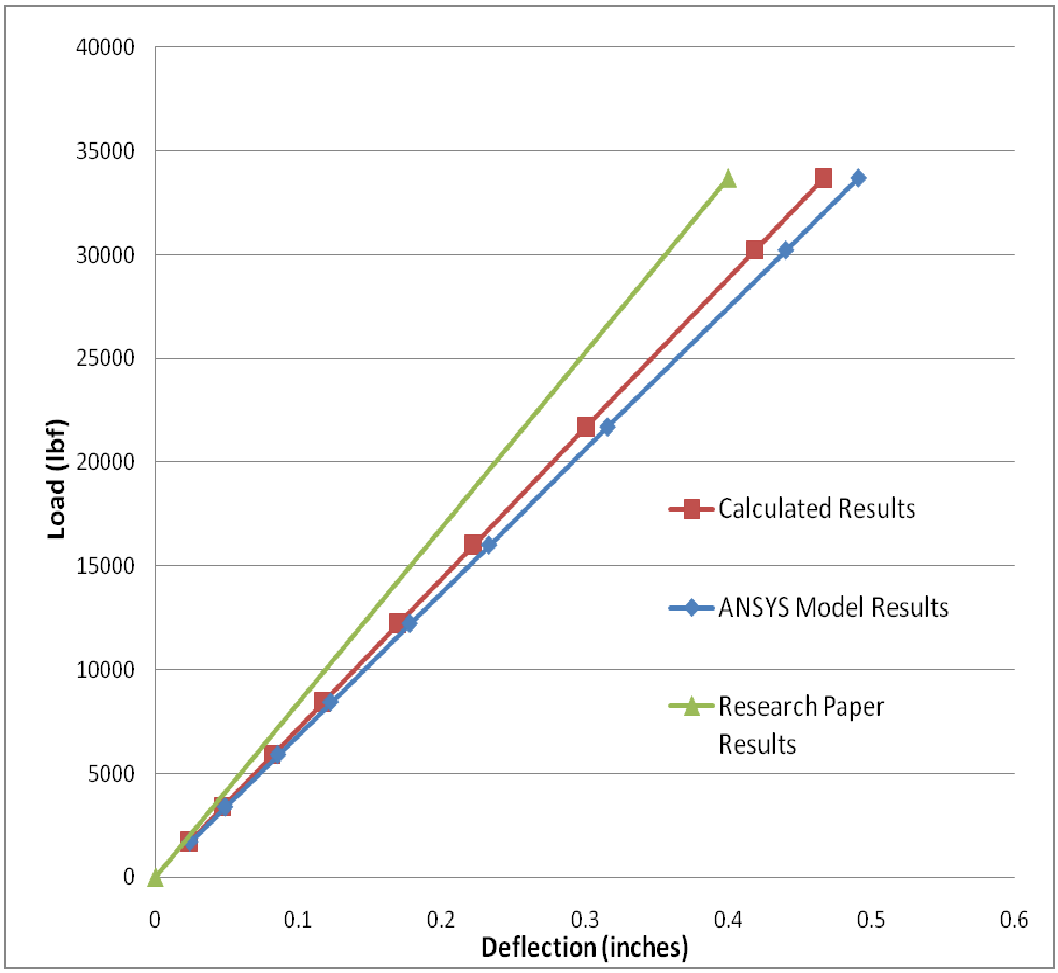

Figure 24 CBM3 Verification Graph

3.5 CBM4 Model Description

The composite beam model CBM4 has no research paper model with which it may be compared. It was created as composite beam typical to the author's experience (Figure 25).

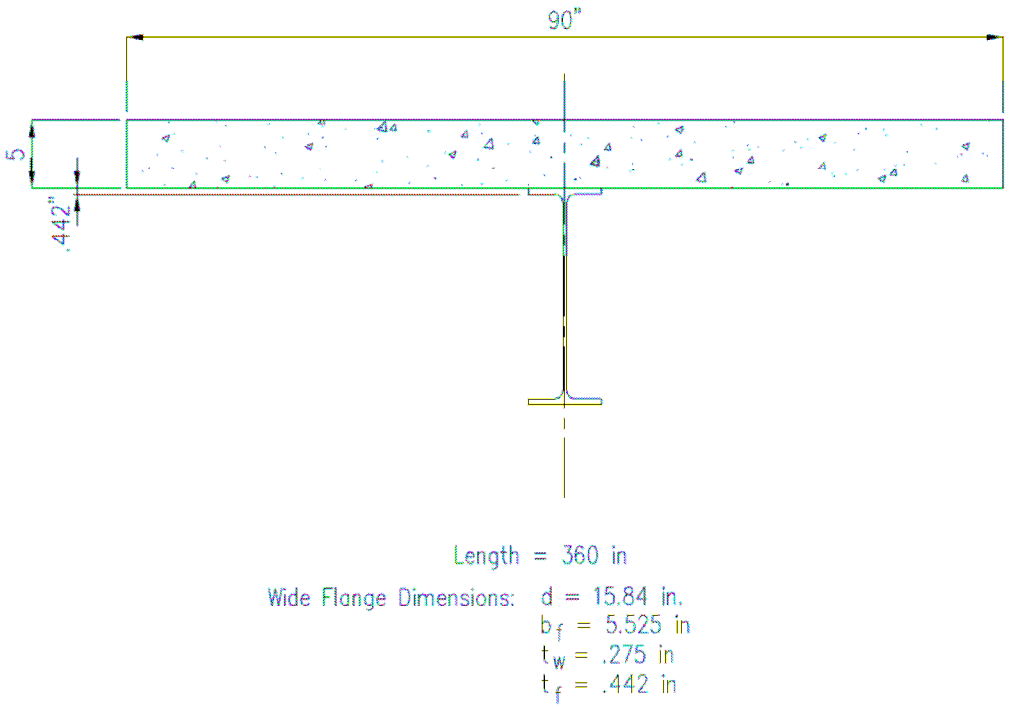

Figure 25 CBM4 Composite Cross Section

The material model for the steel beam assumes linear isotropic properties defined by a Young's modulus of 29000 ksi and a poisson ratio of .3; multilinear isotropic properties are defined by the stress/strain curve for steel with a yield stress of 50 ksi. The material model for the slab assumes linear isotropic properties defined by a Young's modulus of 4074 ksi and a poisson's ratio of .15; concrete properties as calculated below.

1. Open shear transfer coef., 0.15

2. Closed shear transfer coef., 0.85 (The open shear transfer coefficient added to the closed shear transfer coefficient must equal 1.0)
3. Uniaxial Cracking Stress, 740.5 (Approximately 13% of the Uniaxial Crushing Stress)
4. Uniaxial Crushing Stress, 5000 ($f`_c$, the allowable concrete compressive stress)
5. Biaxial Crushing Stress, 6000 (1.2 x $f`_c$)
6. Hydrostatic Pressure, 8660.3 (f'_c x $\sqrt{3}$)
7. Hydro Biax Crush Stress, 7250 (1.45 x $f`_c$)
8. Hydro Uniax Crush Stress, 8625 (1.725 x $f`_c$)
9. Tensile Crack Factor, 0.6 (a value < 1.0)

The results of the first loading condition, a simply supported beam with a point load located in the middle of the beam, are indicated in order to verify the accuracy of the model. The difference in the calculated versus ANSYS model results is just a bit over 2% (Figure 26).

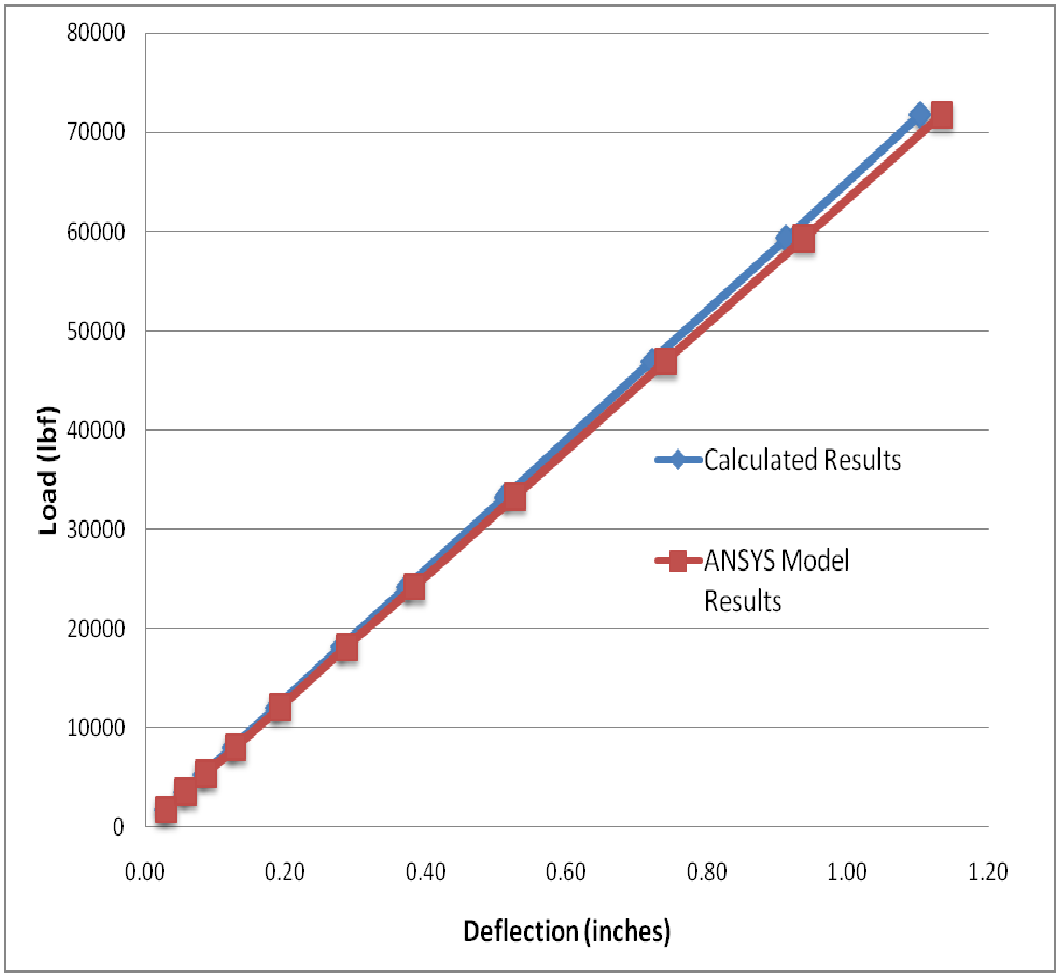

Figure 26 CBM4 Verification Graph

CHAPTER 4
PARAMETRIC STUDY RESULTS

4.1 Introduction to Results

The parameters of the study of the composite beams were end conditions (fixed or pinned), loading conditions (single, two-point, distributed), and shear stud placement (full composite, partially composite, increased or decreased shear connector area, and increased slab thickness). The fixed end condition was utilized to in order to create regions of negative moment.

Each of the four composite beam models was examined in light of the different parameters. Models CBM2, CBM3, and CBM4 were studied with the distributed load condition only. Calculations using well established methods were performed in order to create the sketches of the Plastic Neutral Axis (PNA) and concrete stress blocks as well as the stress distribution graphs.

4.2 CBM1 Results

Calculations of the CBM1 composite section indicate the section is fully composite. Note, the PNA, and the stress block, "a", are located in the slab, which indicates the slab and WF section are acting a together as a composite section (Figure 27). The stress distribution also indicates the section is acting in a composite manner (Figure 28).

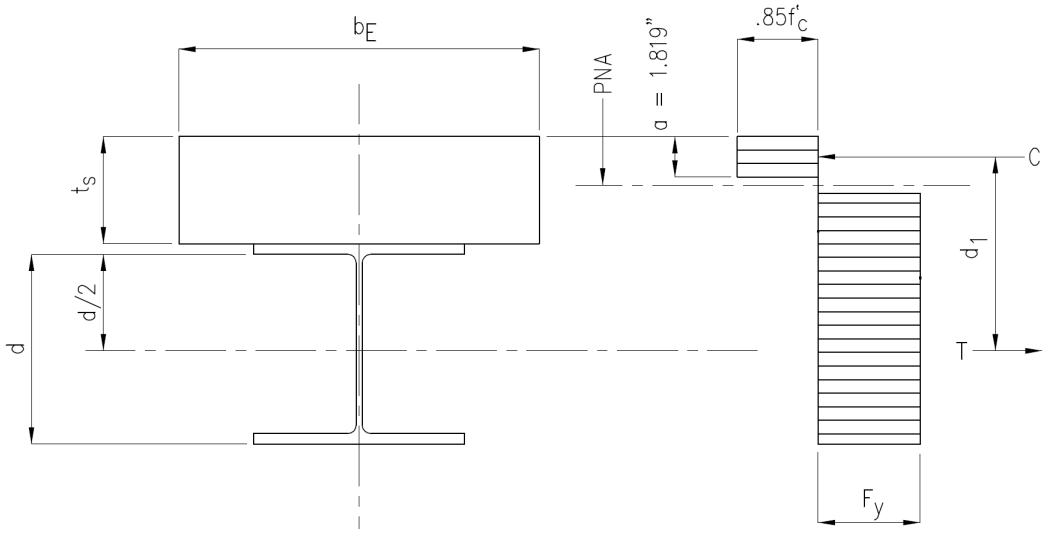

Figure 27 CBM1 Location of Plastic Neutral Axis and Concrete Stress Block.

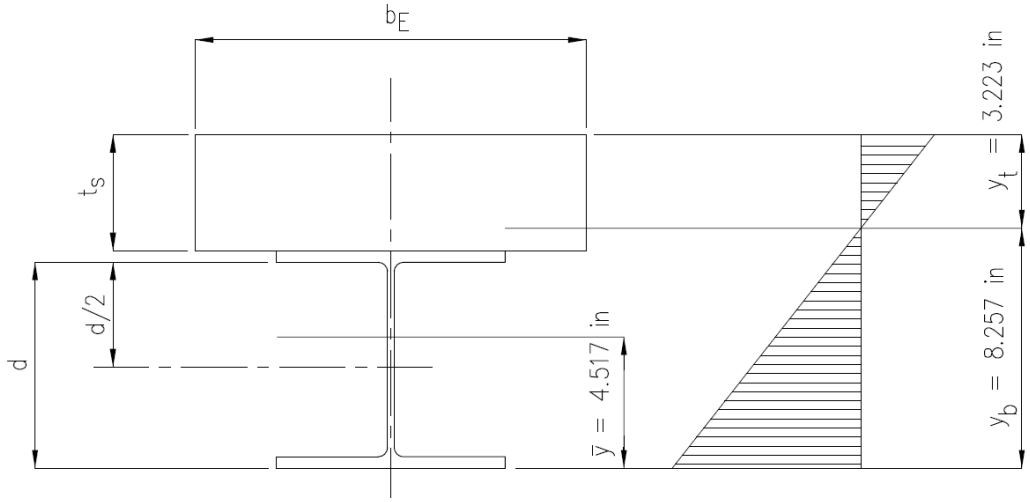

Figure 28 CBM1 Stress Distribution

The loading conditions compared to form the graph are noted. The results of the graph indicated the end condition is more important than the load condition in determining the amount of deflection (Figure 29). The shear (Figure 30) and moment (Figure 31) diagrams of the fully composite section provide a means of comparing the effects of reducing the number of studs at the mid span and end spans of the beam with the fully composite section.

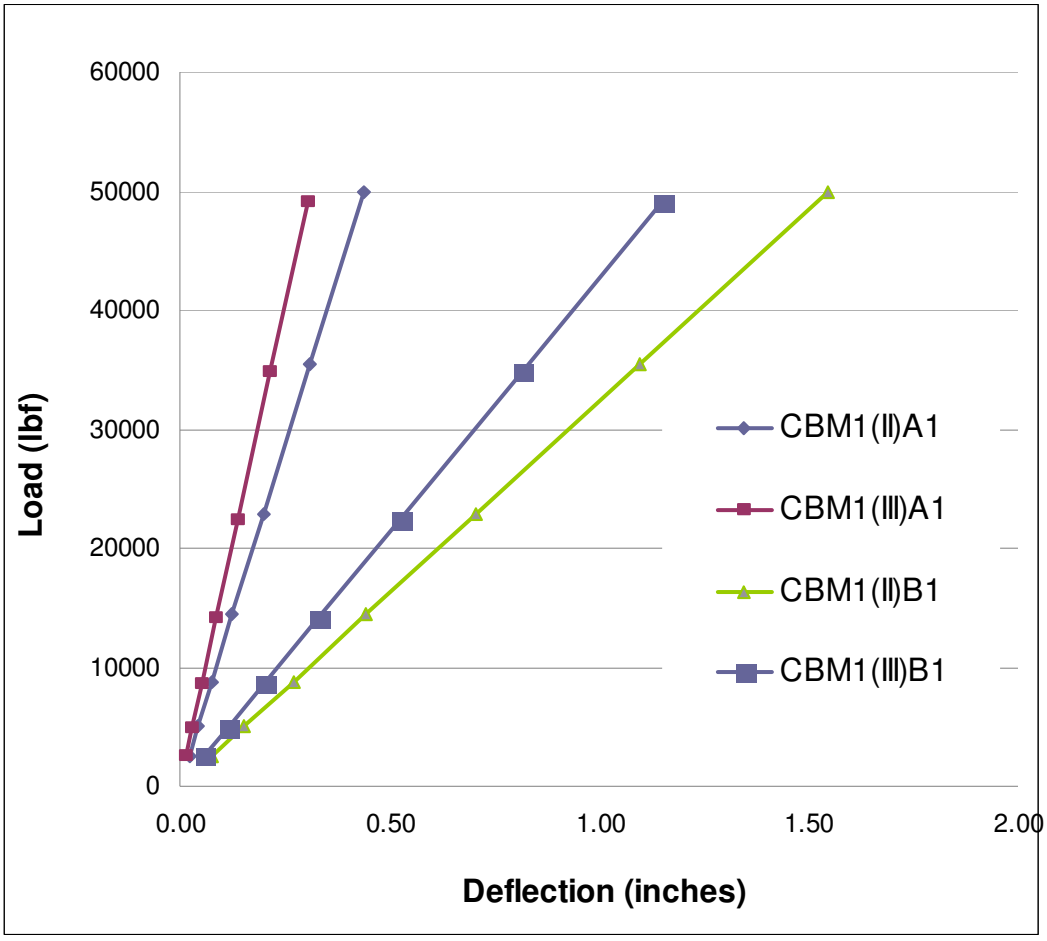

Figure 29 CBM1 Two-Point Load and Distributed Load Curves, Fully Composite Section.

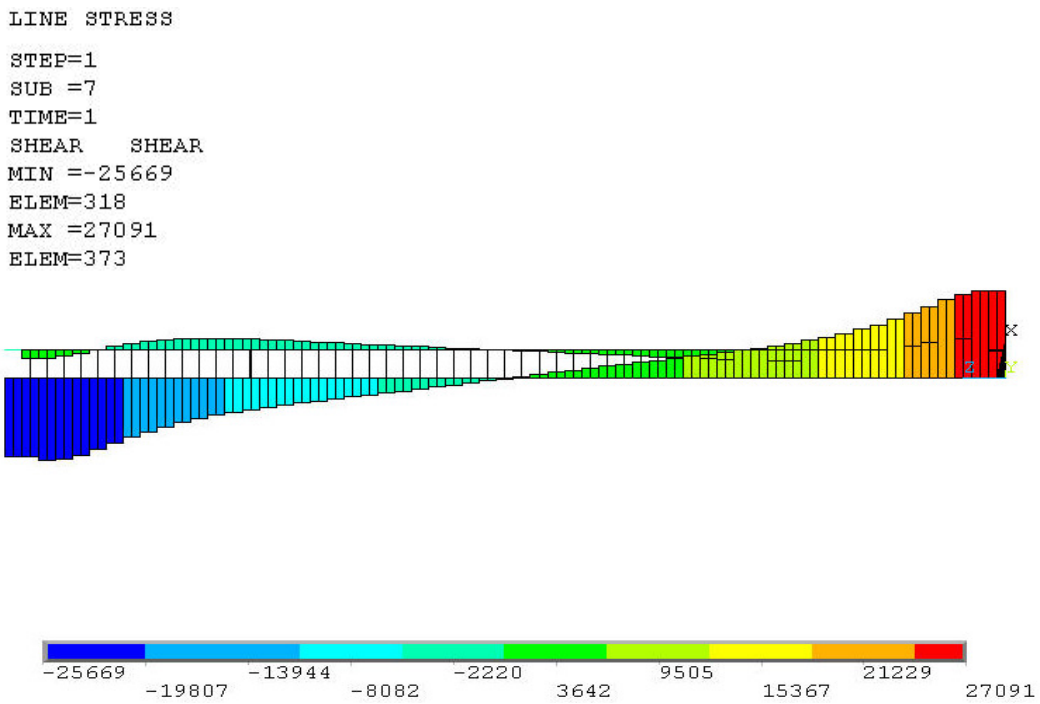

Figure 30 CBM1(III)A1 Shear Diagram

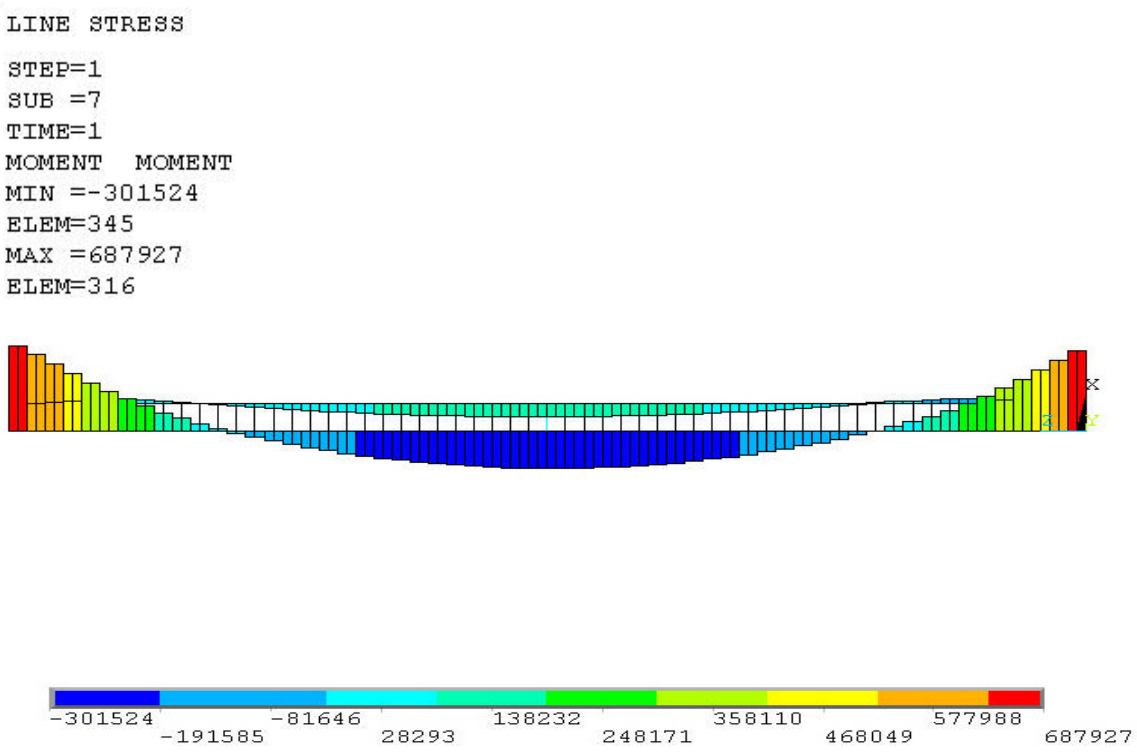

Figure 31 CBM1(III)A1 Moment Diagram

The curves in the graph below indicate there is difference in deflection based on the load condition (Figure 32). The most rigid condition is the fully composite, distributed load condition. Both partially composite conditions and the two-point fully composite load condition display similar amounts of deflection.

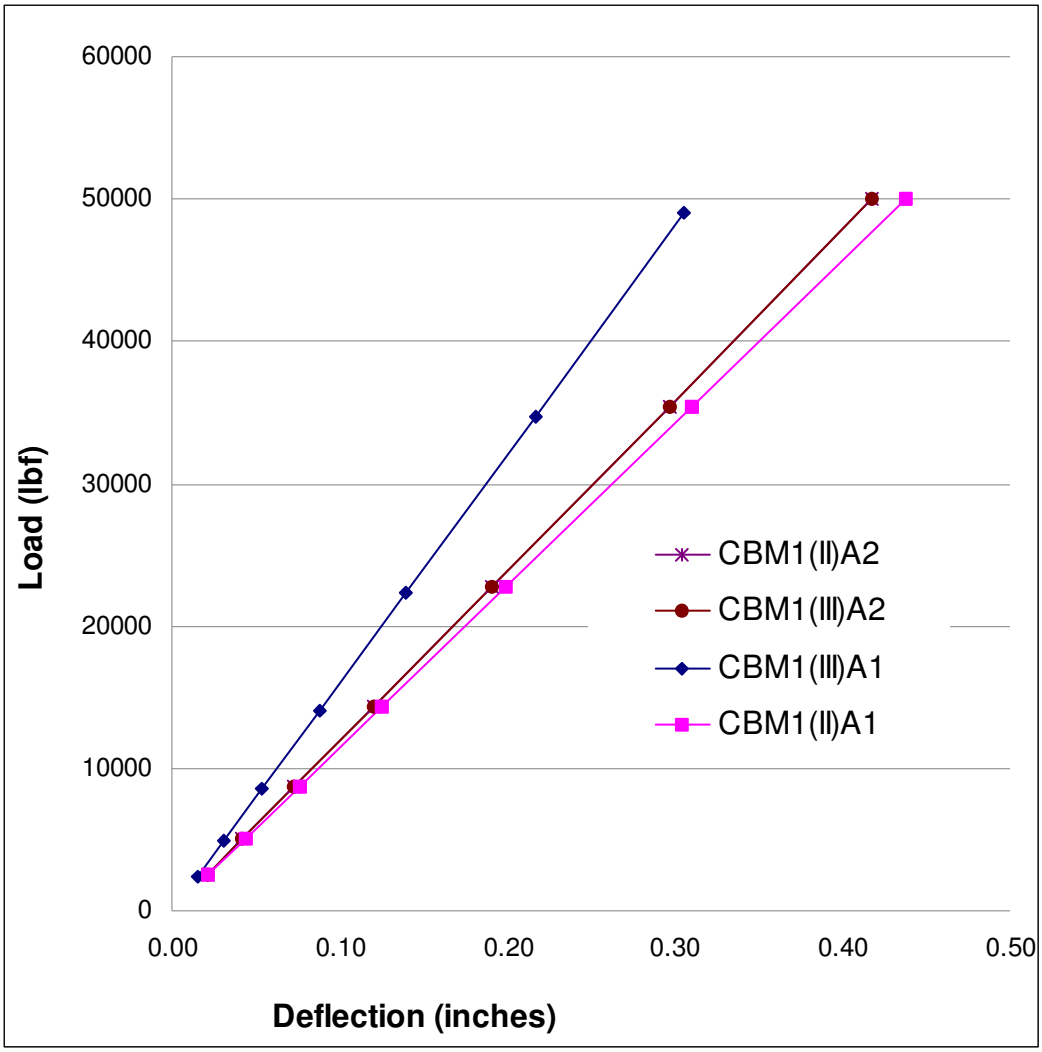

Figure 32 CBM1 Two-Point and Distributed Load Curves, Partially Composite Section, Fixed Ends

There is little difference in the degree of deflection between the partially and fully composite sections (Figure 33).

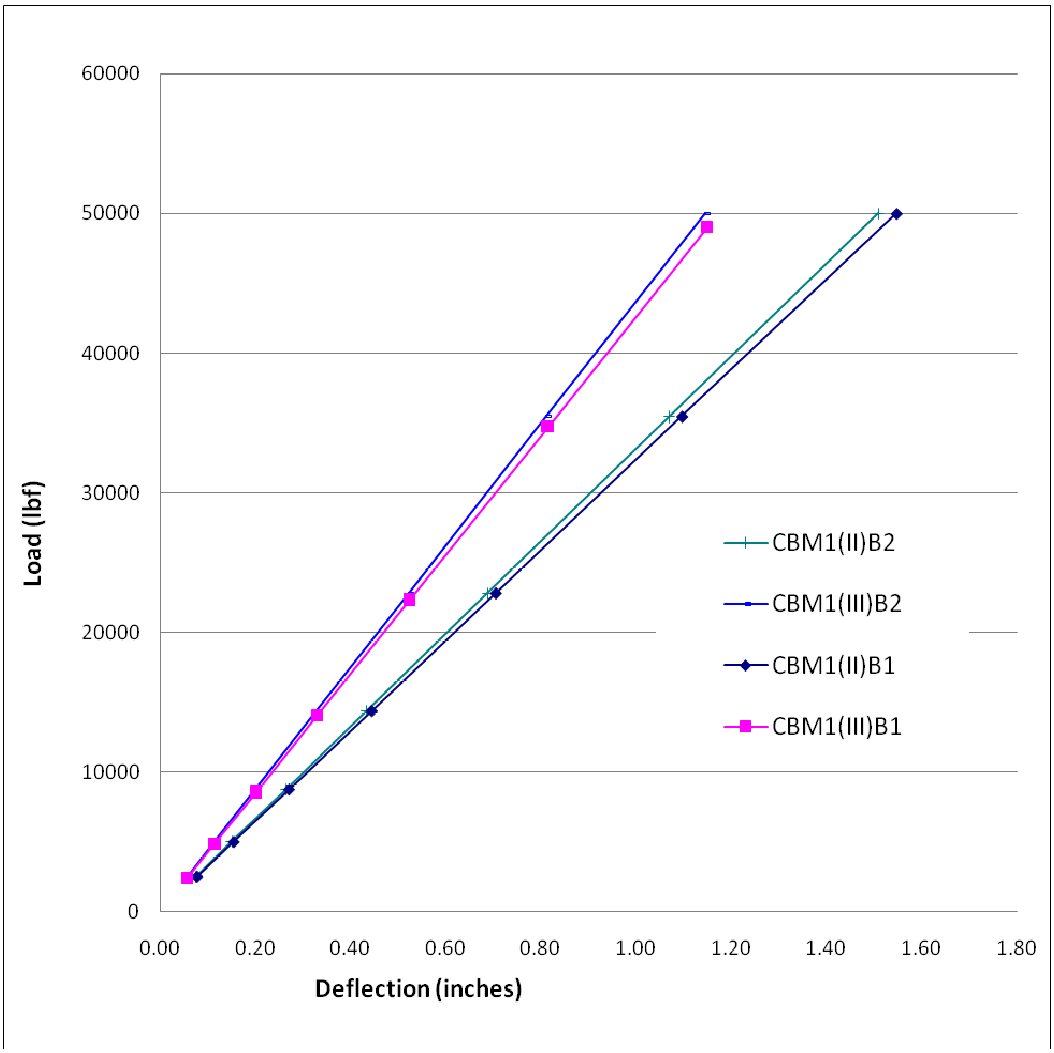

Figure 33 CBM1 Distributed and Two-Point Load Curves, Pinned End Condition, Partially Composite Section.

The curves in the graph below indicate that under a two-point load a reduction in the number of shear studs at either the mid span or end spans of the beam makes little difference in the amount of deflection (Figure 34).

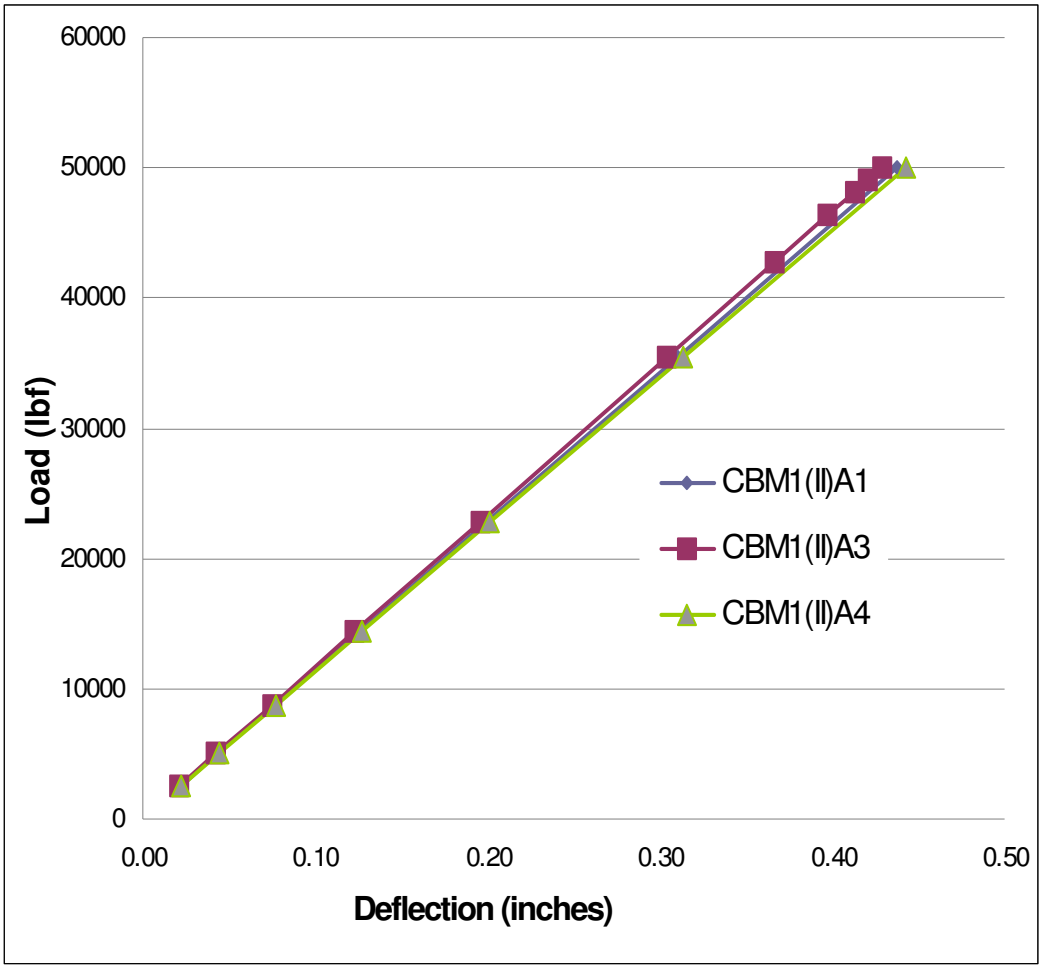

Figure 34 CBM1 Two-Point Load Curves, Fixed End Condition, Partially Composite Sections.

The curves in the graph below indicate that under a two-point load a reduction in the number of shear studs at either the mid span or end spans of the beam makes little difference in the amount of deflection (Figure 35).

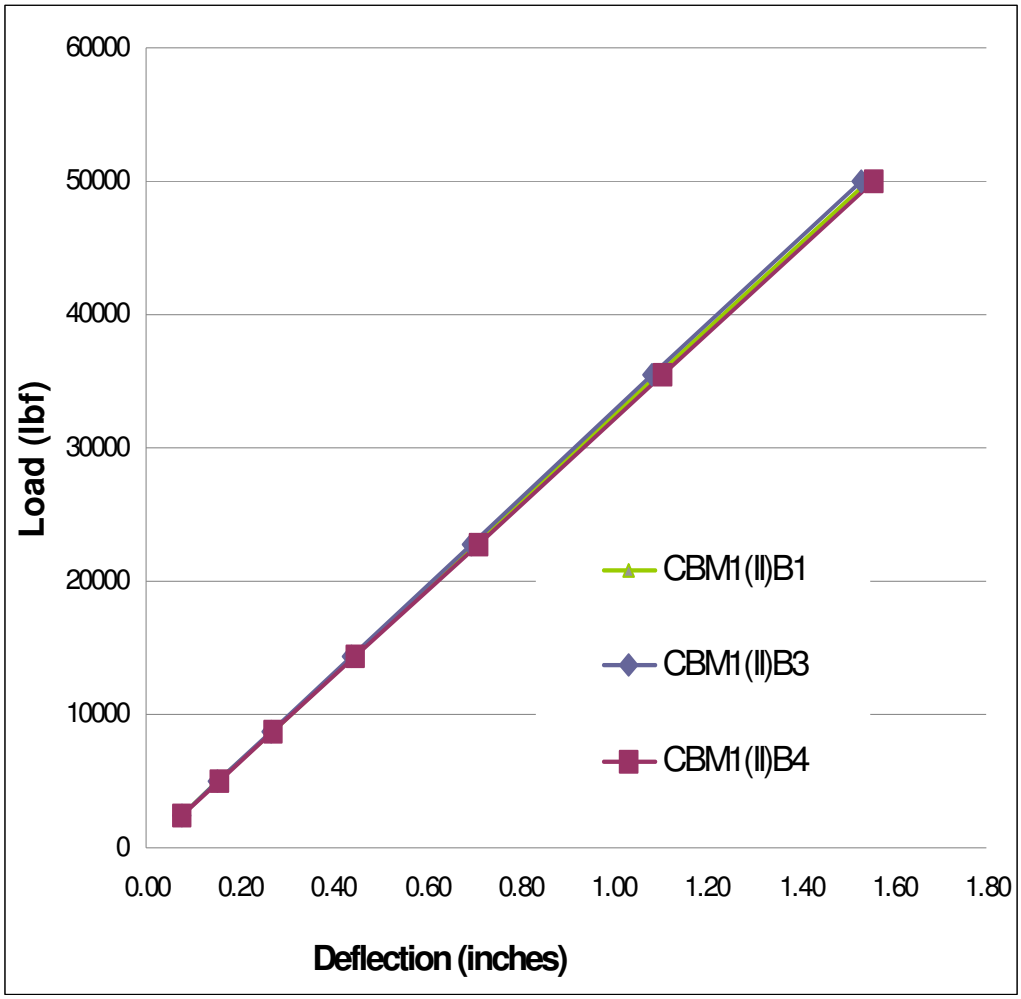

Figure 35 CBM1 Two-Point Load Curves, Pinned End Condition, Partially Composite Sections.

This graph (Figure 36) shows the results of a 2/3 reduction in the number of shear connectors in the middle of the beam with one curve and the results of a 2/3 reduction atg the end spans in another curve. There is not much change in the degree of deflection in any condition. The shear (Figure 37) and moment (Figure 38) diagrams of mid span partially composite section provide a means of comparing the effects of reducing the number of studs at the mid span with the fully composite section.

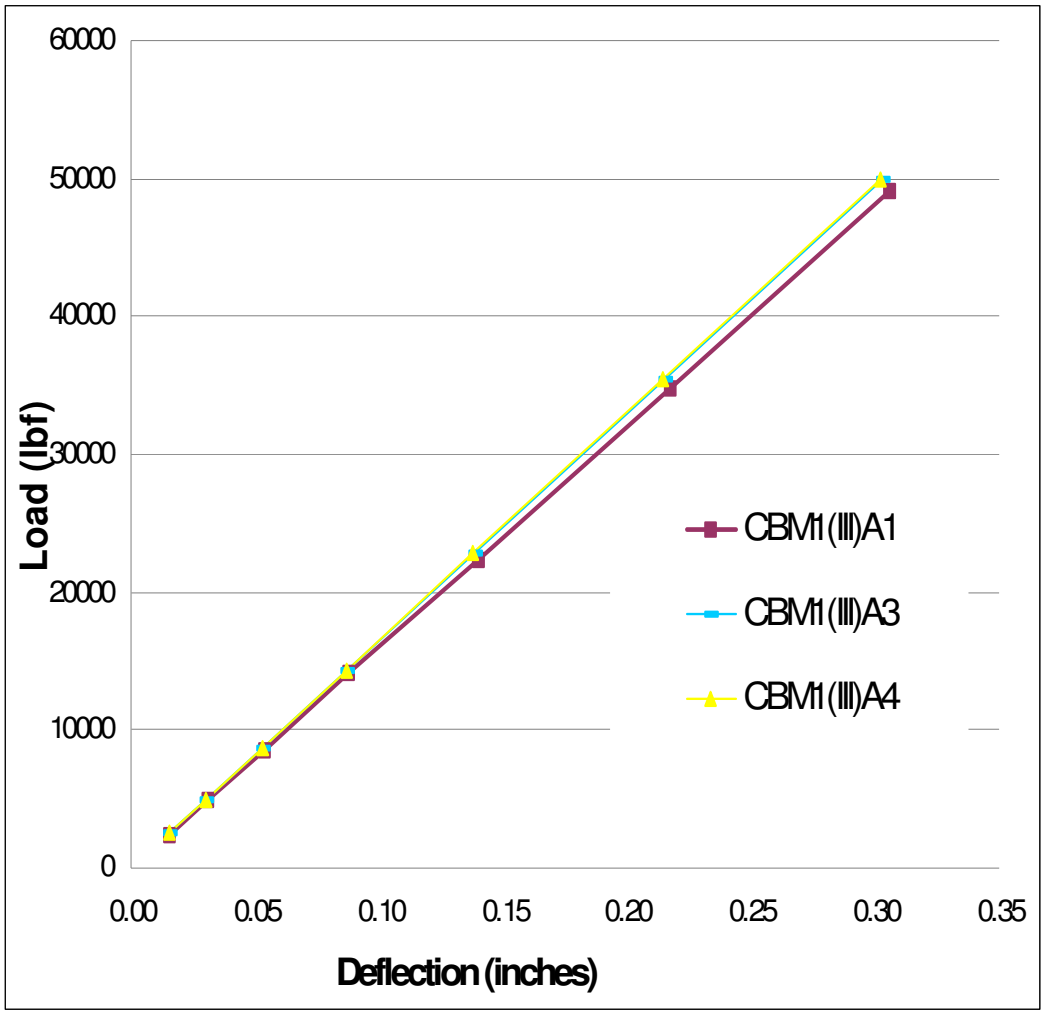

Figure 36 CBM1 Two-Point Load Curves, Fixed End Condition, Partially Composite Sections.

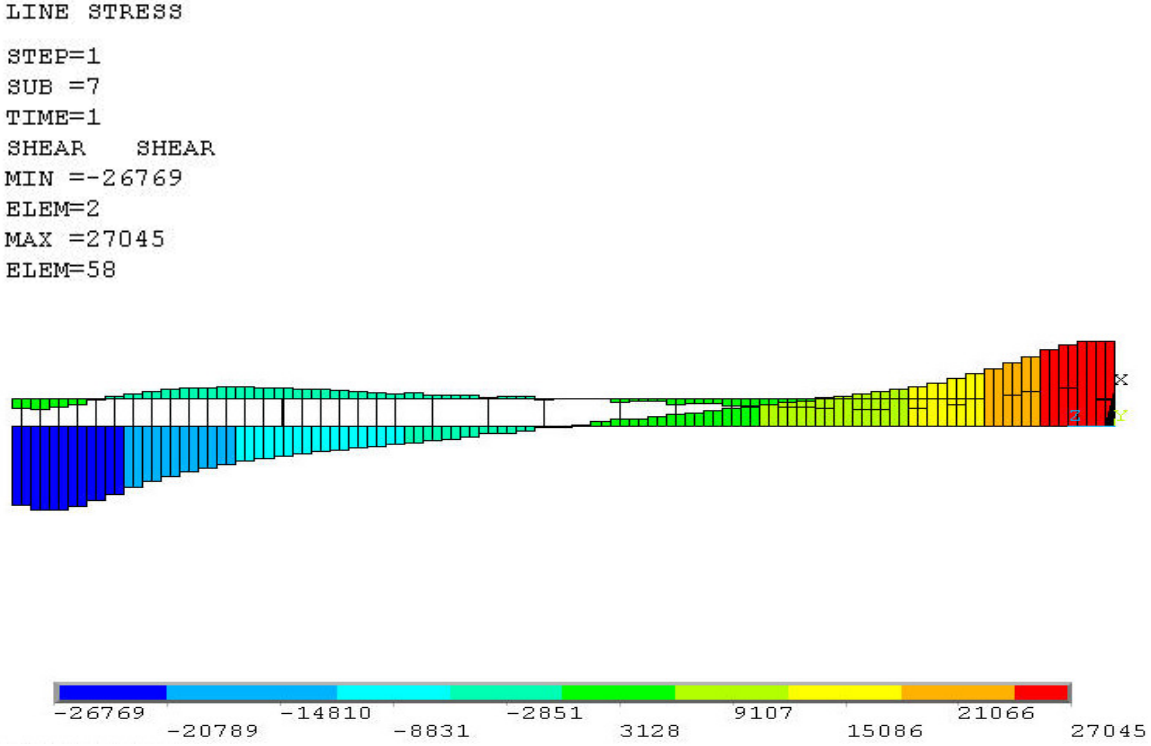

Figure 37 CBMI(III)A3 Shear Diagram

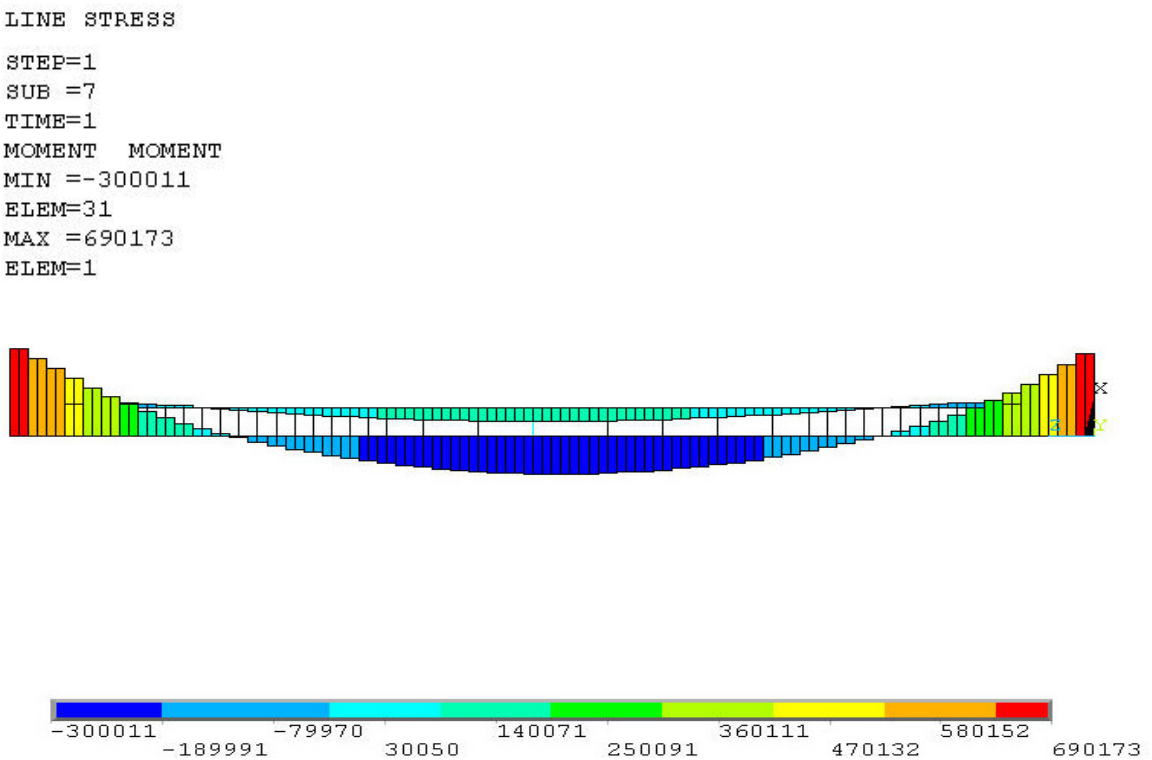

Figure 38 CBM1(III)A3 Moment Diagram

The shear (Figure 39) and moment (Figure 40) diagrams of end span partially composite section provide a means of comparing the effects of reducing the number of studs at the mid span with the fully composite section.

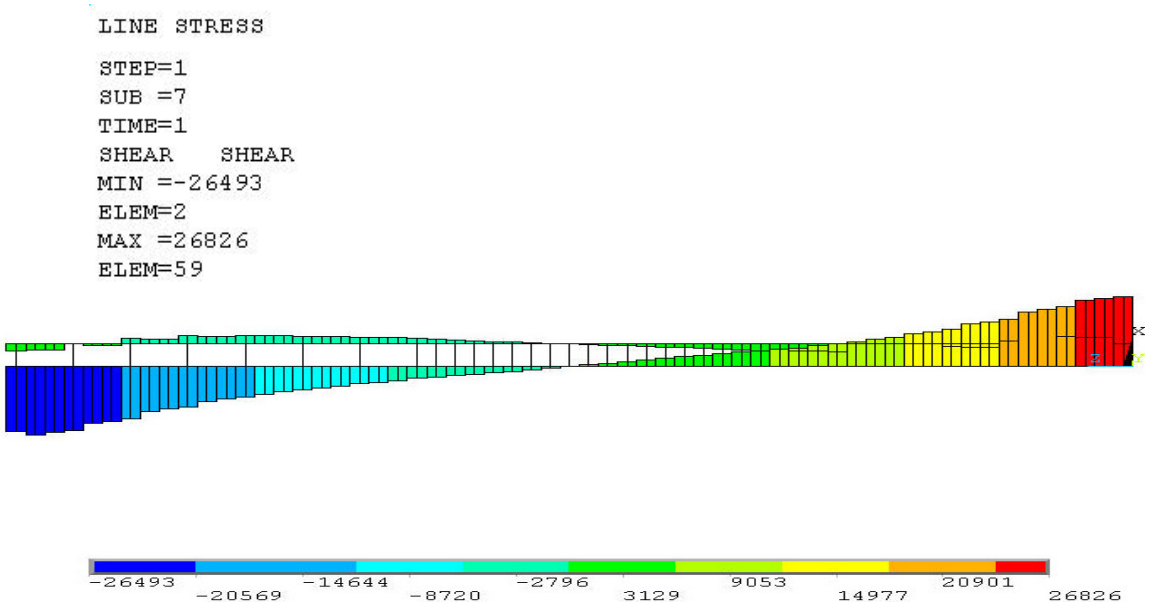

Figure 39 CBM1(III)A4 Shear

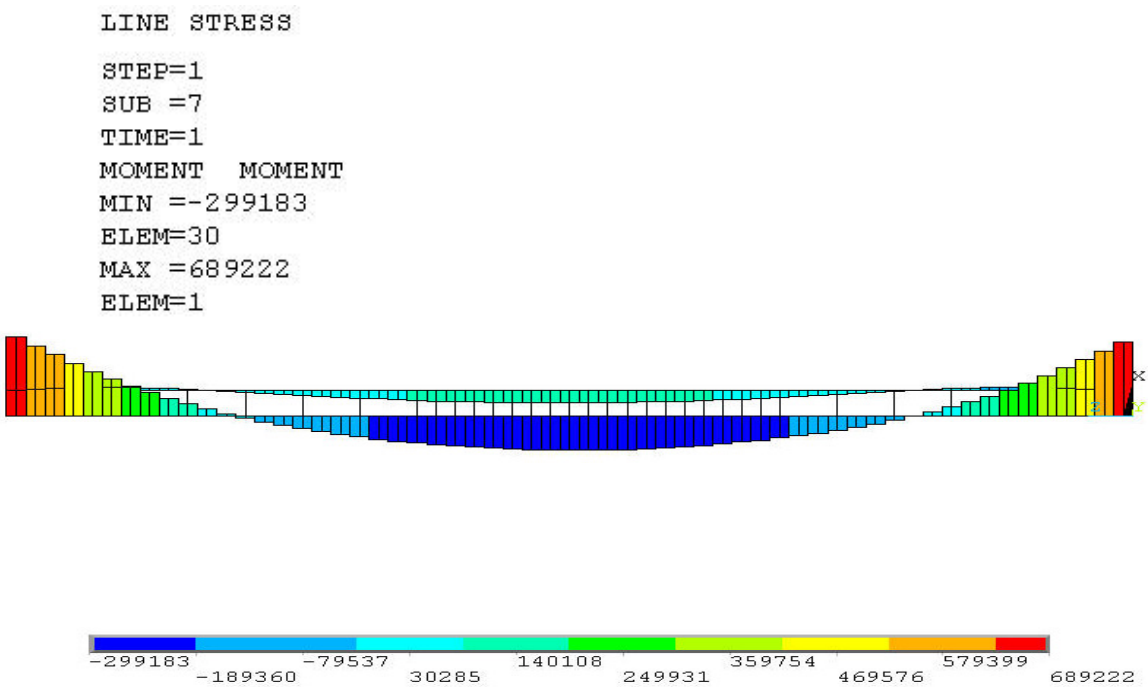

Figure 40 CBM1(III)A4 Moment

This graph (Figure 41)shows the results of a 2/3 reduction in the number of shear connectors in the middle of the beam with one curve and the results of a 2/3 reduction atg the end spans in another curve. There is not much change in the degree of deflection in any condition.

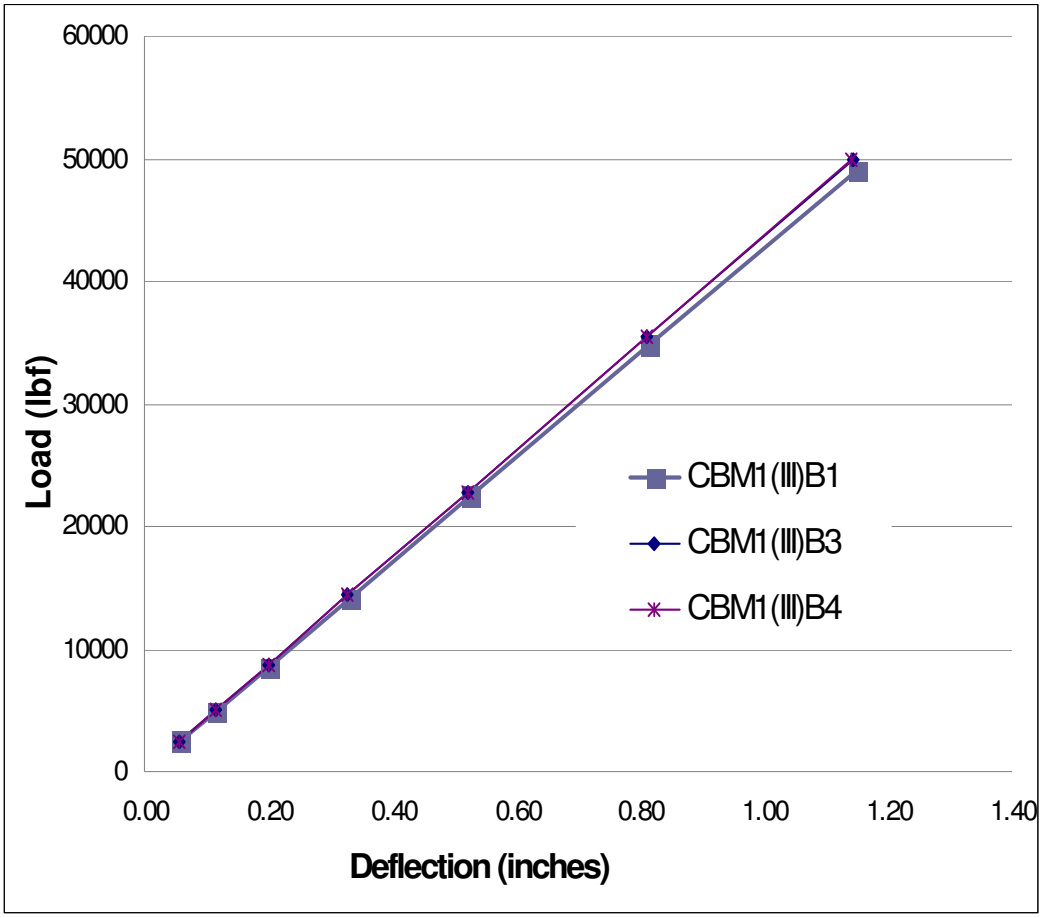

Figure 41 CBM1 Distributed and Two-Point Load Curves, Pinned Ends, Fully Composite and Partially Composite

The change in shear area was not enough to affect the load deflection curves shown in the graph (Figure 42). The curve showing the reduced shear connector area is based on the original shear connector area being reduced by 36%. The curve showing the increase shear connector area is base on the original shear connector area being increased by 300%.

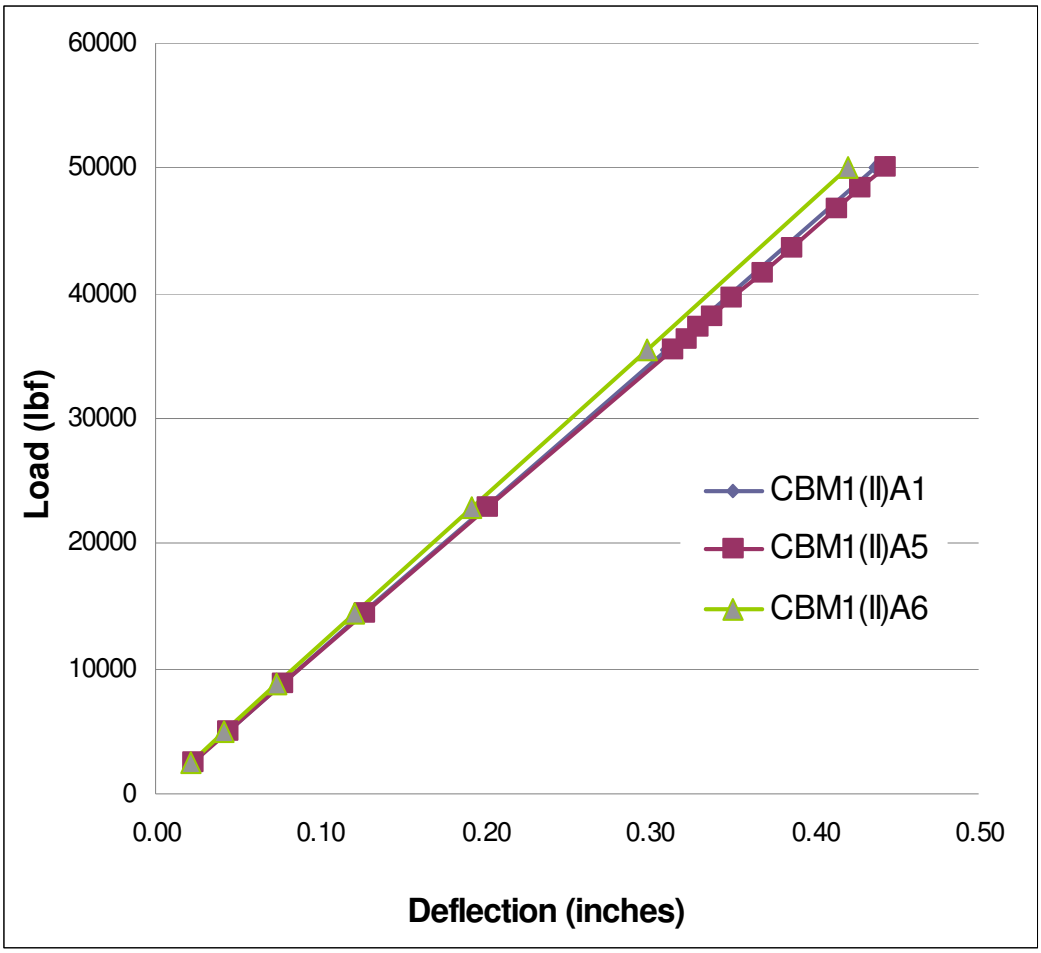

Figure 42 CBM1 Two-Point Load Curves, Fixed Ends, Fully Composite, Reduced and Increased Shear Connector Areas.

The change in shear area was not enough to affect the load deflection curves shown in the graph (Figure 43). The curve showing the reduced shear connector area is based on the original shear connector area being reduced by 36%. The curve showing the increase shear connector area is base on the original shear connector area being increased by 300%.

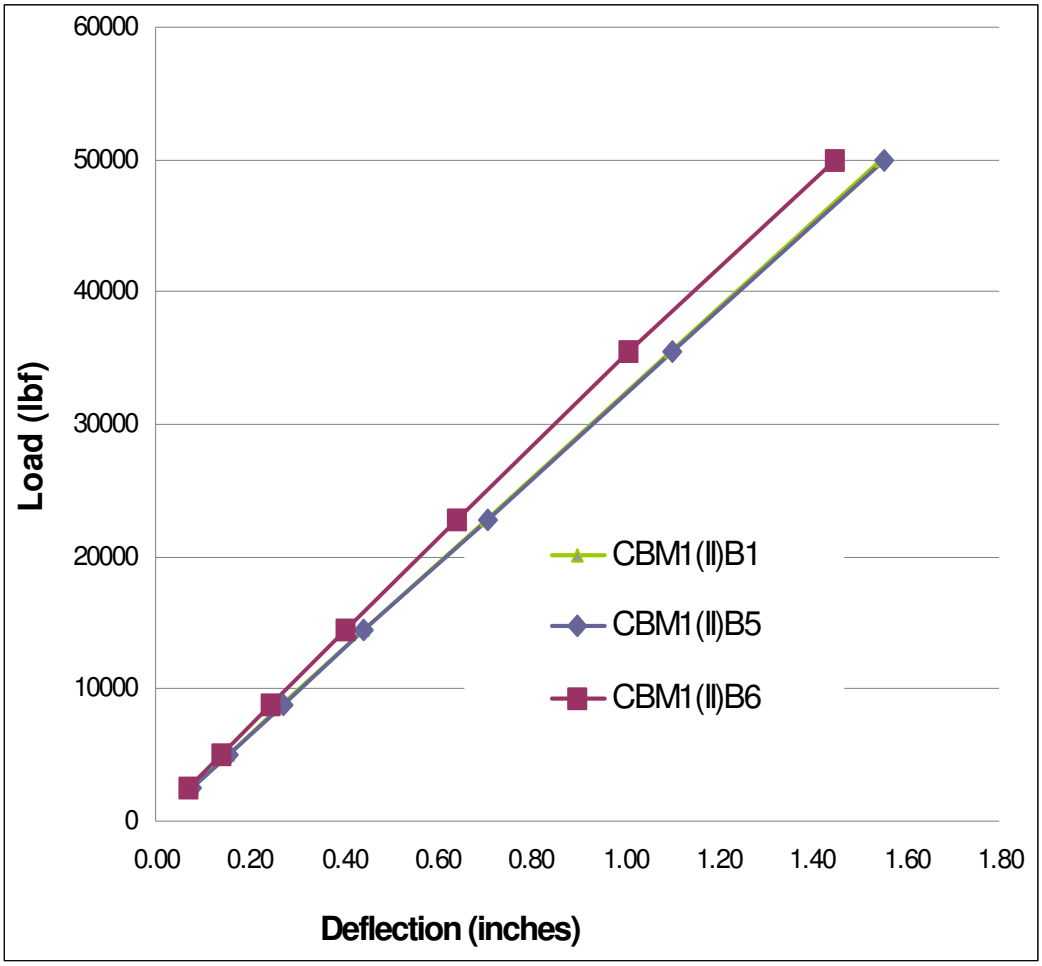

Figure 43 CBM1 Distributed Load Curves, Pinned Ends,
Fully Composite, Reduced and Increased Shear Connector Areas.

The change in shear area was not enough to affect the load deflection curves shown in the graph (Figure 44). The curve showing the reduced shear connector area is based on the original shear connector area being reduced by 36%. The curve showing the increase shear connector area is base on the original shear connector area being increased by 300%.

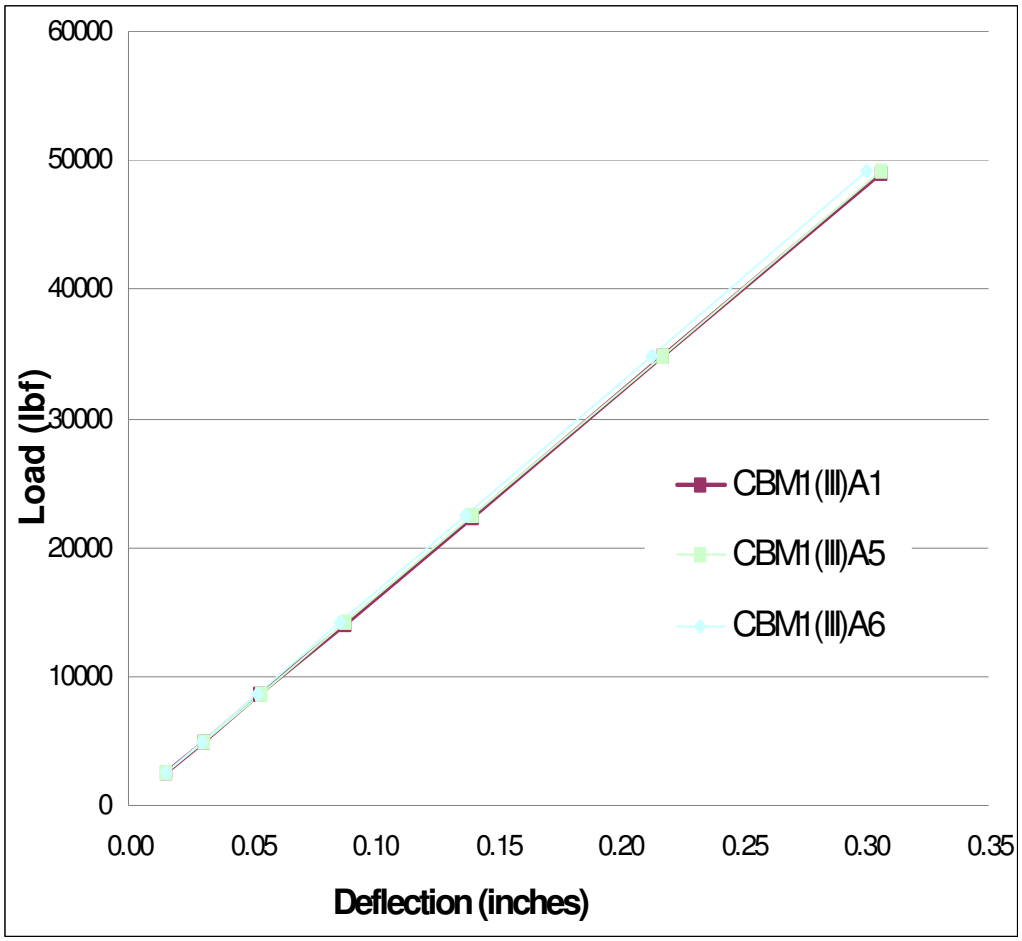

Figure 44 CBM1 Distributed Load Curves, Pinned Ends,
Fully Composite, Reduced and Increased Shear Connector Areas.

The change in shear area was not enough to affect the load deflection curves shown in the graph (Figure 45). The curve showing the reduced shear connector area is based on the original shear connector area being reduced by 36%. The curve showing the increase shear connector area is base on the original shear connector area being increased by 300%.

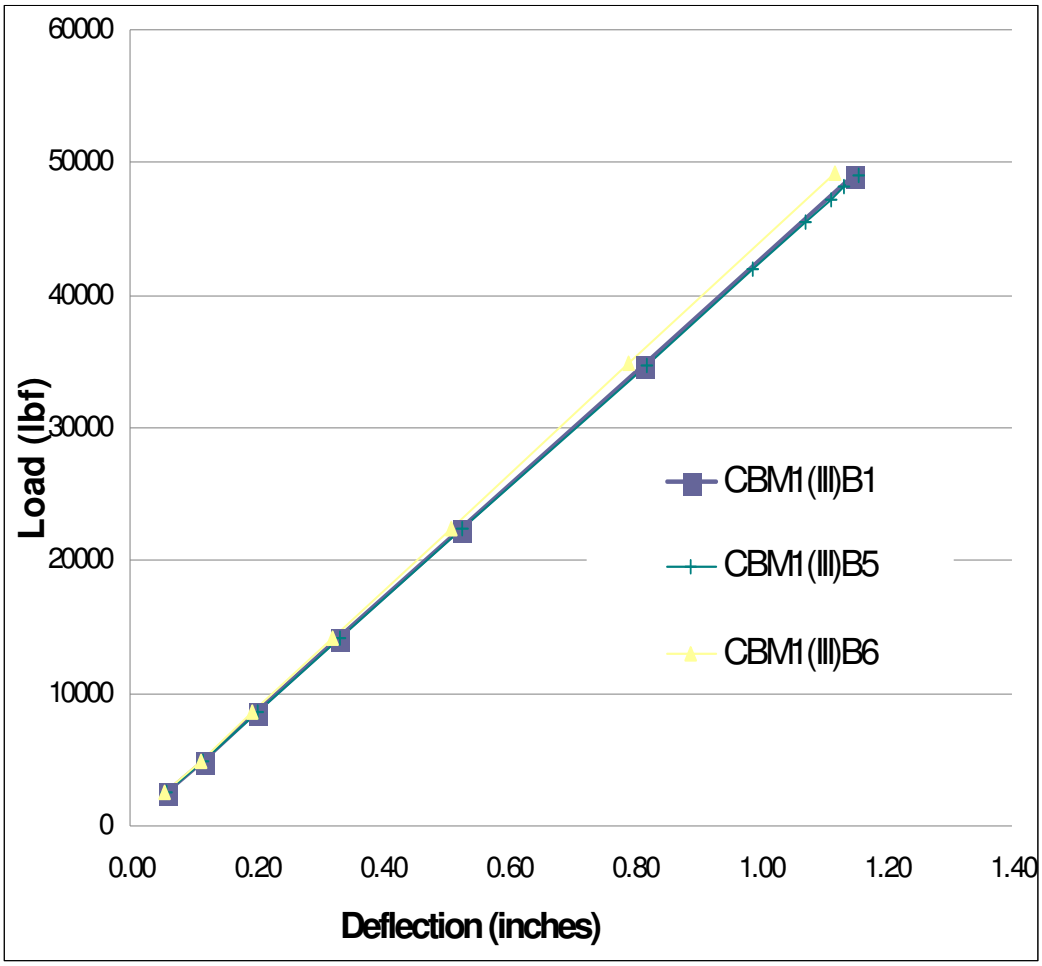

Figure 45 CBM1 Distributed Load Curves, Pinned Ends,
Fully Composite, Reduced and Increased Shear Connector Areas.

The curves in the graph indicate and increased slab thickness stiffens the composite section. The slab was thickened by 50% over the original slab thickness in model from which the curves are derived (Figure 46).

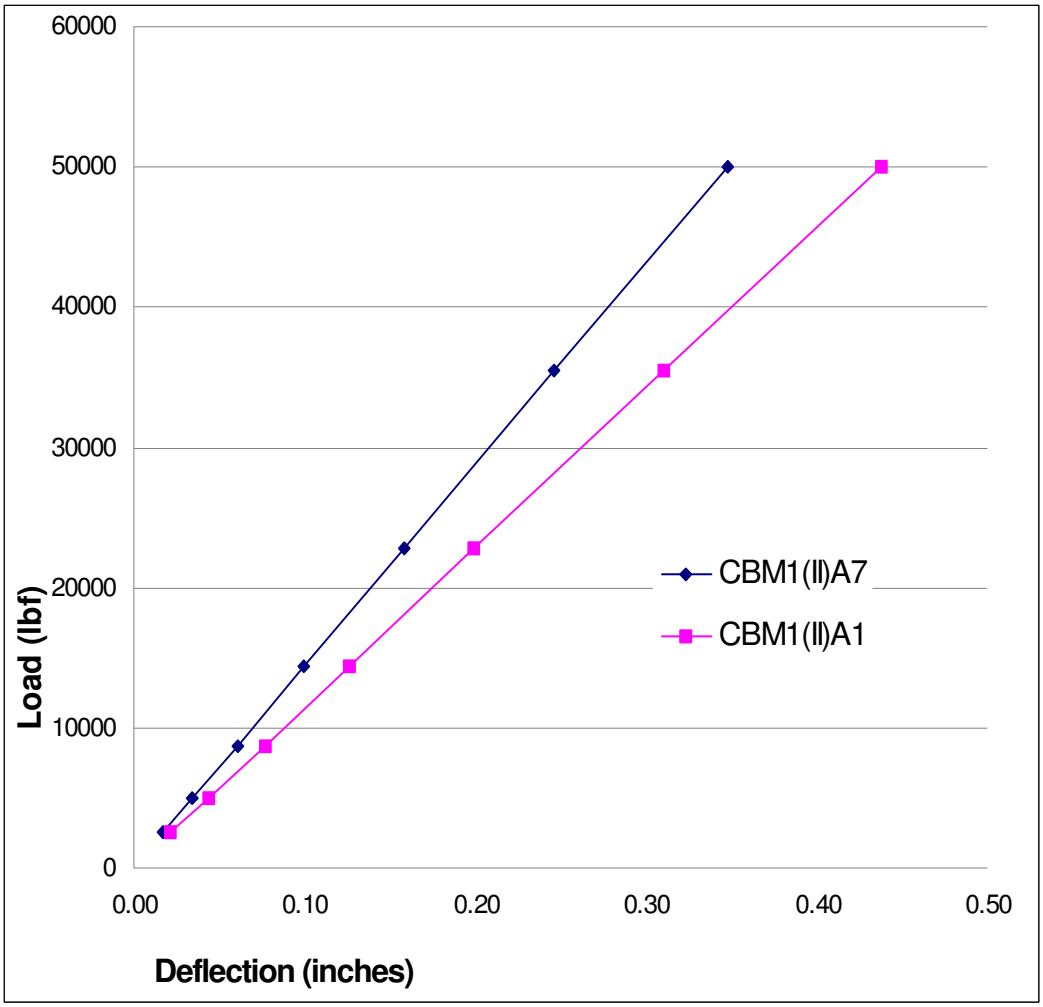

Figure 46 CBM1 Two-Point Load Curves, Fixed Ends, Fully Composite, Thickened Slab.

The curves in the graph indicate and increased slab thickness stiffens the composite section. The slab was thickened by 50% over the original slab thickness in model from which the curves are derived (Figure 47).

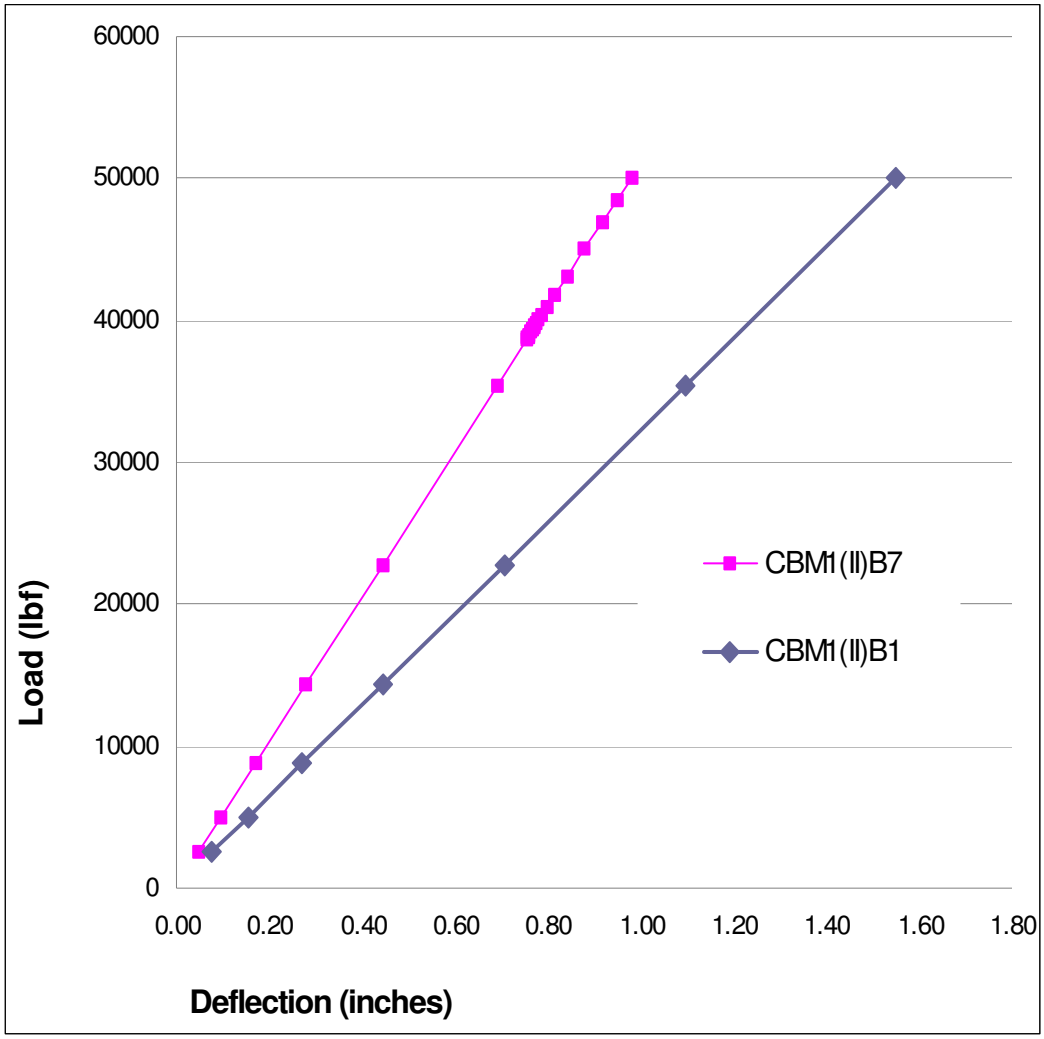

Figure 47 CBM1 Distributed Load Curves, Pinned Ends, Fully Composite, Thickened Slab.

The curves in the graph indicate and increased slab thickness stiffens the composite section. The slab was thickened by 50% over the original slab thickness in model from which the curves are derived (Figure 48)

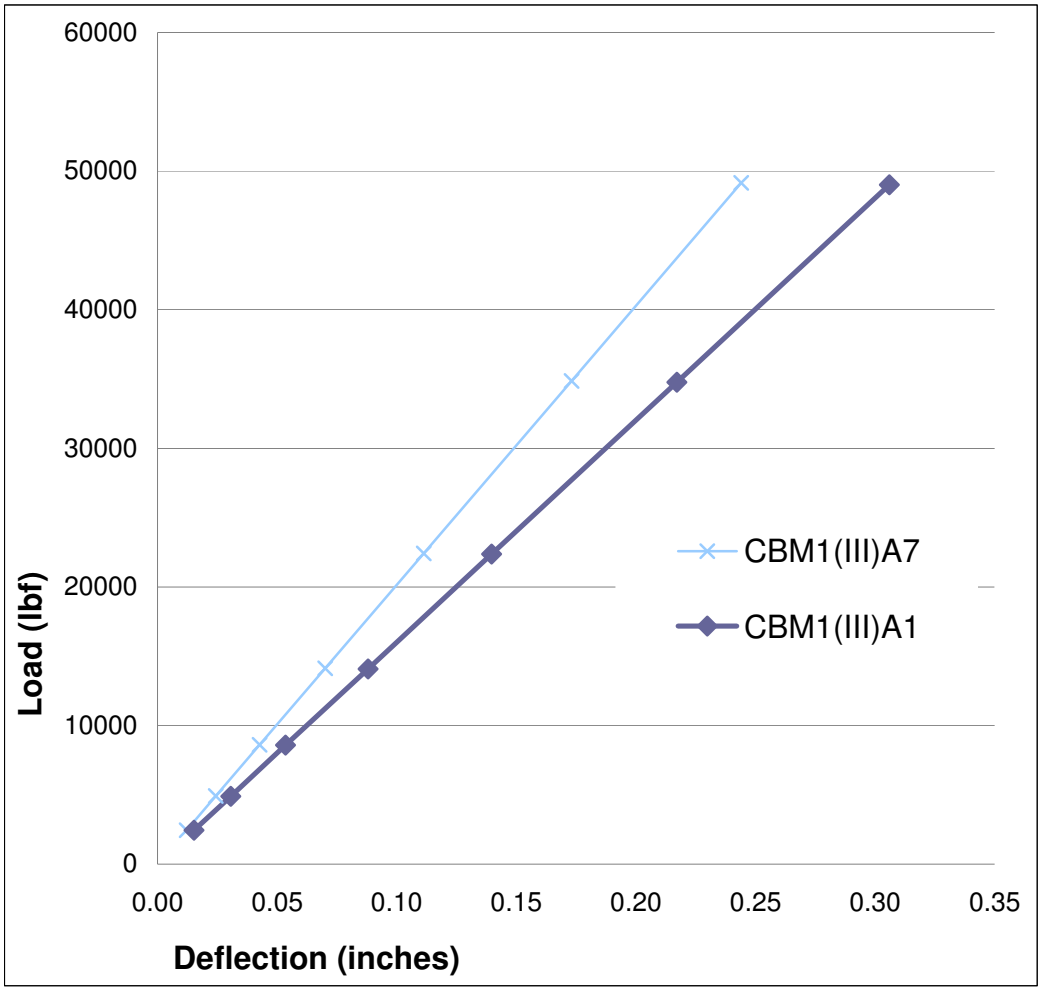

Figure 48 CBM1 Distributed Load Curves, Fixed Ends, Fully Composite, Thickened Slab.

The curves in the graph indicate and increased slab thickness stiffens the composite section. The slab was thickened by 50% over the original slab thickness in model from which the curves are derived (Figure 49).

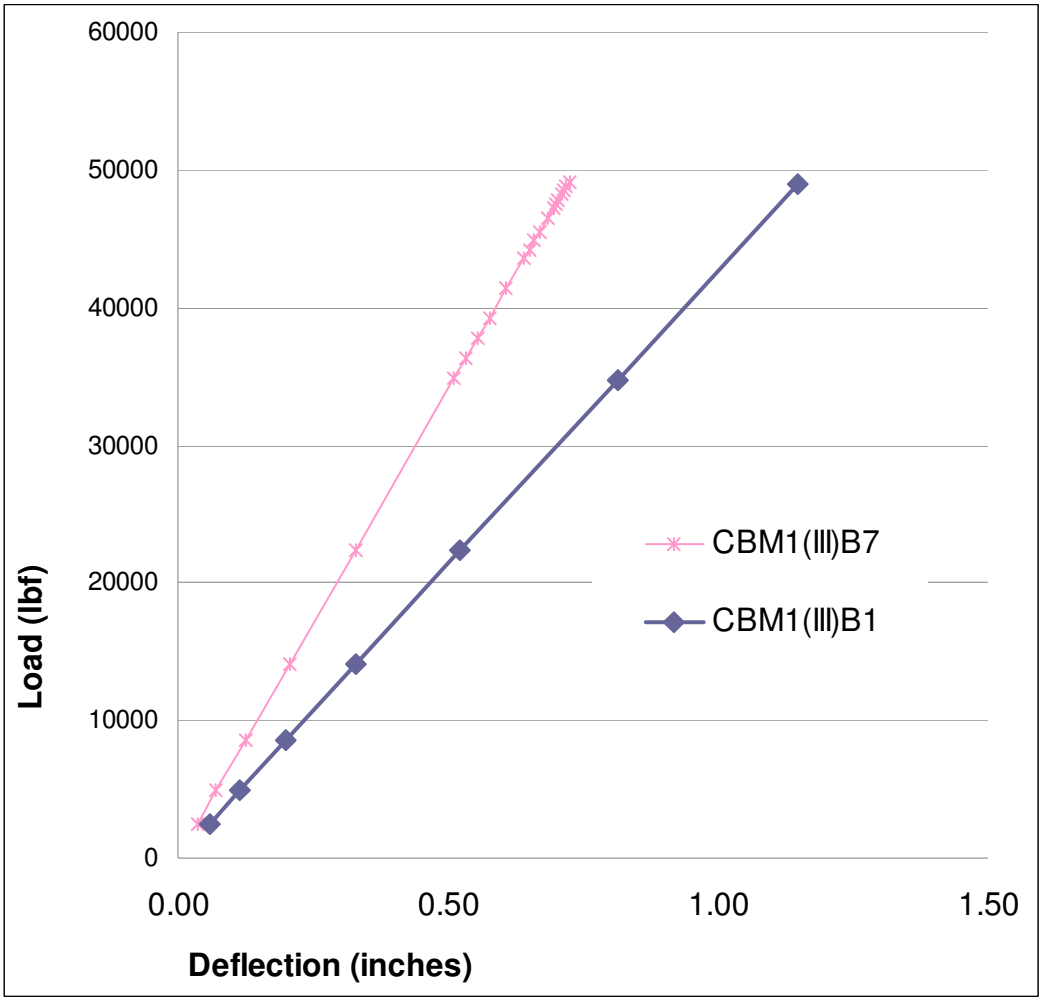

Figure 49 CBM1 Two-Point Load Curves, Pinned Ends, Fully Composite, Thickened Slab.

4.3 CBM2 Results

Calculations of the CBM2 composite section indicate the section is not fully composite. Note, the PNA, and the stress block, "a", are located in the WF section, which indicates the slab and WF section are not acting a together as a composite section (Figure 50). The stress distribution also indicates the section is not acting in a composite manner (Figure 51).

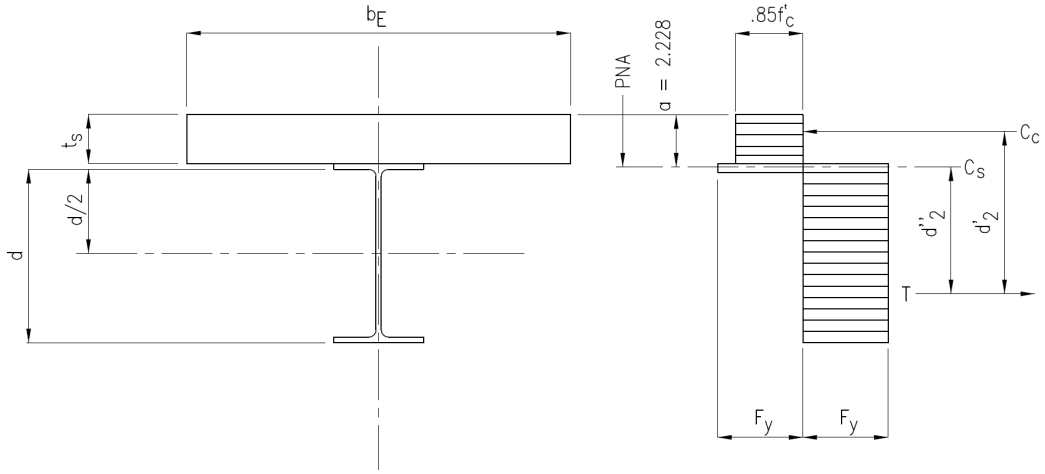

Figure 50 CBM2 Location of Plastic Neutral Axis and Concrete Stress Block.

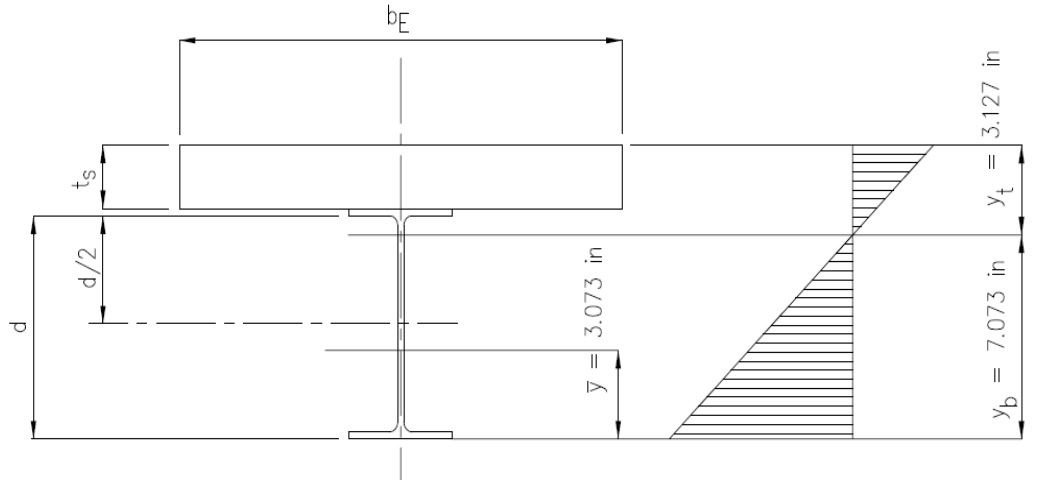

Figure 51 CBM2 Stress Distribution

The end condition in the full composite section has an impact on the amount of deflection (Figure 52). The fixed end condition deflects less than the pinned condition. The shear (Figure 53) and moment (Figure 54) diagrams of the fully composite section provide a means of comparing the effects of reducing the number of studs at the mid span and end spans of the beam with the fully composite section.

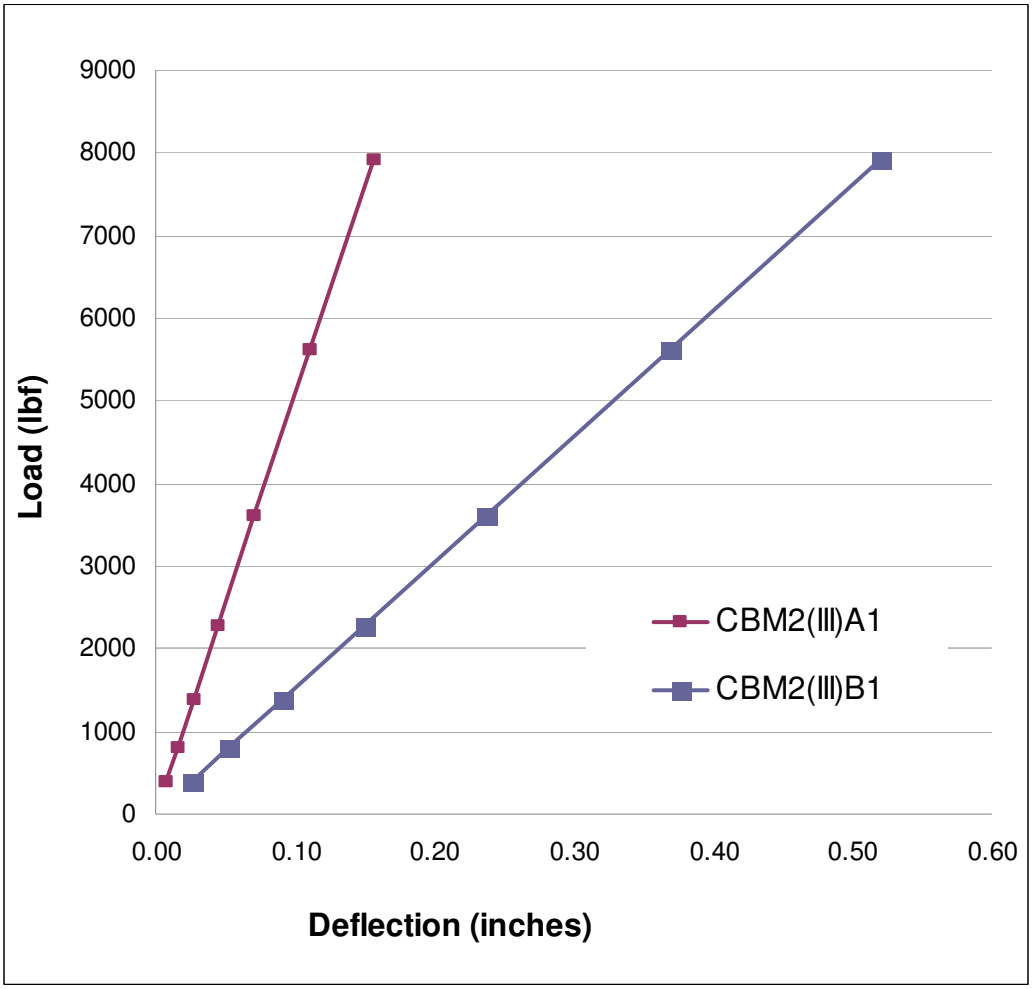

Figure 52 CBM2 Distributed Load, Fully Composite, Pinned and Fixed Ends.

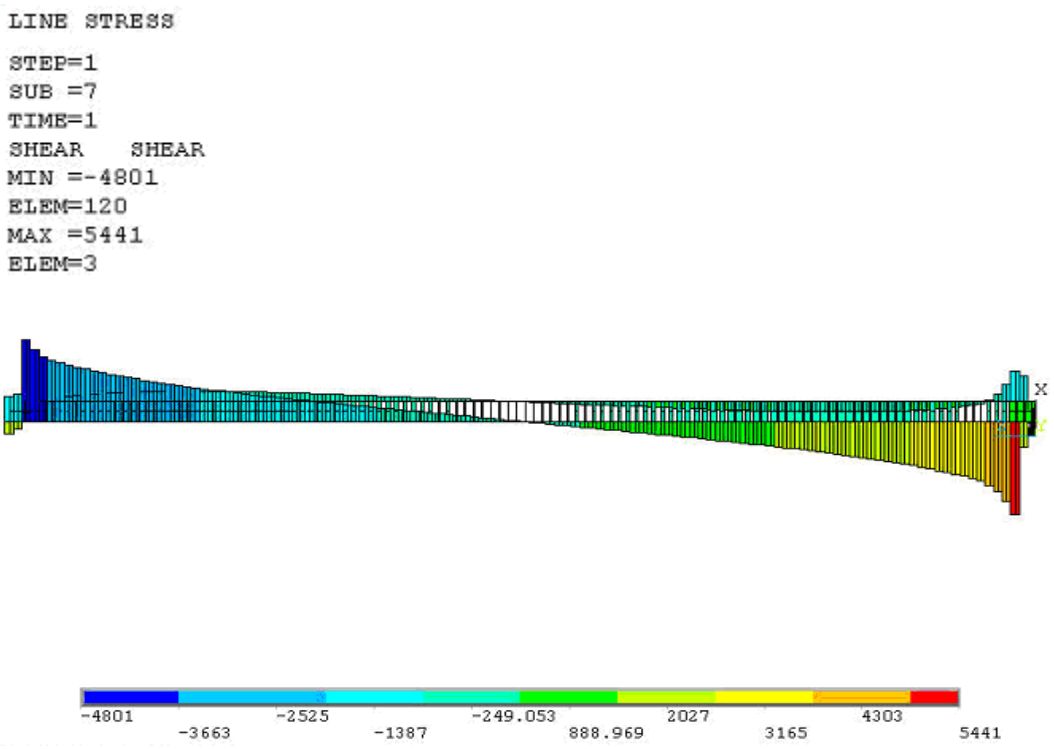

Figure 53 CBM2(III)A1 Shear Diagram

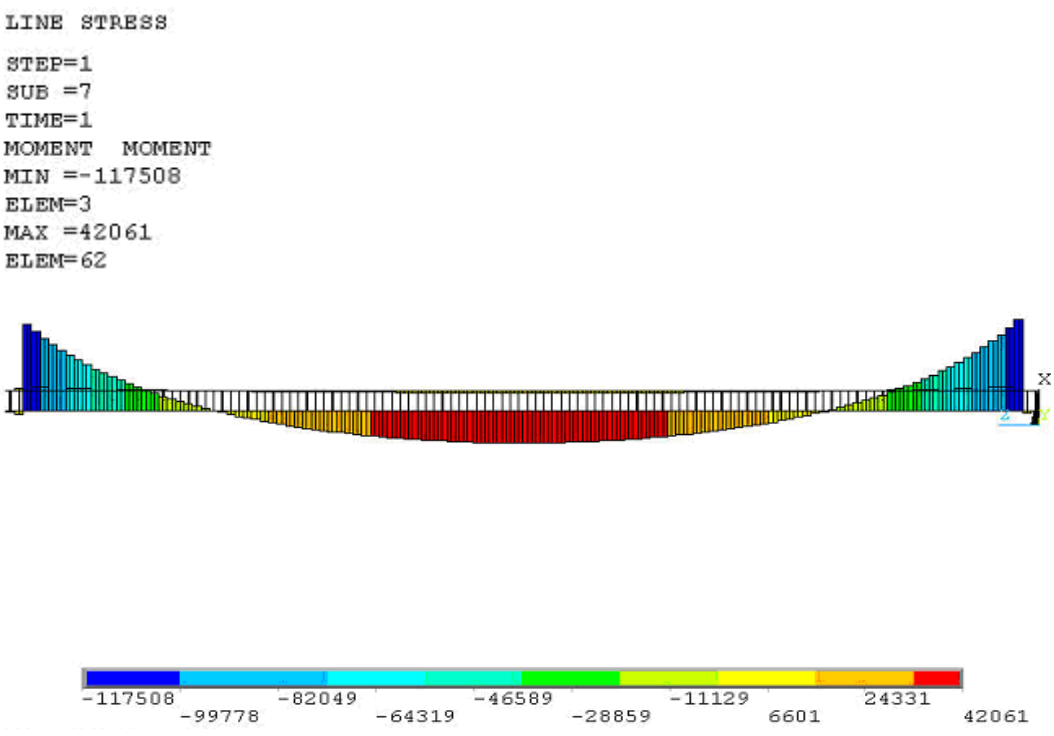

Figure 54 CBM2(III)A1 Moment Diagram

The end condition is a consistent factor in the degree of deflection, be it the two-point load condition or the distributed load condition (Figure 55).

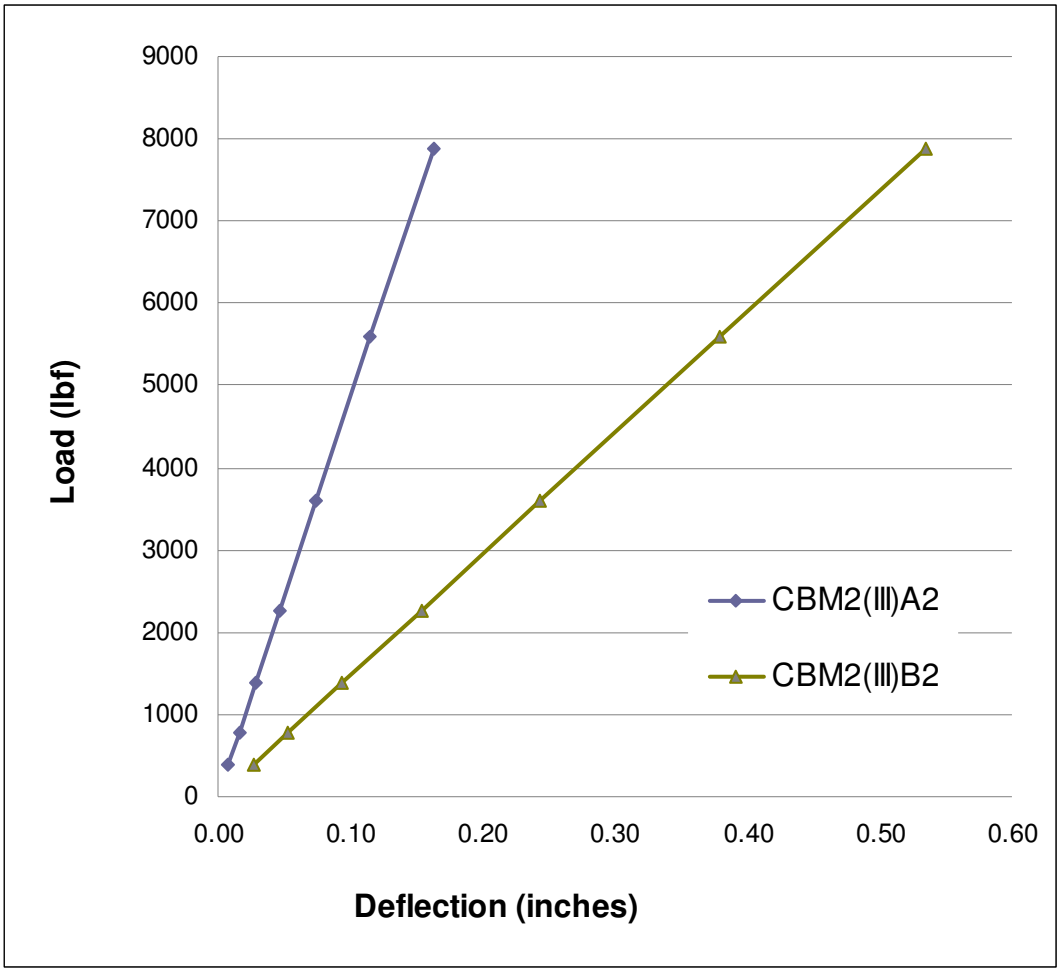

Figure 55 CBM2 Distributed Load, Partially Composite, Pinned and Fixed Ends.

A comparison of the partially composite section with the fully composite section indicates the partially composite section will deflect more due to the fewer number of shear connectors. A 1/3 reduction in shear connectors over the length of the composite beam does not yield a great degree of difference though (Figure 56).

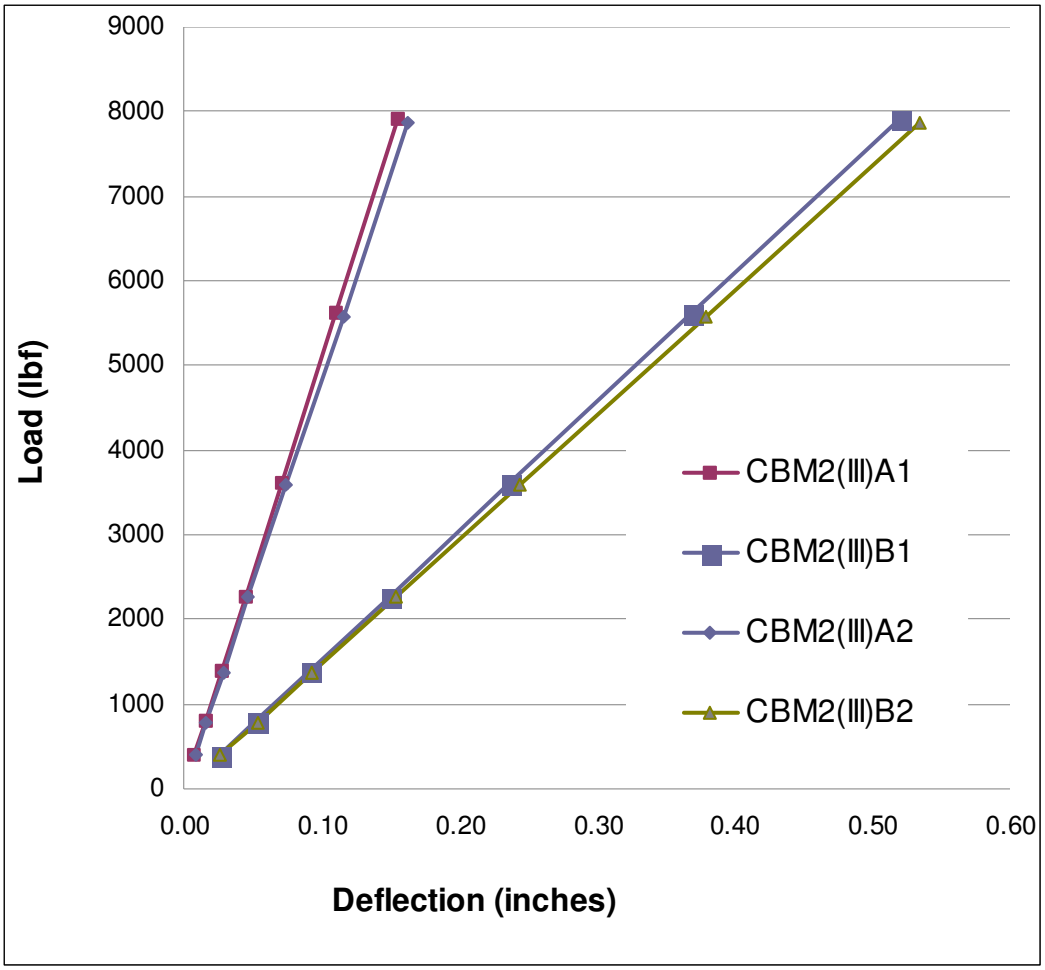

Figure 56 CBM2 Comparison of Fully and Partially Composite Models

The curves of the partially composite mid span (Figure 57) area a close match the fully composite section. The shear (Figure 58) and moment (Figure 59) diagrams of the partially composite section provide a means of comparing the effects of reducing the number of studs at the mid span with the fully composite section.

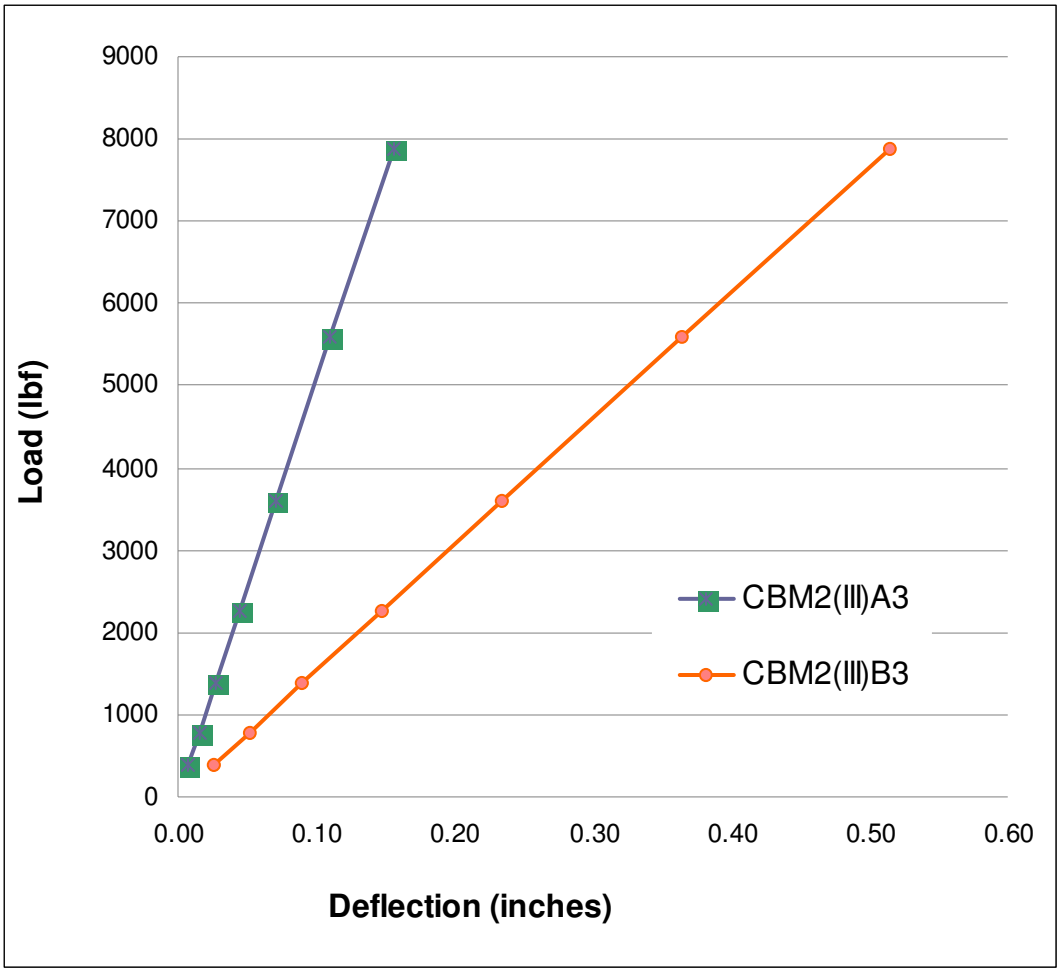

Figure 57 CBM2 Distributed Load, Partially Composite at Mid Span, Pinned and Fixed Ends.

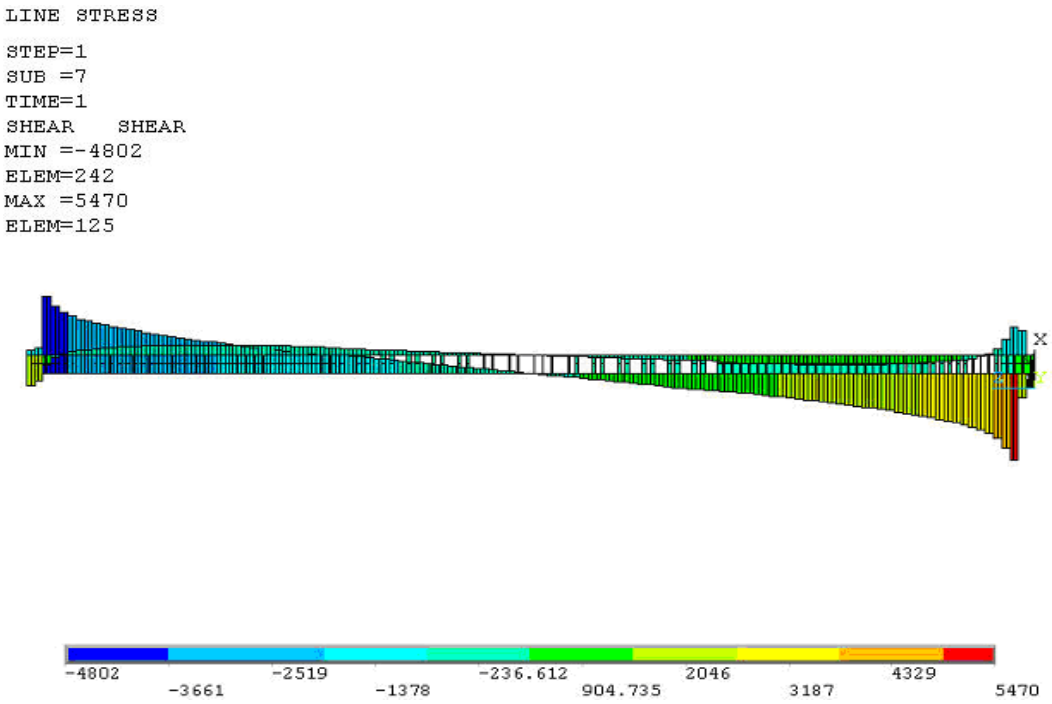

Figure 58 CBM2(III)A3 Shear Diagram

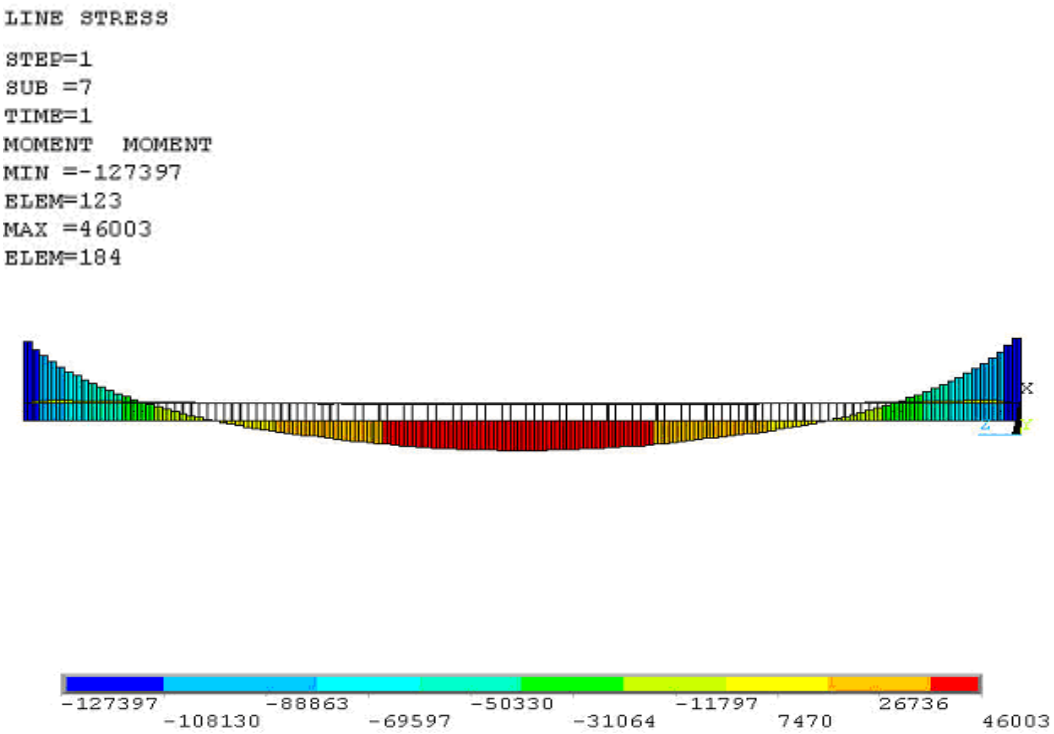

Figure 59 CBM2(III)A3 Moment Diagram

The curves of the partially composite end spans (Figure 60) are also a close match the fully composite section. The shear (Figure 61) and moment (Figure 62) diagrams of the partially composite section provide a means of comparing the effects of reducing the number of studs at the end spans with the fully composite section.

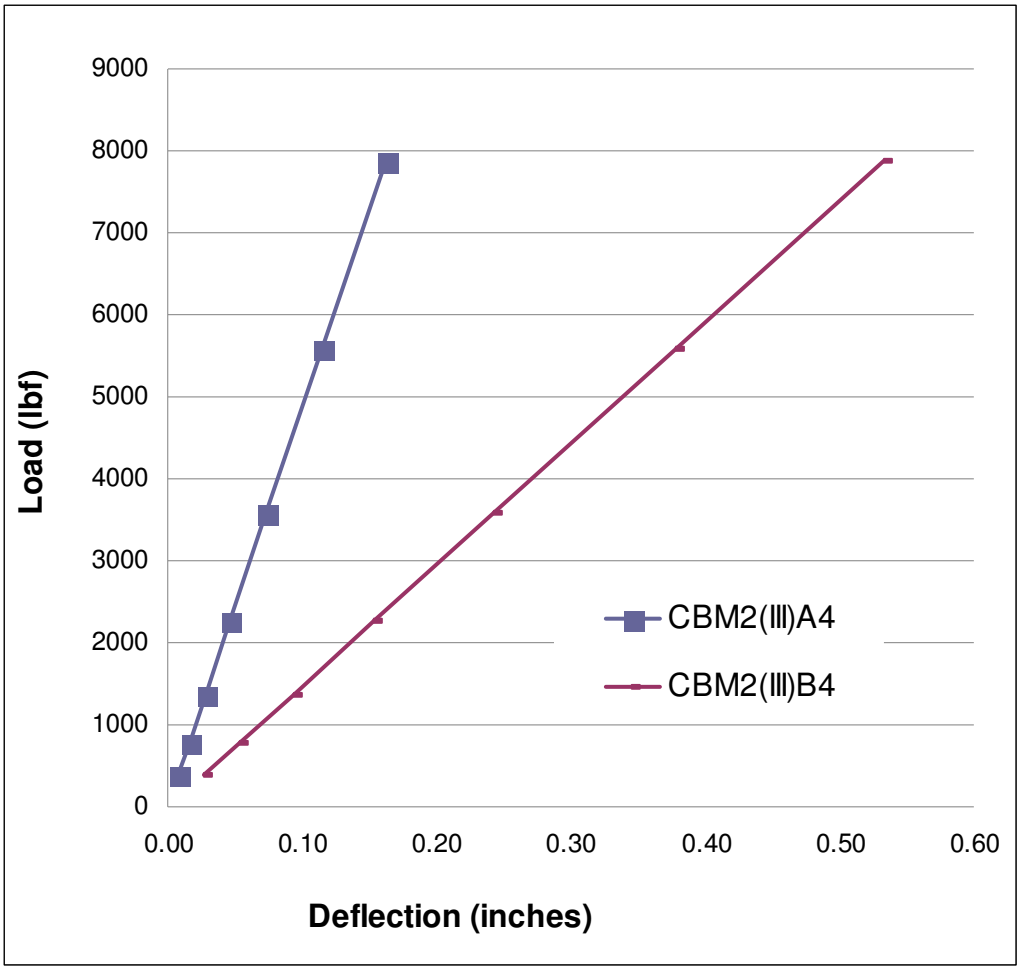

Figure 60 CBM2 Distributed Load, Partially Composite at End Spans, Pinned and Fixed Ends.

.

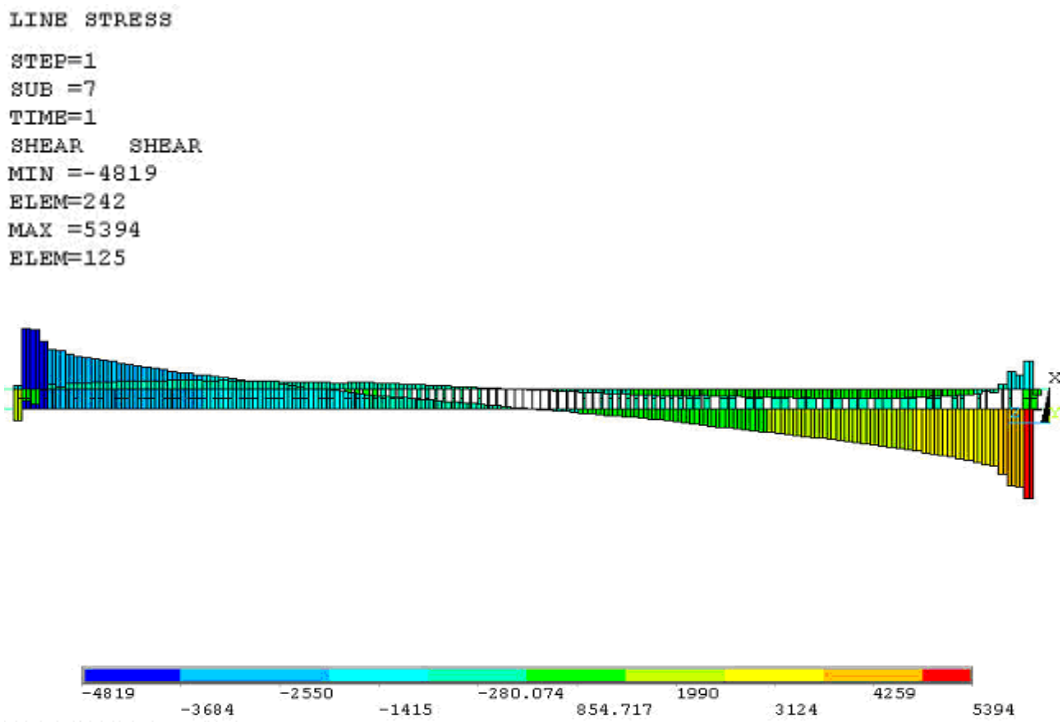

Figure 61 CBM2(III)A4 Shear Diagram

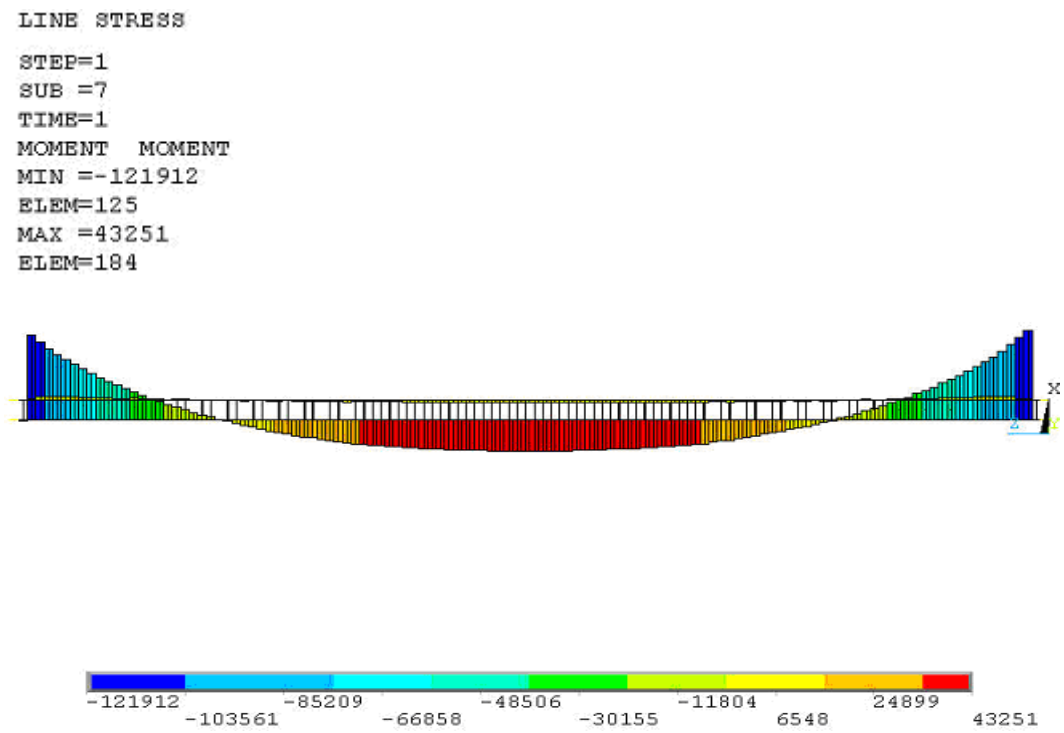

Figure 62 CBM2(III)A4 Moment Diagram

A comparison of the mid span partially composite section and end spans partially composite sections with the fully composite section does not indicate much difference in the amount of deflection (Figure 63). Even though the number of shear connectors was reduced at either the mid span or beam end spans; the remaining shear connectors prevented large deflections.

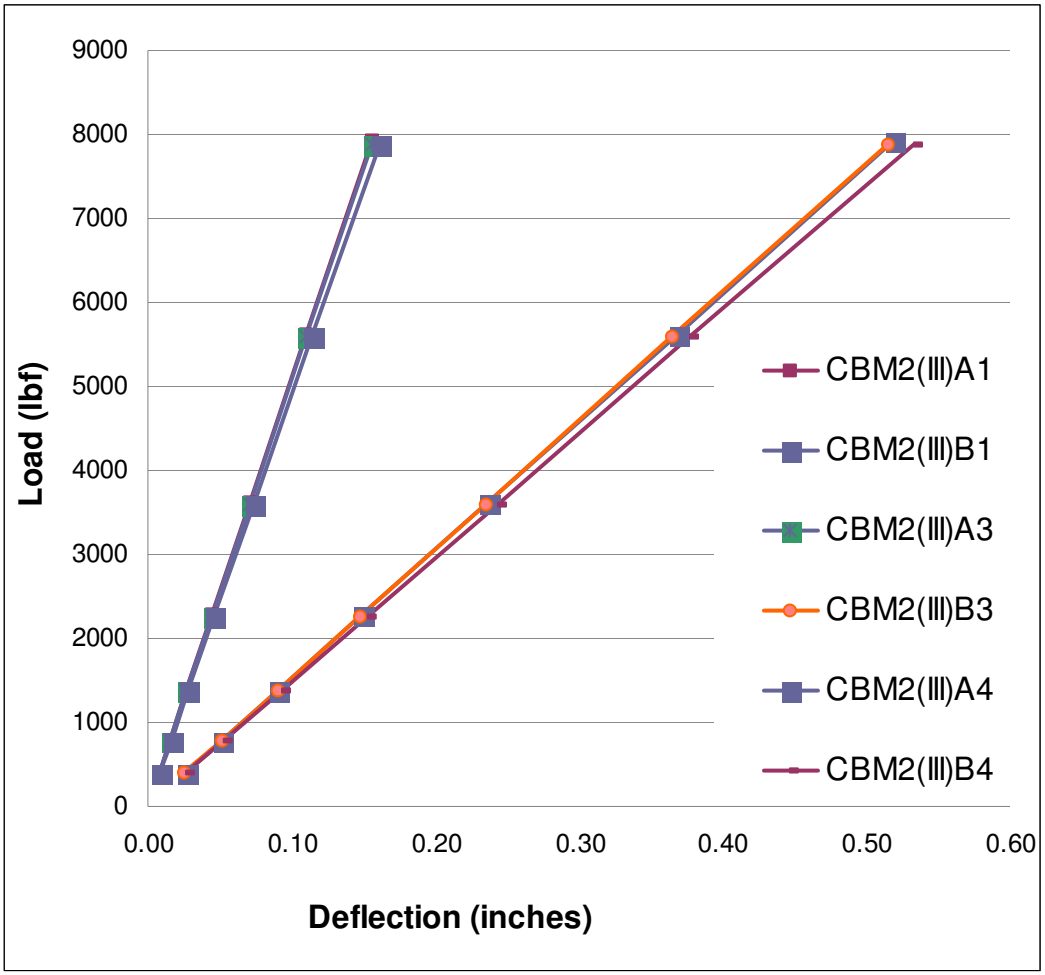

Figure 63 CBM2 Comparison of Fully and Partially Composite Beams

A decrease in the shear area results in a greater amount of deflection (Figure 64).

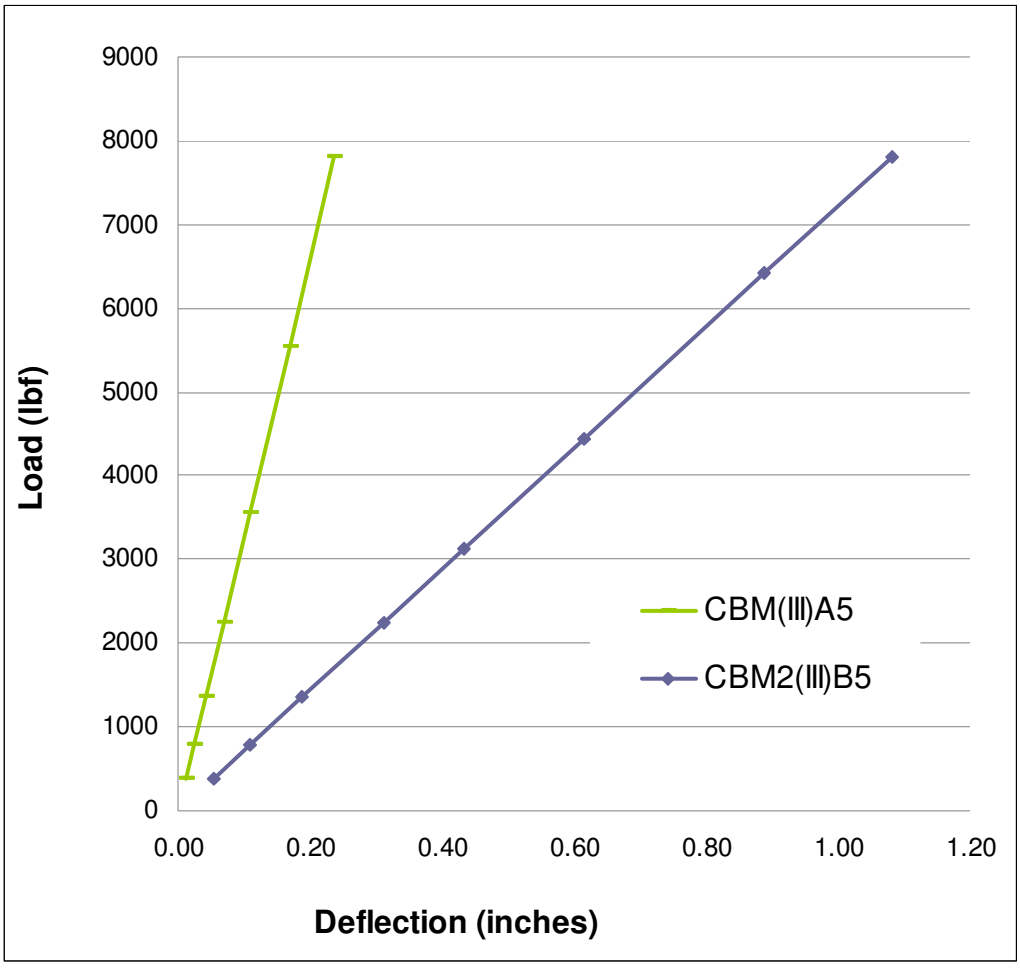

Figure 64 CBM2 Distributed Load, Fully Composite, Reduced Shear Area, Pinned and Fixed Ends.

An increase in the shear area results in less deflection (Figure 65)

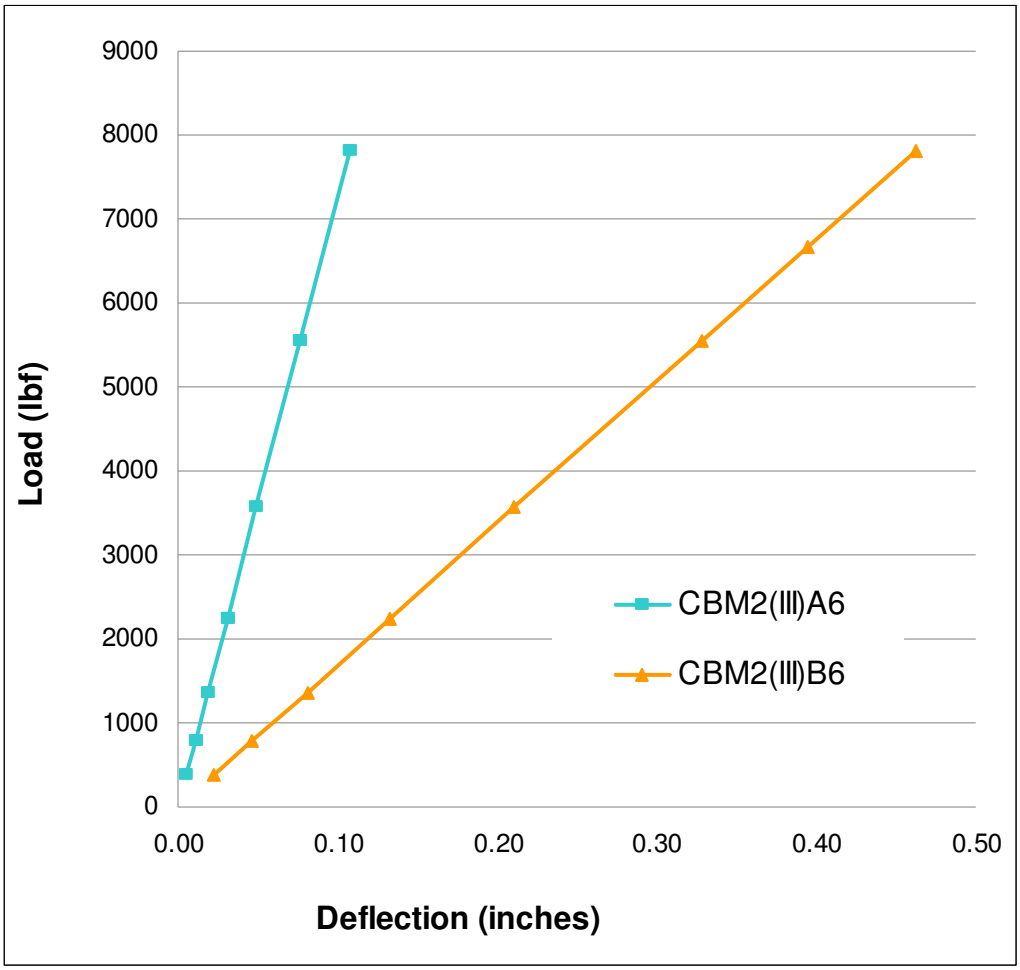

Figure 65 CBM2 Distributed Load, Fully Composite, Increased Shear Area, Pinned and Fixed Ends.

A comparison of the original shear areas with the modified shear areas makes the results more apparent (Figure 66). The results may be summed up: more shear connector area results in less deflection; less shear area results in more deflection. The curves showing the reduced shear connector area is based on the original shear connector area being reduced by 91%. The curve showing the increase shear connector area is base on the original shear connector area being increased by 800%.

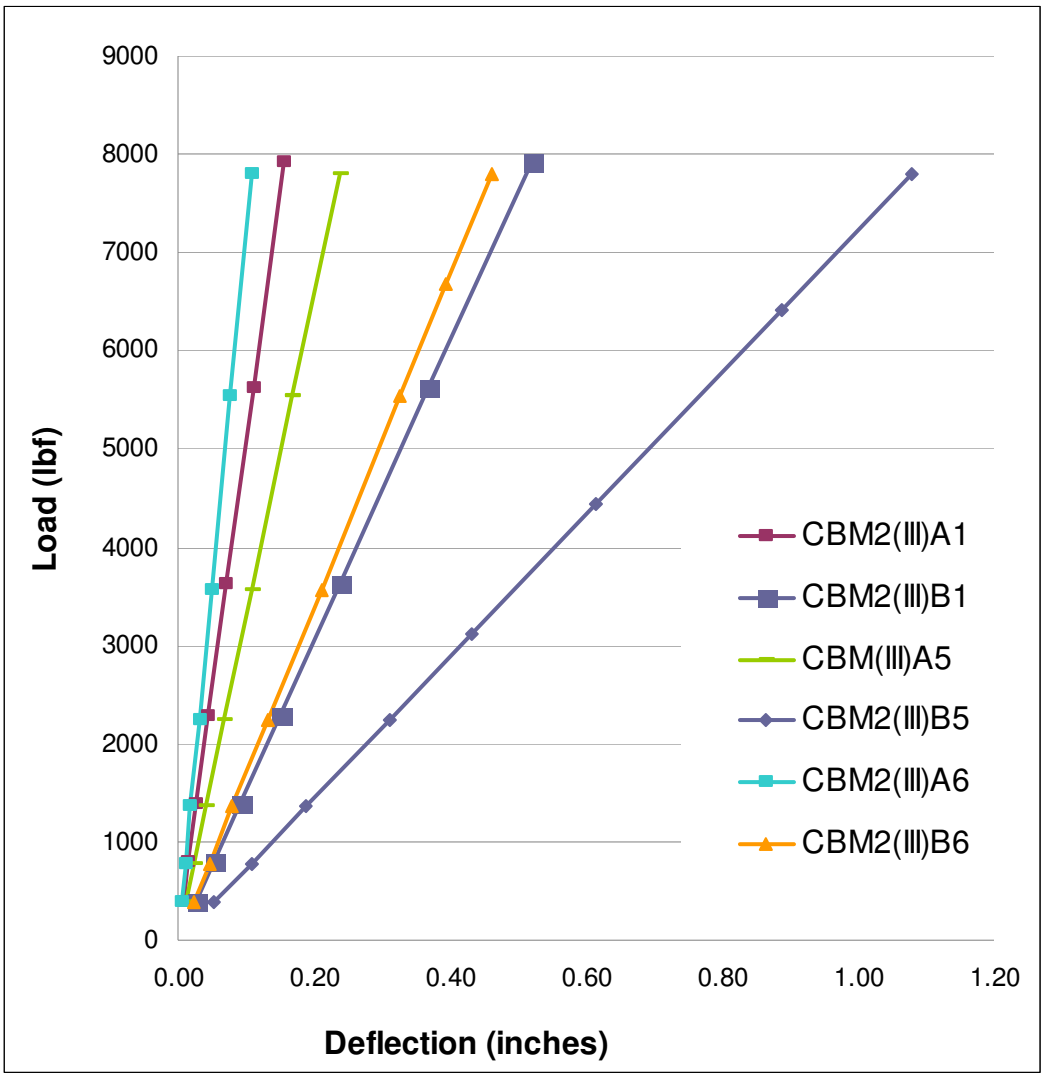

Figure 66 CBM2 Comparison of Shear Connector Areas

The curves in the graph indicate and increased slab thickness stiffens the composite section (Figure 67).

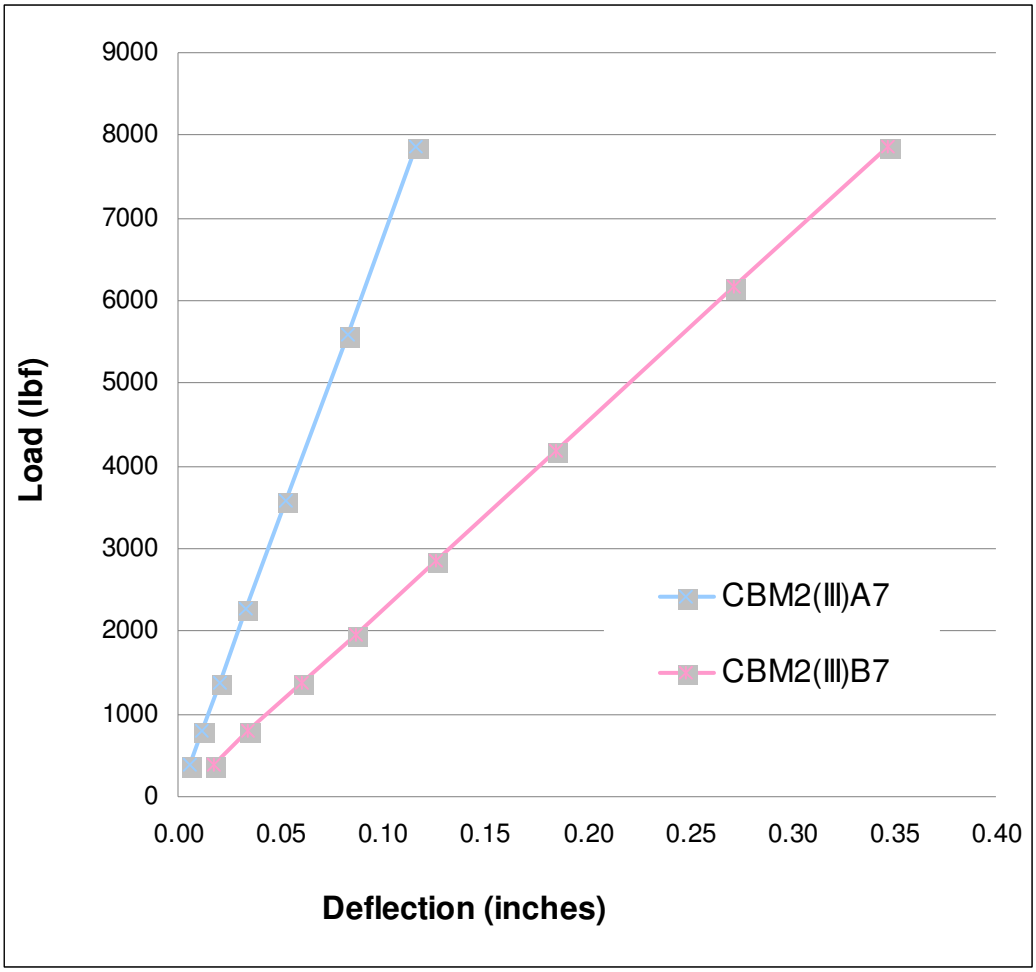

Figure 67 CBM2 Distributed Load, Fully Composite, Increased Slab Thickness, Pinned and Fixed Ends

A comparison of the original slab thickness with an increased slab thickness makes the results of a thicker slab more apparent (Figure 68). In both end conditions a thicker slab resulted in less deflection. The curves in the graph indicate and increased slab thickness stiffens the composite section. The slab was thickened by 100% over the original slab thickness in model from which the curves are derived.

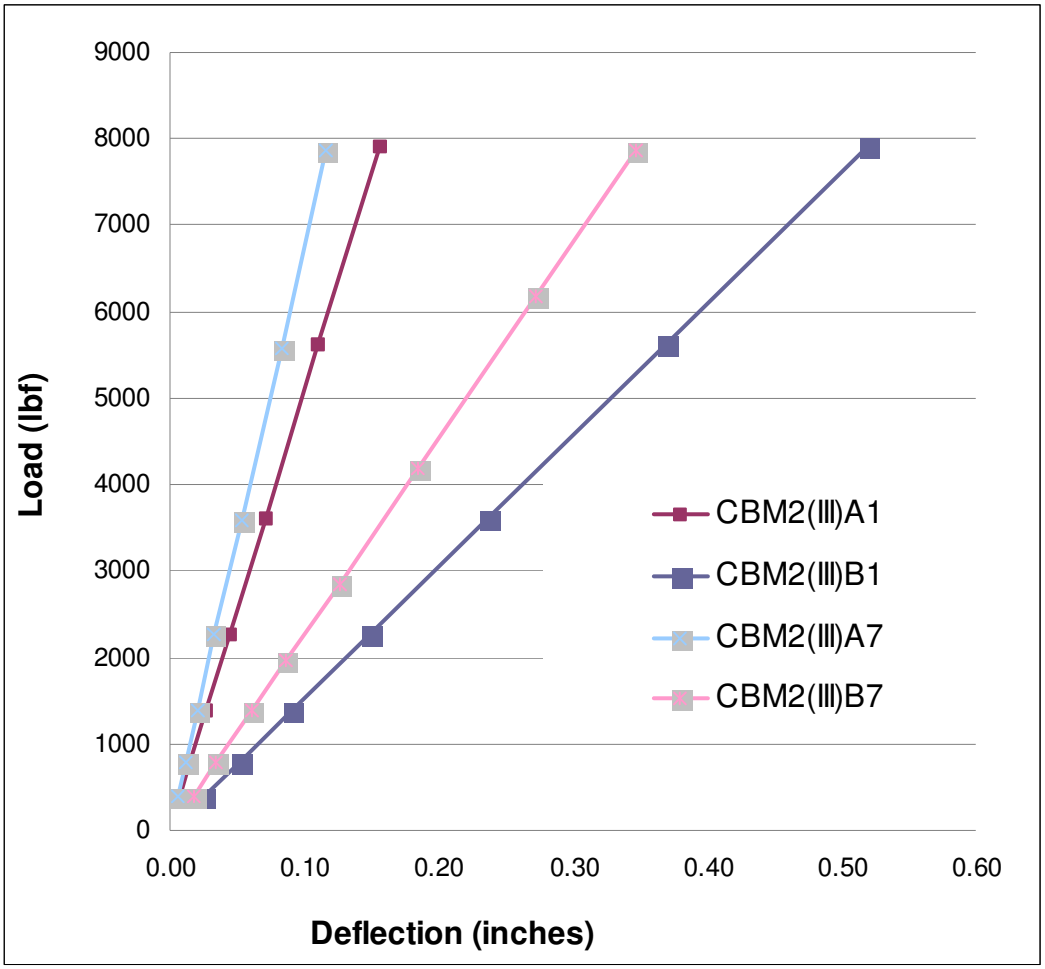

Figure 68 CBM2 Comparison of Slab Thickness

4.4 CBM3 Results

Calculations of the CBM3 composite section indicate the section is fully composite. Note, the PNA, and the stress block, "a", are located in the slab, which indicates the slab and WF section are acting a together as a composite section (Figure 69). The stress distribution also indicates the section is acting in a composite manner (Figure 70).

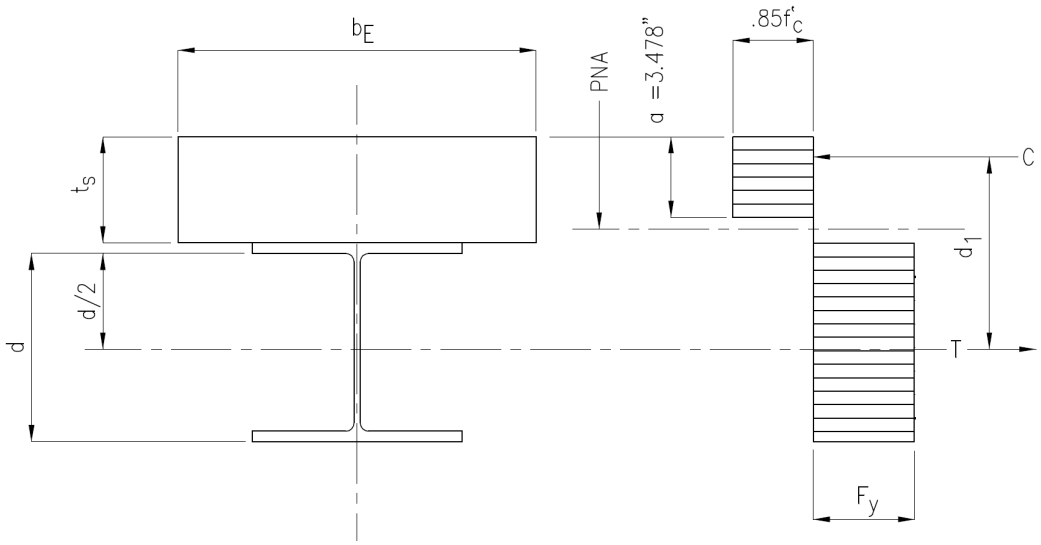

Figure 69 CBM3 Location of Plastic Neutral Axis and Concrete Stress Block.

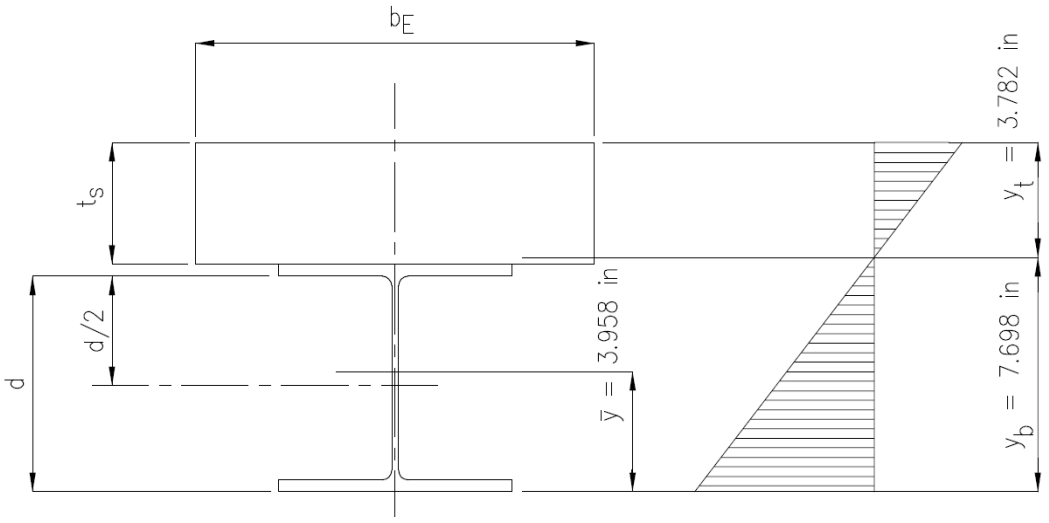

Figure 70 CBM3 Stress Distribution

The end condition in the full composite section has an impact on the amount of deflection (Figure 71). The fixed end condition deflects less than the pinned condition. The shear (Figure 72) and moment (Figure 73) diagrams of the fully composite section provide a means of comparing the effects of reducing the number of studs at the mid span and end spans of the beam with the fully composite section.

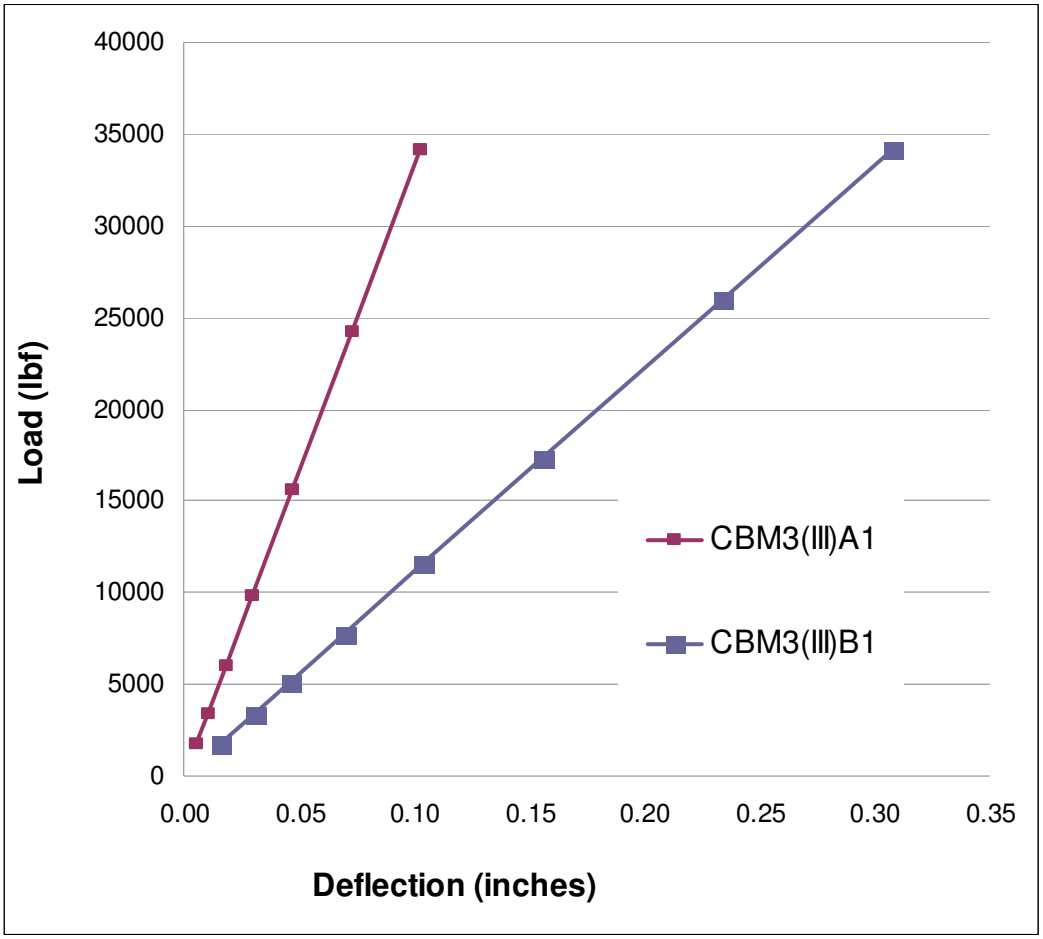

Figure 71 CBM3 Distributed Load, Fully Composite, Pinned and Fixed Ends.

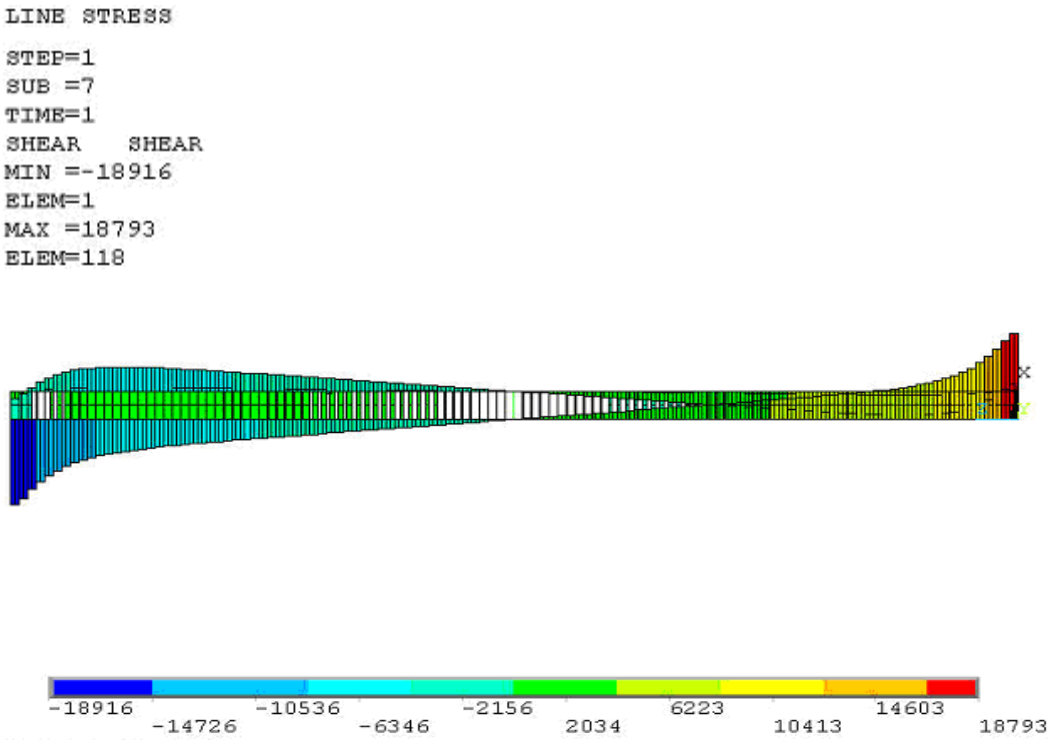

Figure 72 CBM3(III)A1 Shear Diagram

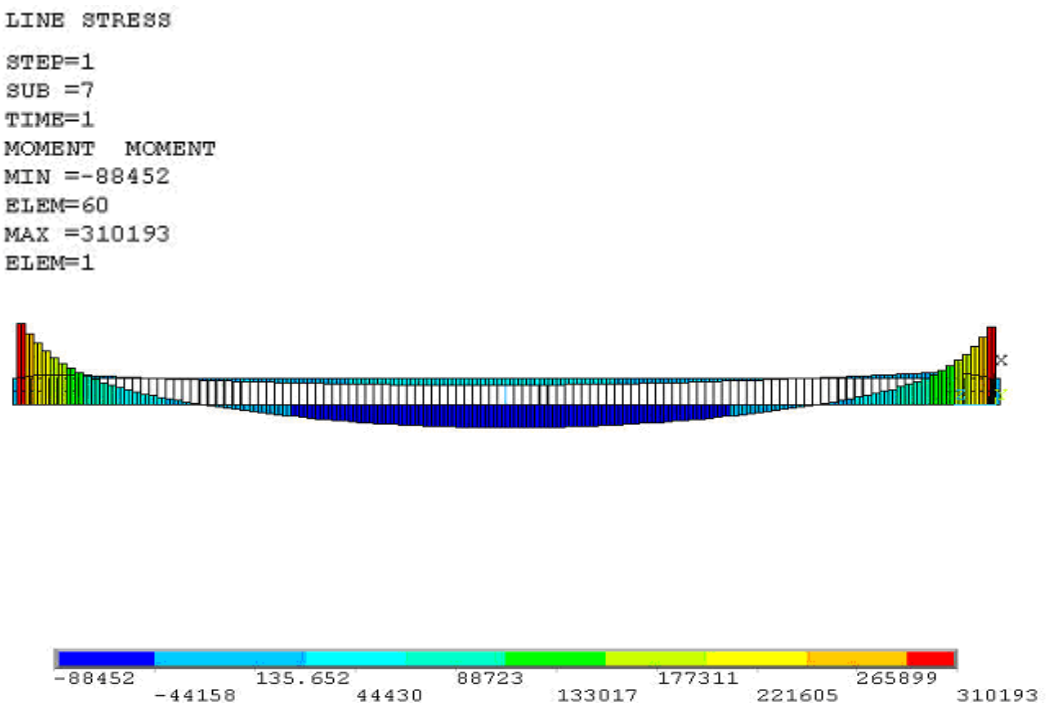

Figure 73 CBM3(III)A1 Moment Diagram

The end condition is a consistent factor in the degree of deflection, be it the two-point load condition or the distributed load condition (Figure 74).

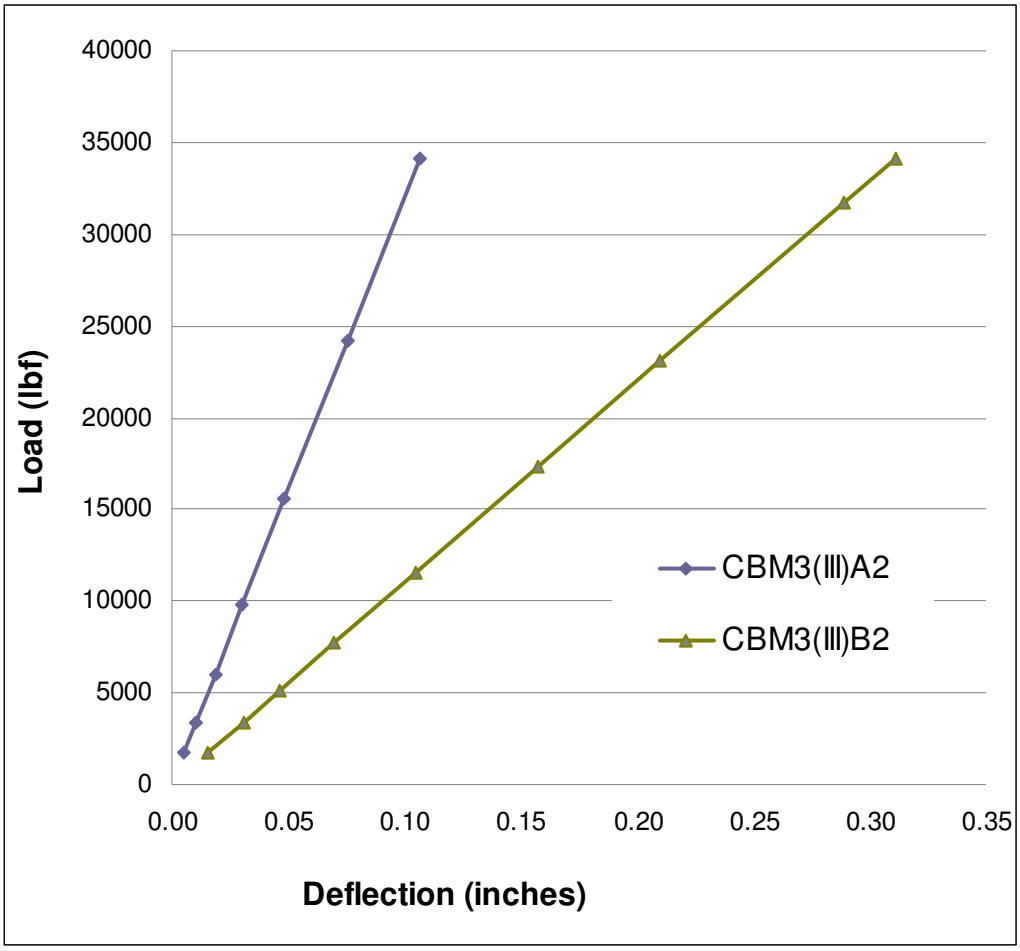

Figure 74 CBM3 Distributed Load, Partially Composite, Pinned and Fixed Ends.

A comparison of the partially composite section with the fully composite section indicates the partially composite section will deflect more due to the fewer number of shear connectors. A 1/3 reduction in shear connectors over the length of the composite beam does not yield a great degree of difference though (Figure 75).

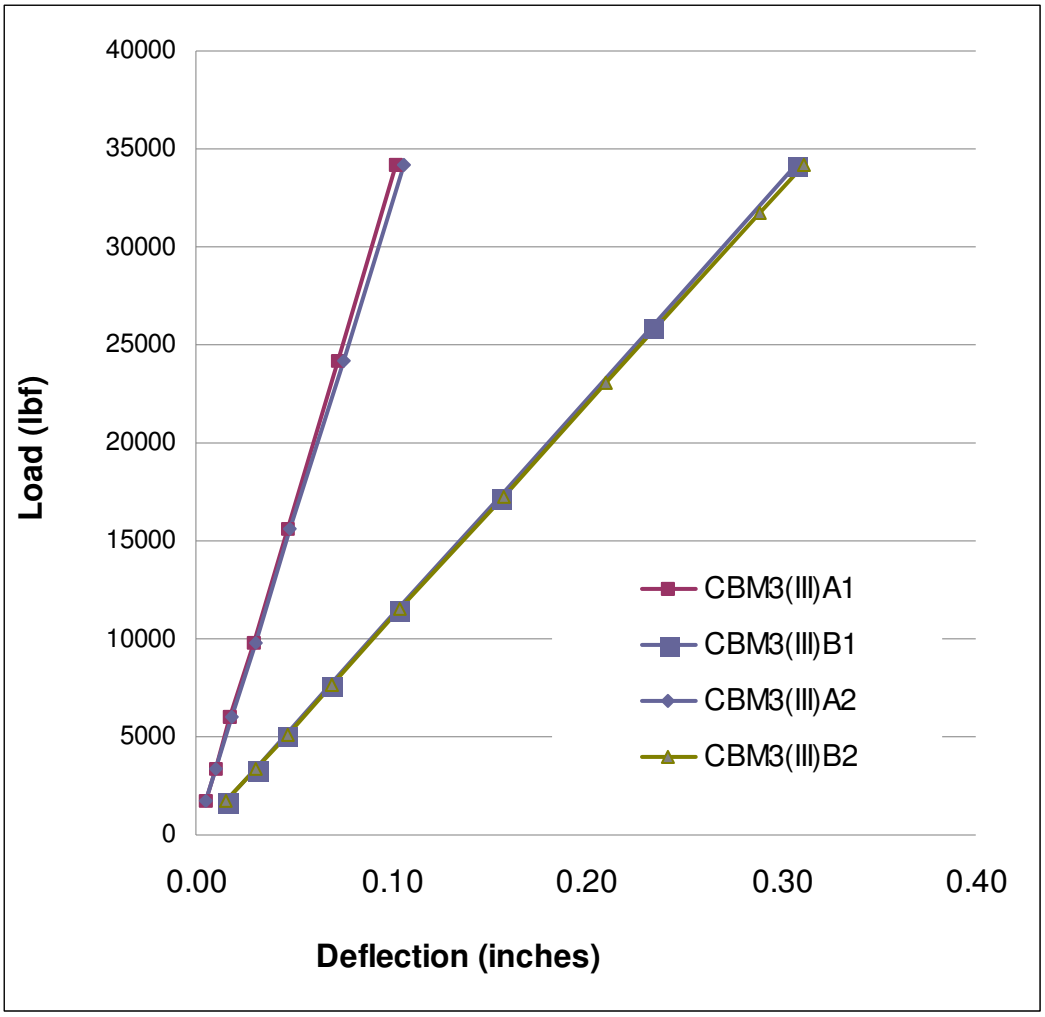

Figure 75 CBM3 Comparison of Fully and Partially Composite Beams

The curves of the partially composite mid span (Figure 76) area a close match the fully composite section. The shear (Figure 77) and moment (Figure 78) diagrams of the partially composite section provide a means of comparing the effects of reducing the number of studs at the mid span with the fully composite section.

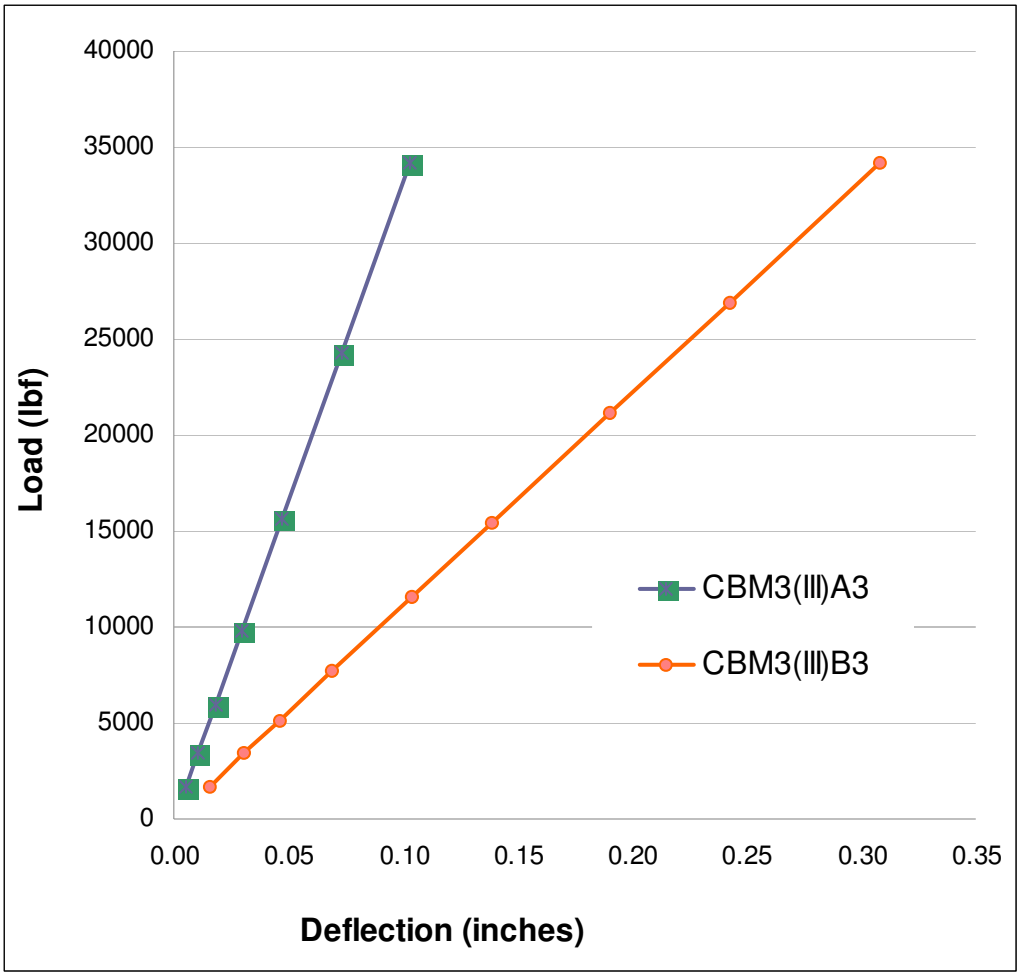

Figure 76 CBM3 Distributed Load, Partially Composite at Mid Span, Pinned and Fixed Ends.

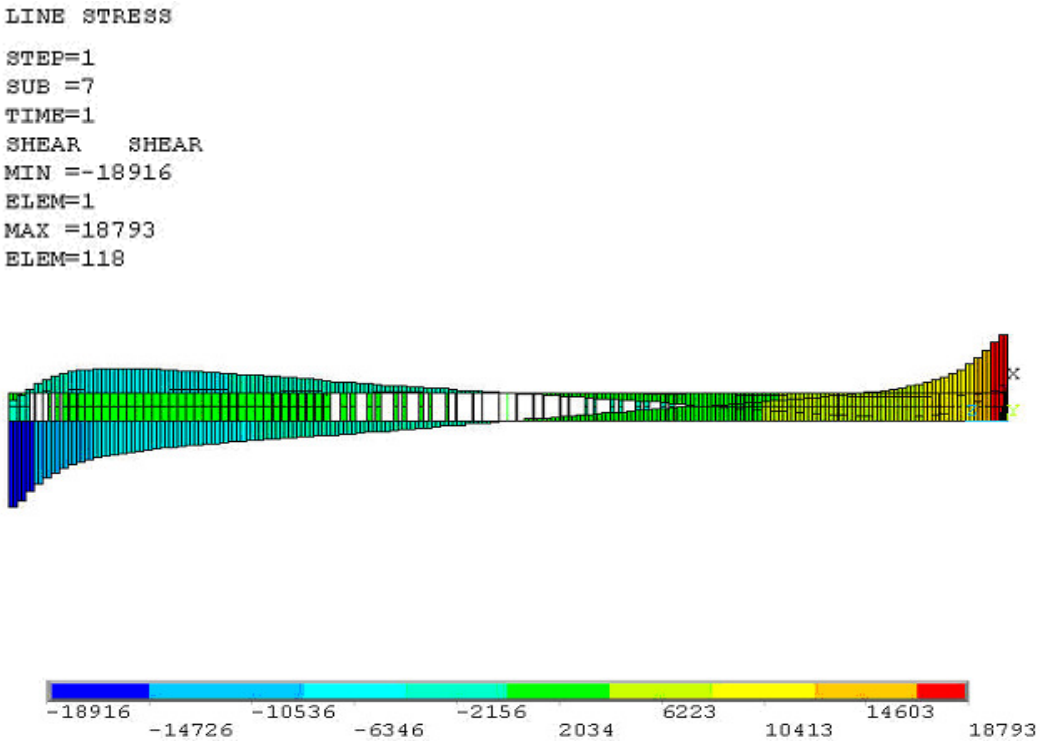

Figure 77 CBM3(III)A3 Shear Diagram

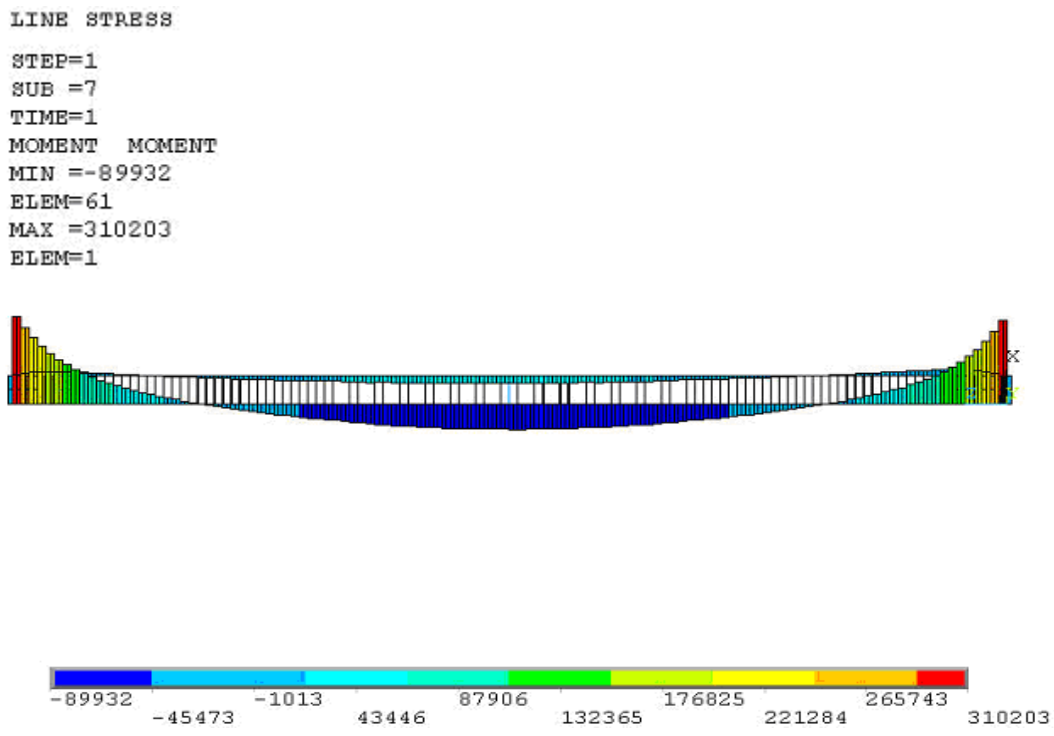

Figure 78 CBM3(III)A3 Moment Diagram

The curves of the partially composite end spans (Figure 79) are also a close match the fully composite section. The shear (Figure 80) and moment (Figure 81) diagrams of the partially composite section provide a means of comparing the effects of reducing the number of studs at the end spans with the fully composite section.

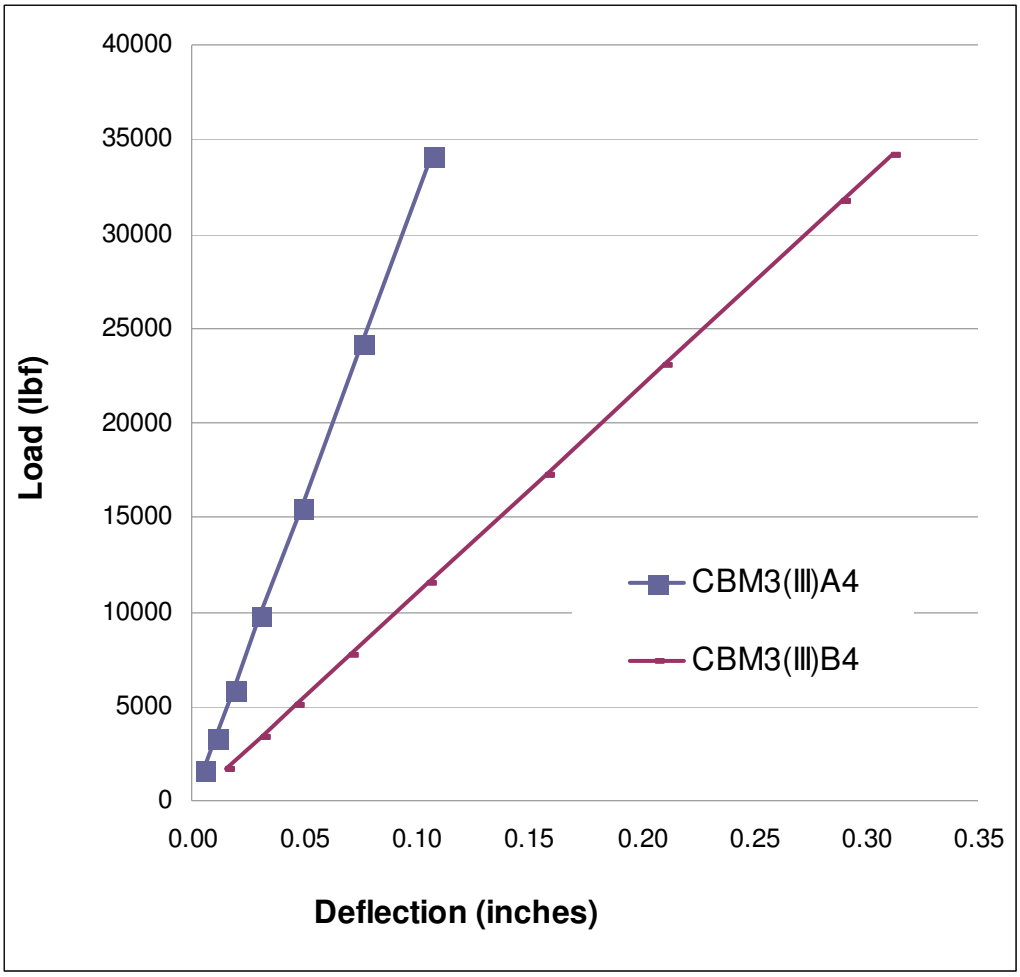

Figure 79 CBM3 Distributed Load, Partially Composite at End Spans, Pinned and Fixed Ends.

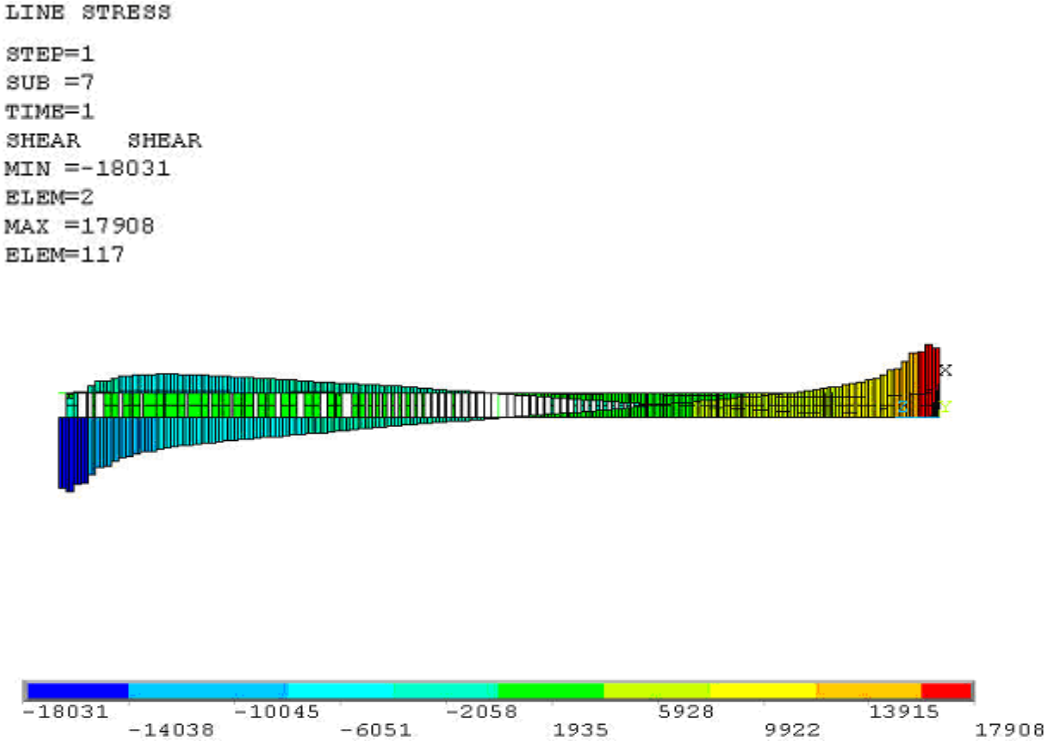

Figure 80 CBM3(III)A4 Shear Diagram

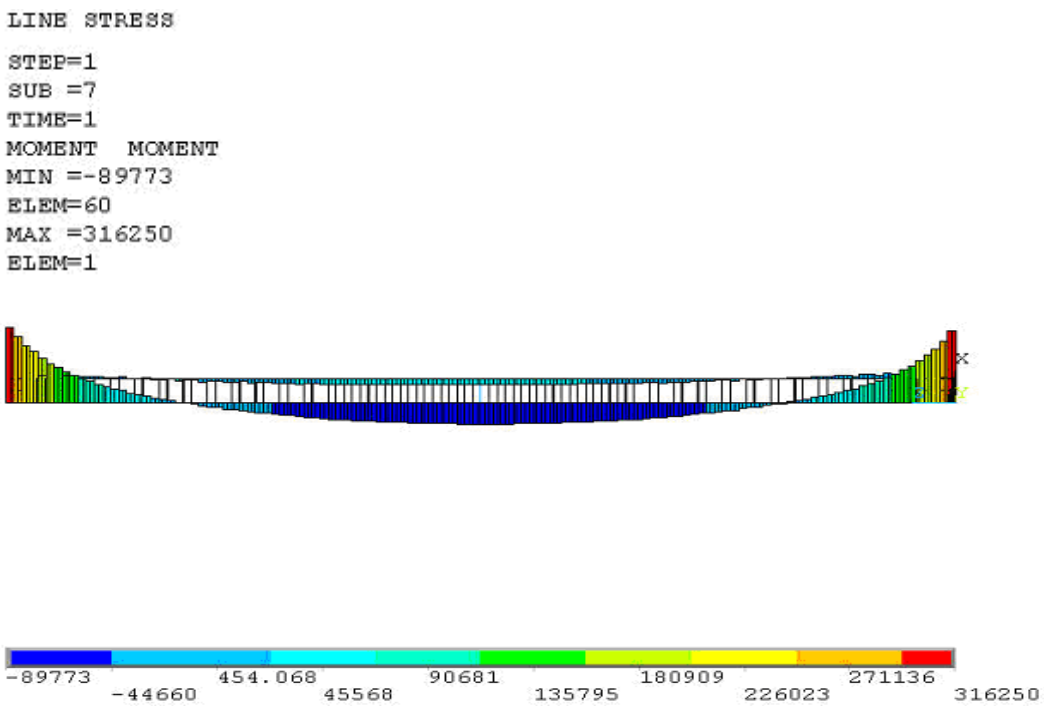

Figure 81 CBM3(III)A4 Moment Diagram

A comparison of the mid span partially composite section and end spans partially composite sections with the fully composite section does not indicate much difference in the amount of deflection (Figure 82). Even though the number of shear connectors was reduced at either the mid span or beam end spans; the remaining shear connectors prevented large deflections.

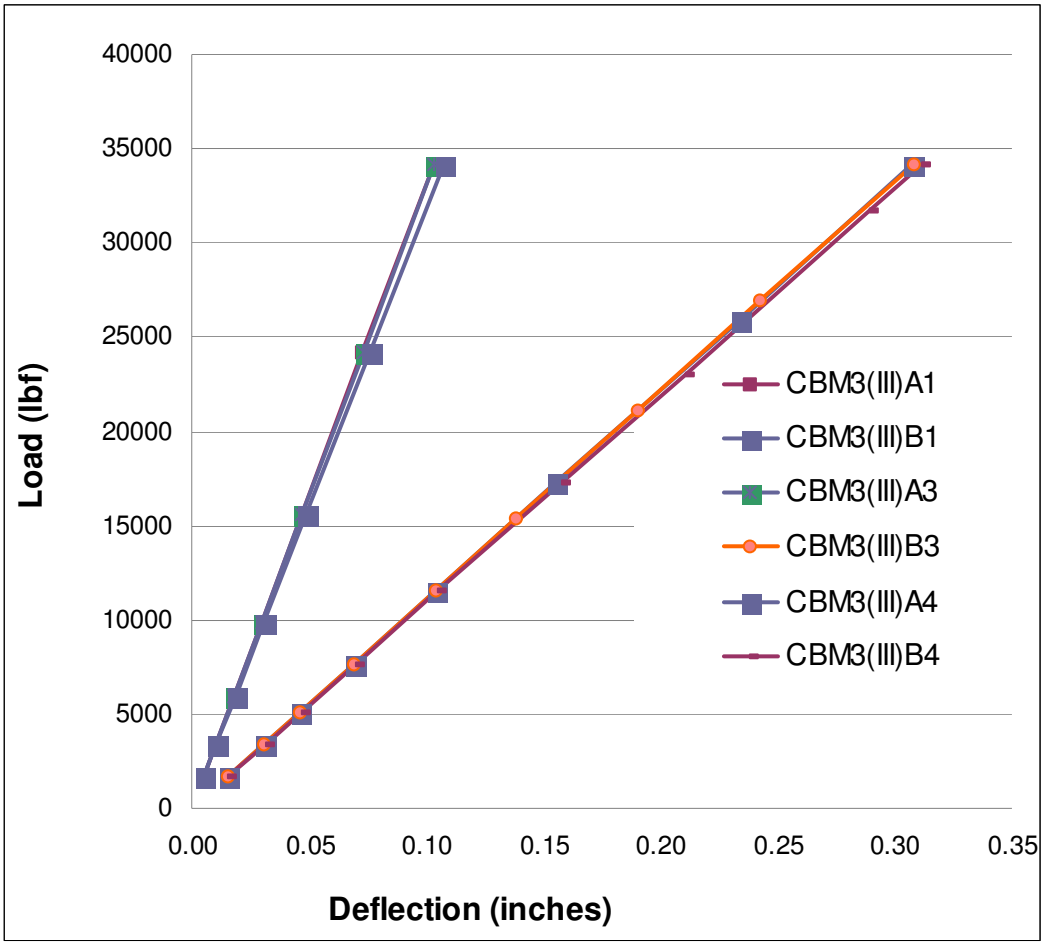

Figure 82 Comparison of Full and Partially Composite Beams

A decrease in the shear area results in a greater amount of deflection (Figure 83).

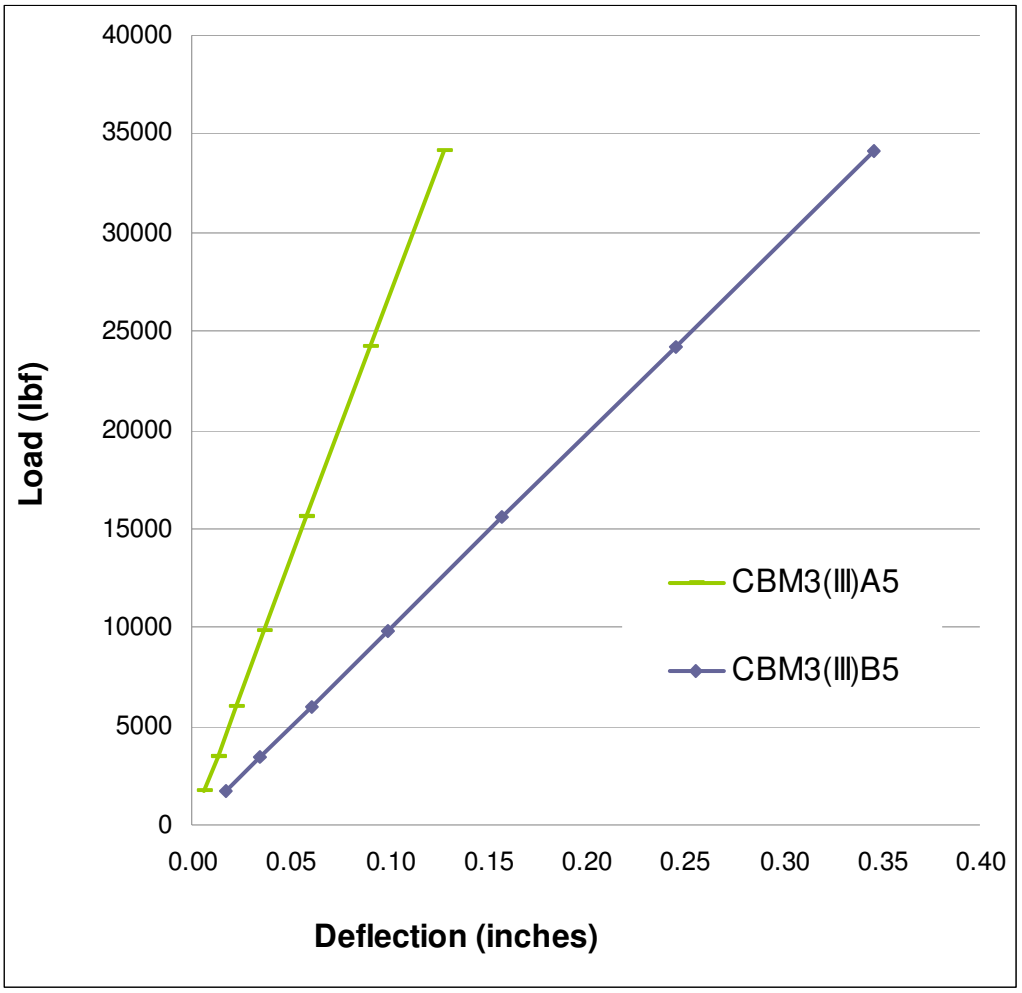

Figure 83 CBM3 Distributed Load, Fully Composite, Reduced Shear Area, Pinned and Fixed Ends.

An increase in the shear area results in less deflection (Figure 84).

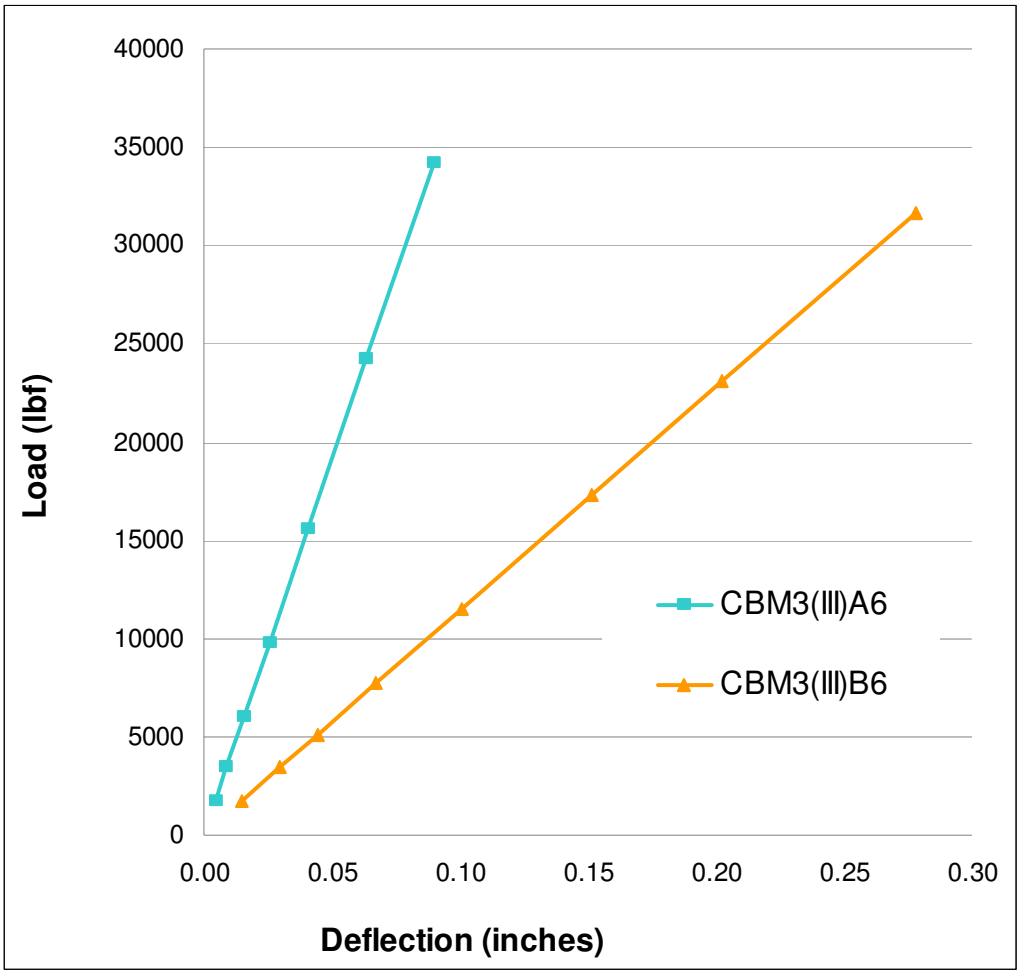

Figure 84 CBM3 Distributed Load, Fully Composite, Increased Shear Area, Pinned and Fixed Ends.

A comparison of the original shear areas with the modified shear areas makes the results more apparent (Figure 85). The results may be summed up: more shear connector area results in less deflection; less shear area results in more deflection. The curves showing the reduced shear connector area is based on the original shear connector area being reduced by 66%. The curve showing the increase shear connector area is base on the original shear connector area being increased by 101%.

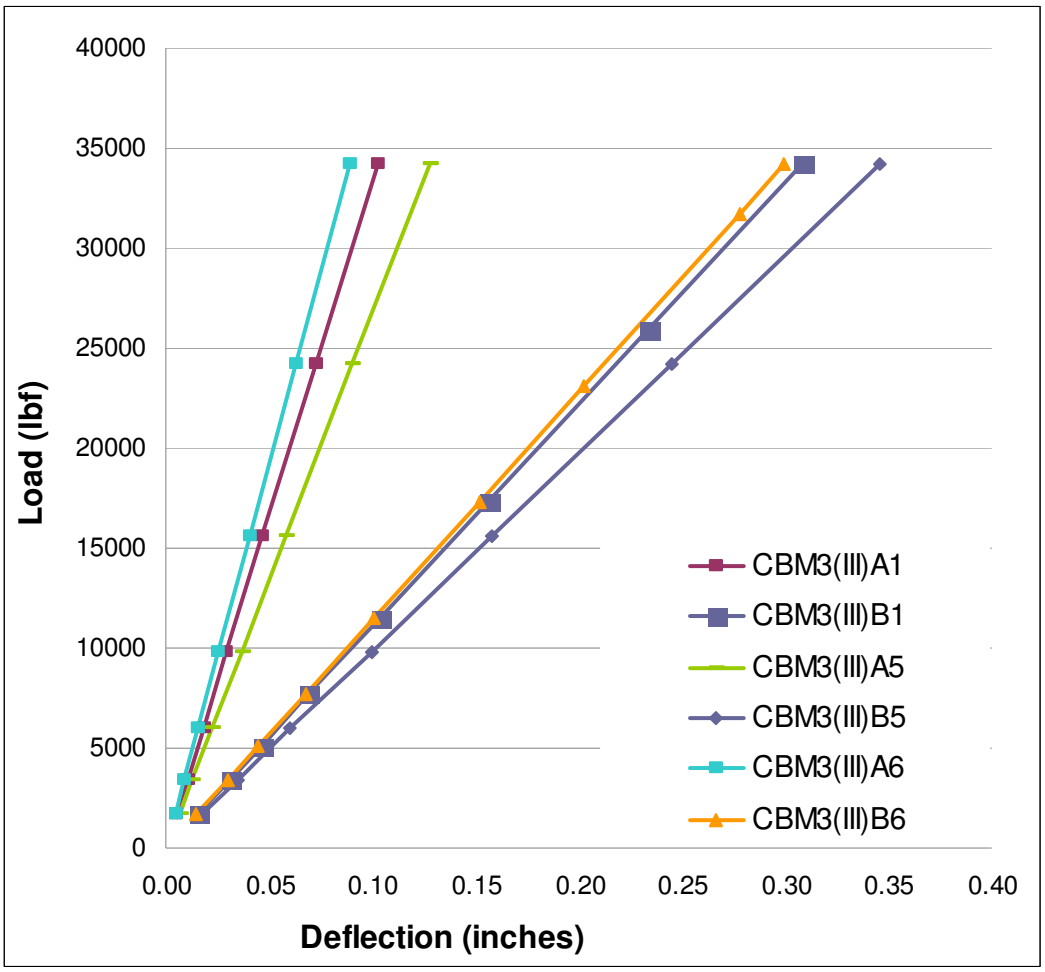

Figure 85 CBM3 Comparison of Shear Connector Areas

Increasing the thickness of the slab results in less deflection (Figure 86).

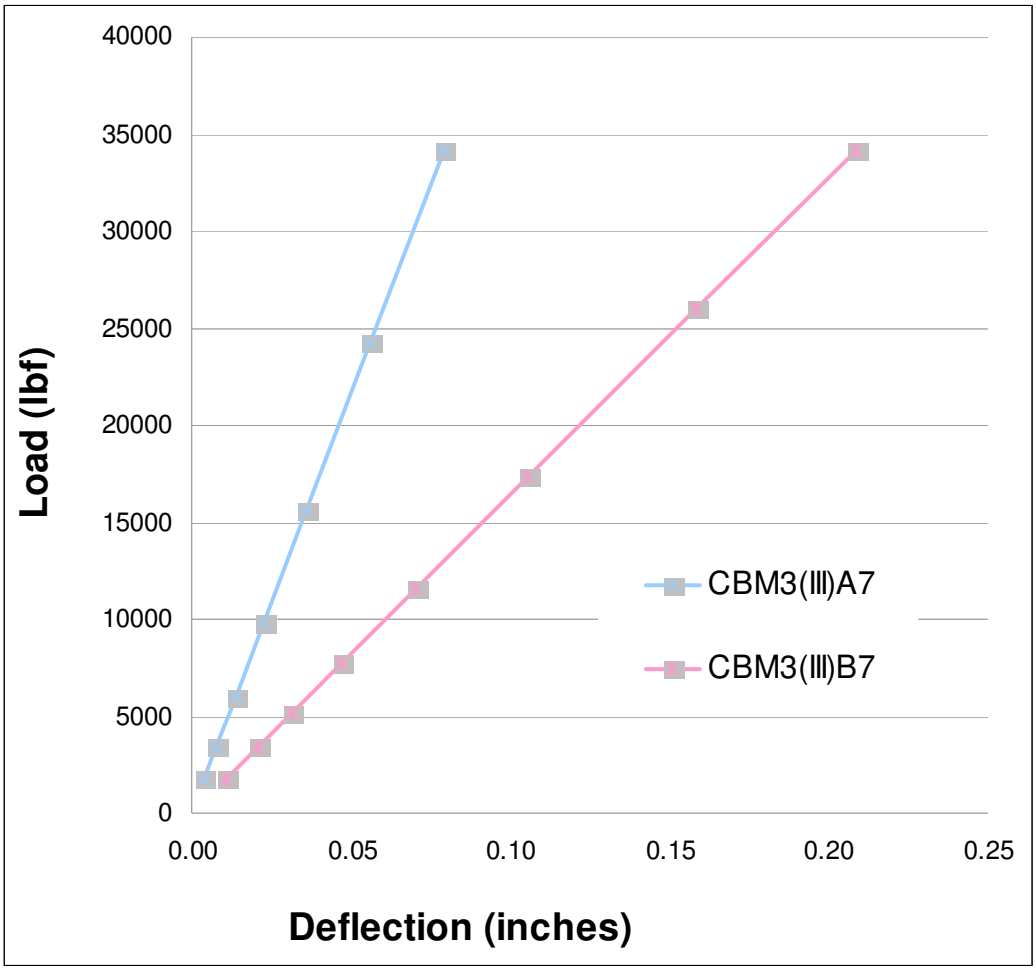

Figure 86 CBM3 Distributed Load, Fully Composite, Increased Slab Thickness Pinned and Fixed Ends

A comparison of the original slab thickness with an increased slab thickness makes the results of a thicker slab more apparent (Figure 87). In both end conditions a thicker slab resulted in less deflection. The curves in the graph indicate and increased slab thickness stiffens the composite section. The slab was thickened by 50% over the original slab thickness in model from which the curves are derived.

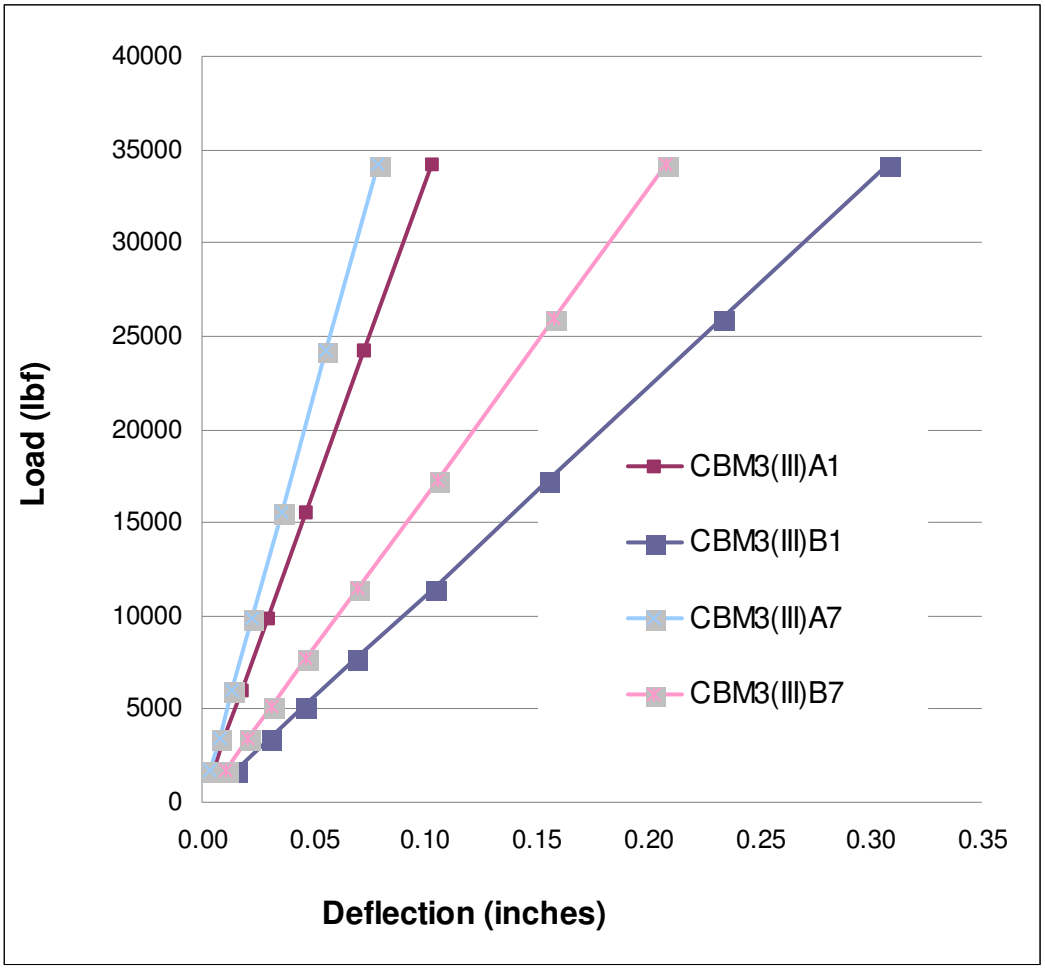

Figure 87 Comparison of Slab Thickness

4.5 CBM4 Results

Calculations of the CBM4 composite section indicate the section is fully composite. Note, the PNA, and the stress block, "a", are located in the slab, which indicates the slab and WF section are acting a together as a composite section (Figure 88). The stress distribution also indicates the section is acting in a composite manner (Figure 89).

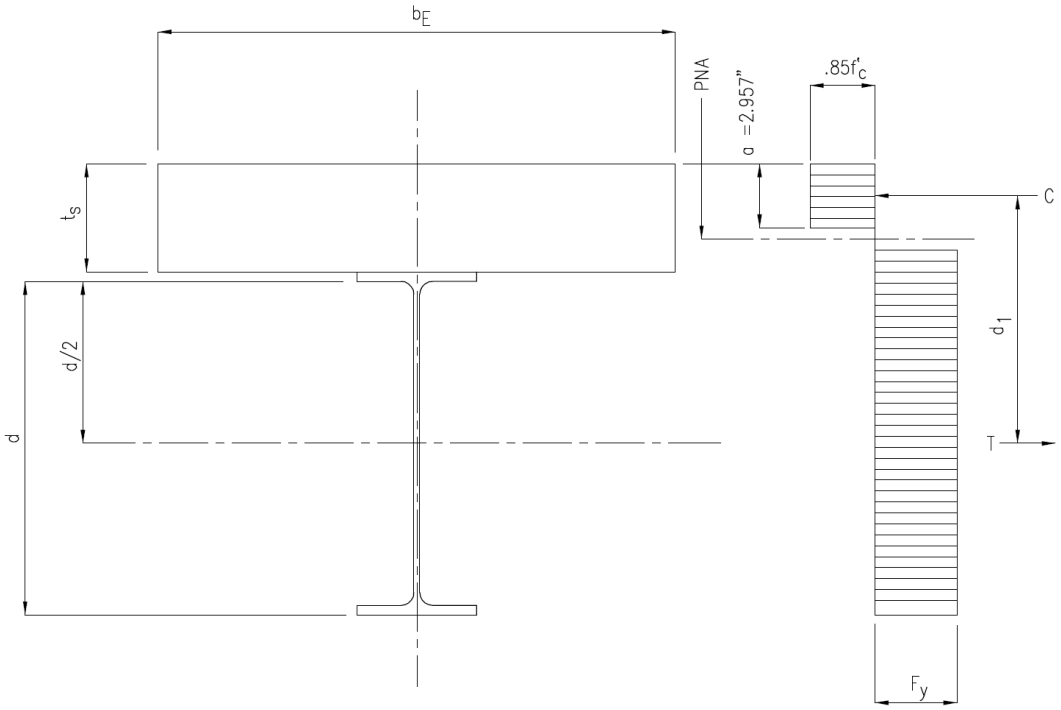

Figure 88 CBM4 Location of Plastic Neutral Axis and Concrete Stress Block.

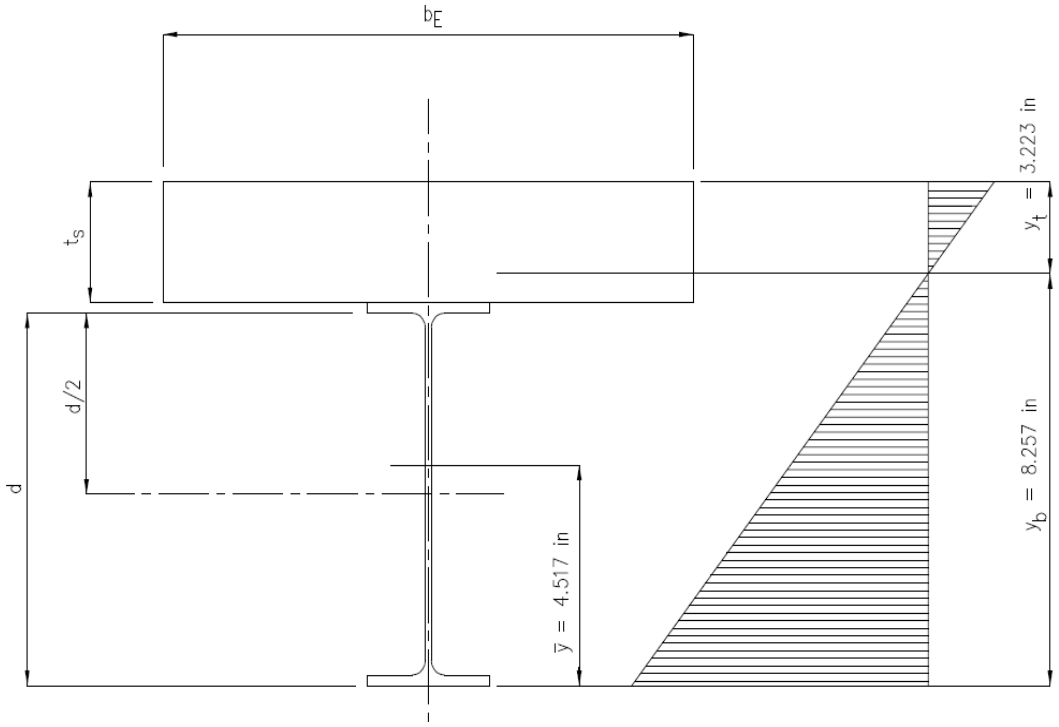

Figure 89 CBM4 Stress Distribution

The end condition in the full composite section has an impact on the amount of deflection (Figure 90). The fixed end condition deflects less than the pinned condition. The shear (Figure 91) and moment (Figure 92) diagrams of the fully composite section provide a means of comparing the effects of reducing the number of studs at the mid span and end spans of the beam with the fully composite section.

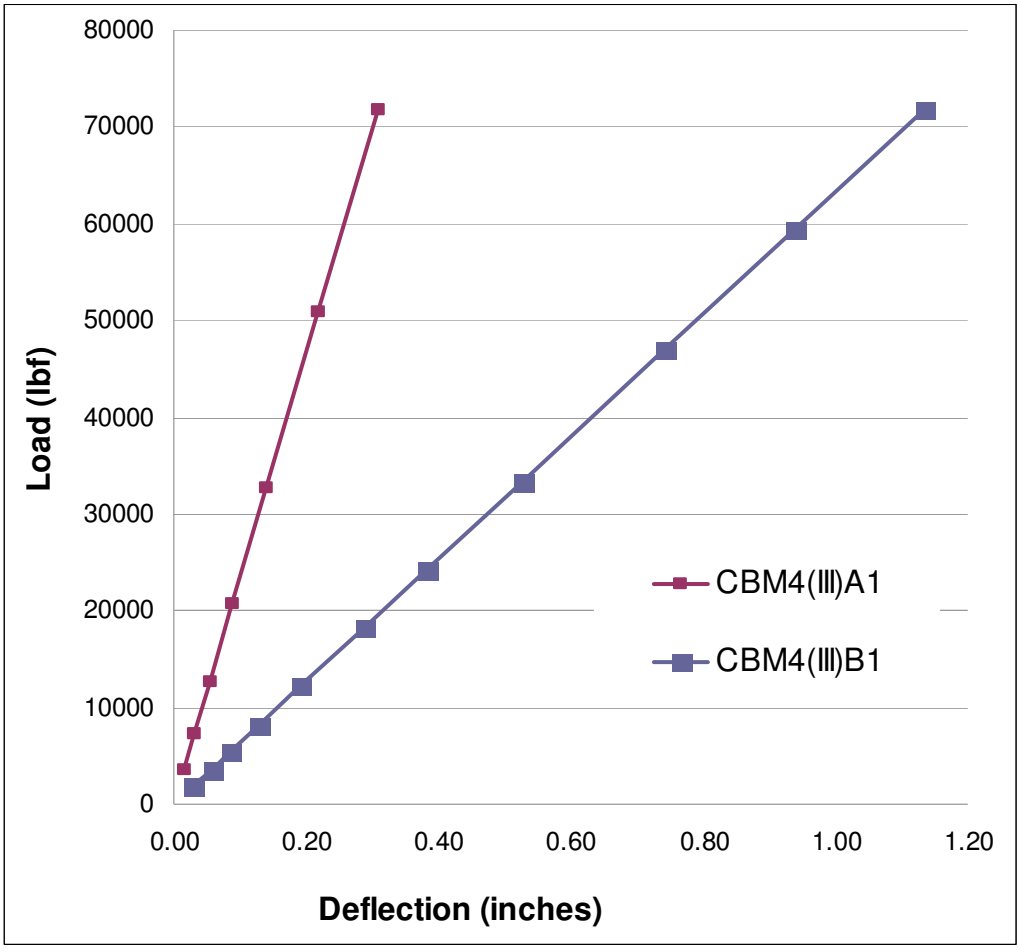

Figure 90 CBM4 Distributed Load, Fully Composite, Pinned and Fixed Ends.

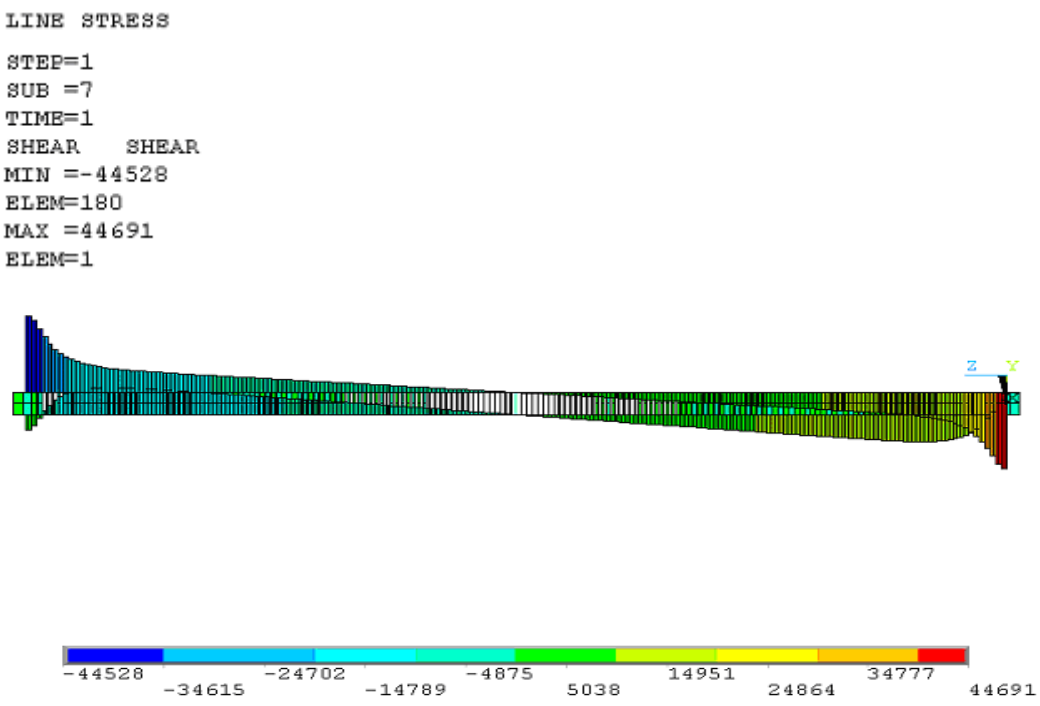

Figure 91 CBM4(III)A1 Shear Diagram

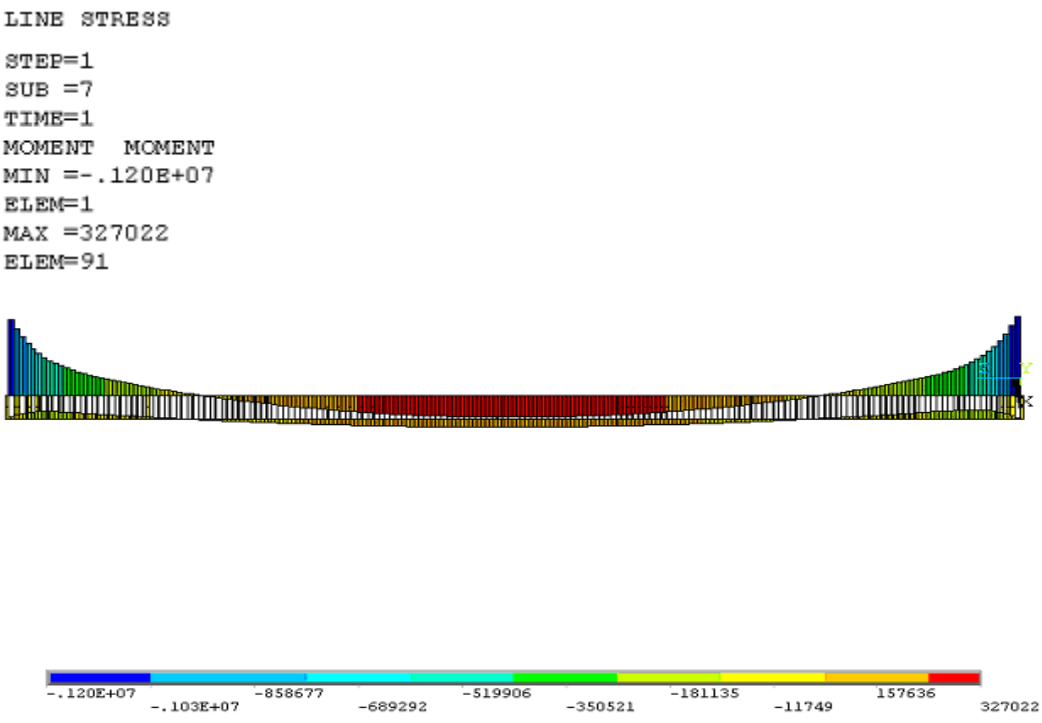

Figure 92 CBM4(III)A1 Moment Diagram

The end condition is a consistent factor in the degree of deflection, be it the two-point load condition or the distributed load condition (Figure 93).

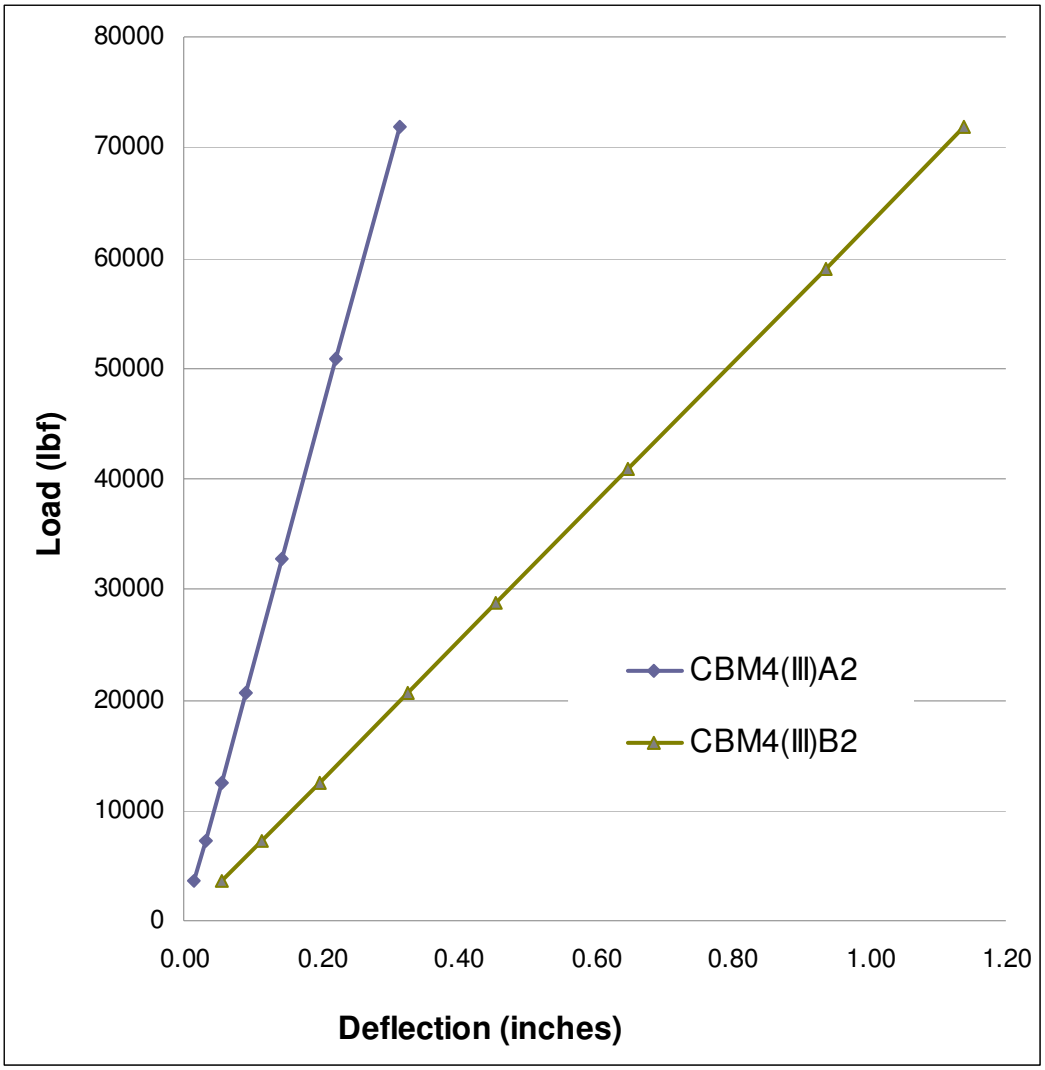

Figure 93 CBM4 Distributed Load, Partially Composite, Pinned and Fixed Ends.

A comparison of the partially composite section with the fully composite section indicates the partially composite section will deflect more due to the fewer number of shear connectors. A 1/3 reduction in shear connectors over the length of the composite beam does not yield a great degree of difference though (Figure 94).

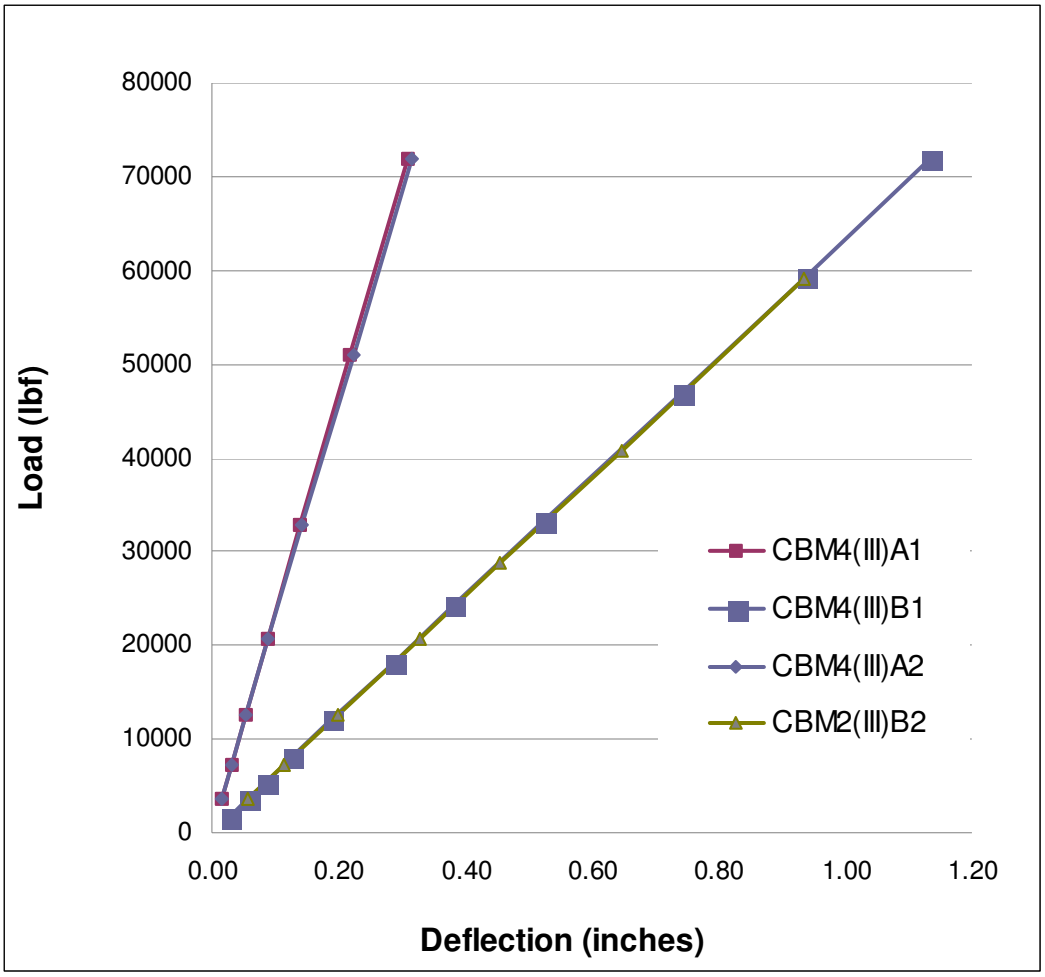

Figure 94 CBM4 Comparison of Fully and Partially Composite Sections

The curves of the partially composite mid span (Figure 95) area a close match the fully composite section. The shear (Figure 96) and moment (Figure 97) diagrams of the partially composite section provide a means of comparing the effects of reducing the number of studs at the mid span with the fully composite section.

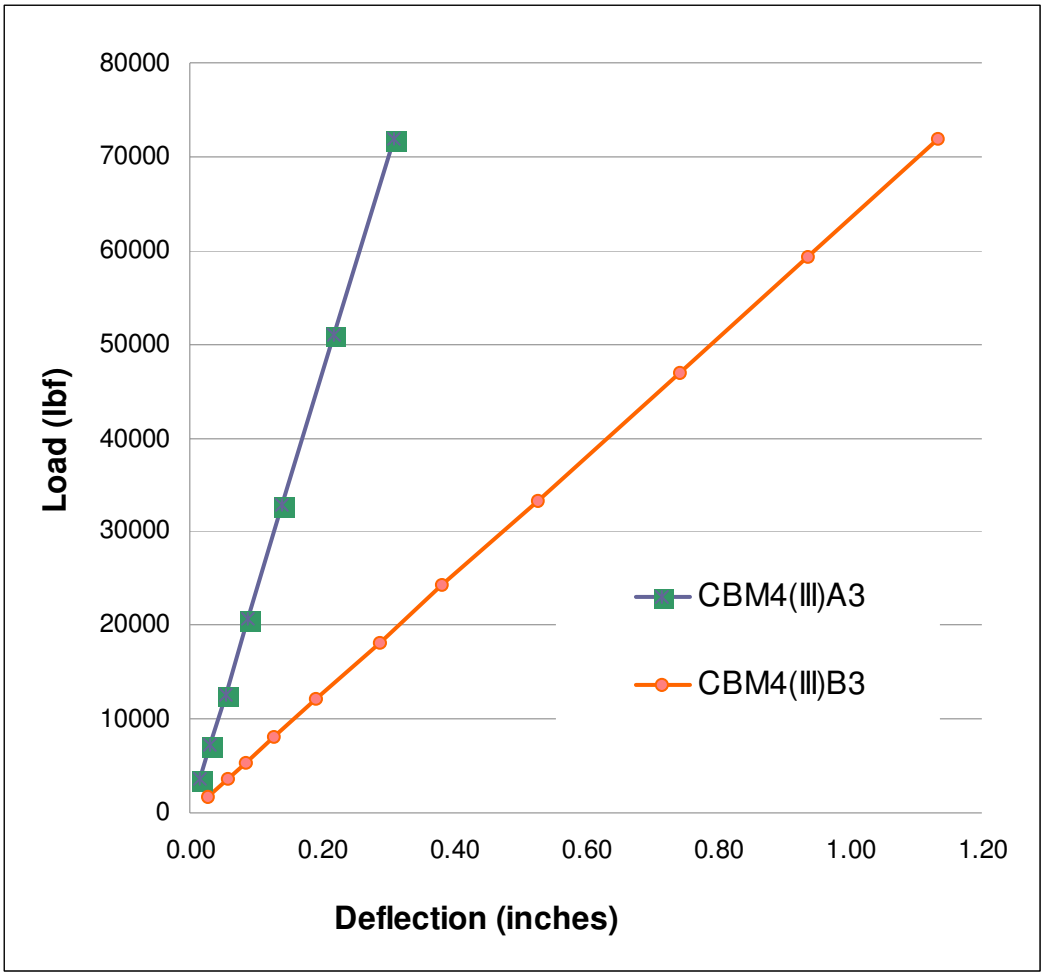

Figure 95 CBM4 Distributed Load, Partially Composite at Mid Span, Pinned and Fixed Ends.

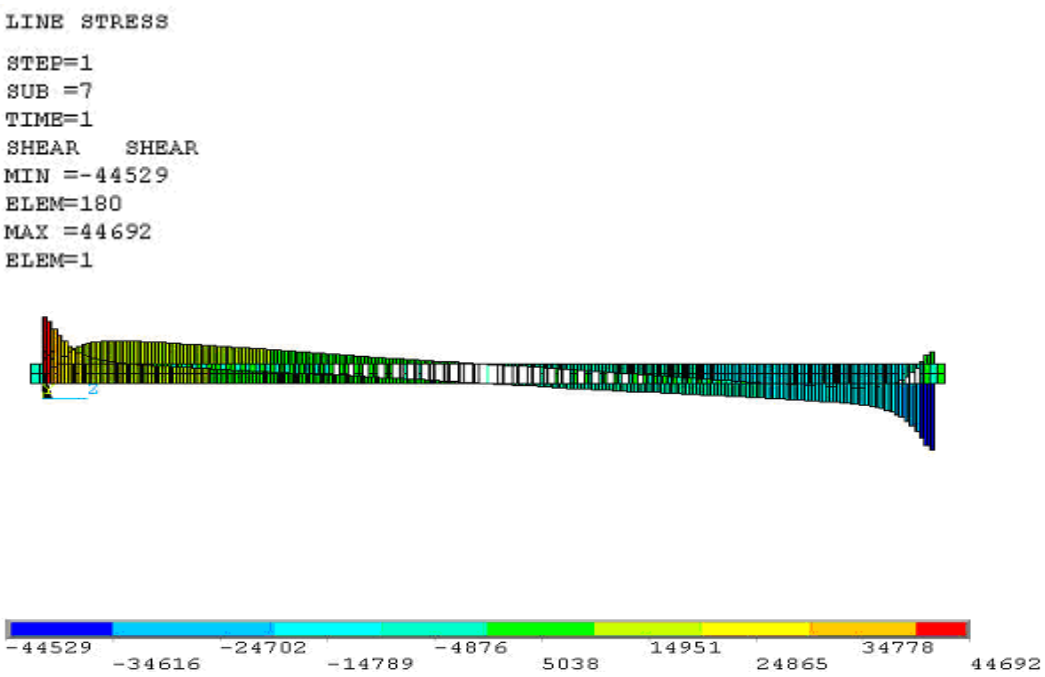

Figure 96 CBM4(III)A3 Shear Diagram

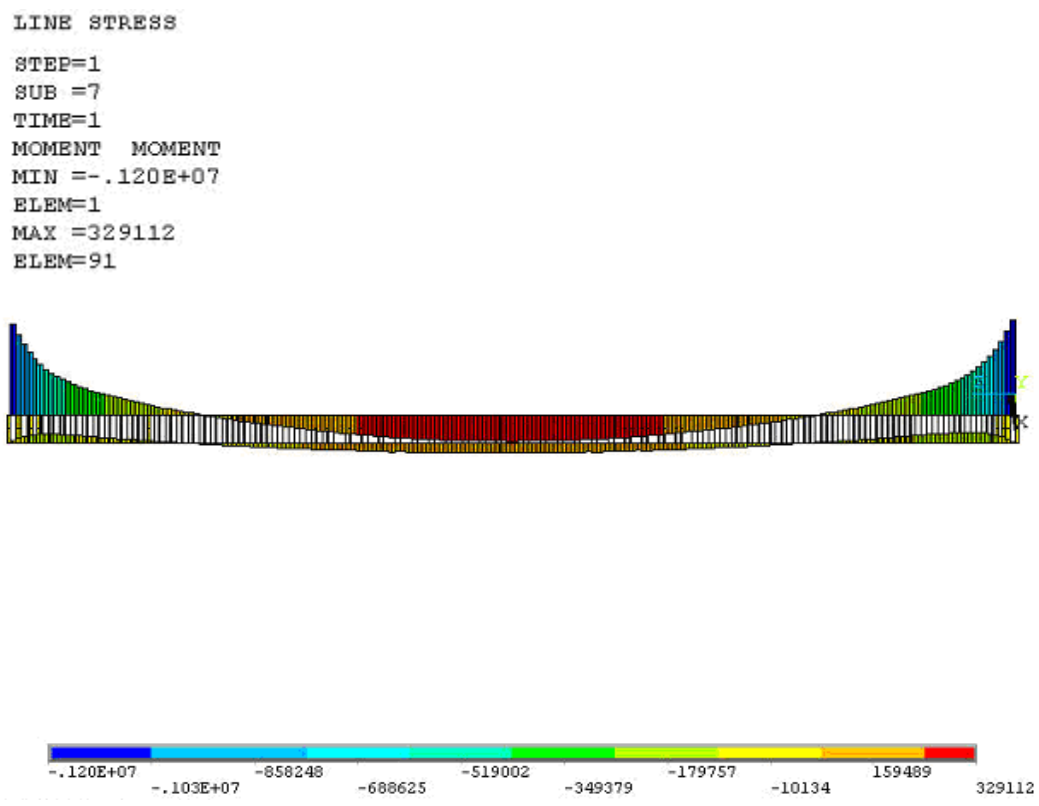

Figure 97 CBM4(III)A3 Moment Diagram

The curves of the partially composite end spans (Figure 98) are also a close match the fully composite section. The shear (Figure 99) and moment (Figure 100) diagrams of the partially composite section provide a means of comparing the effects of reducing the number of studs at the end spans with the fully composite section.

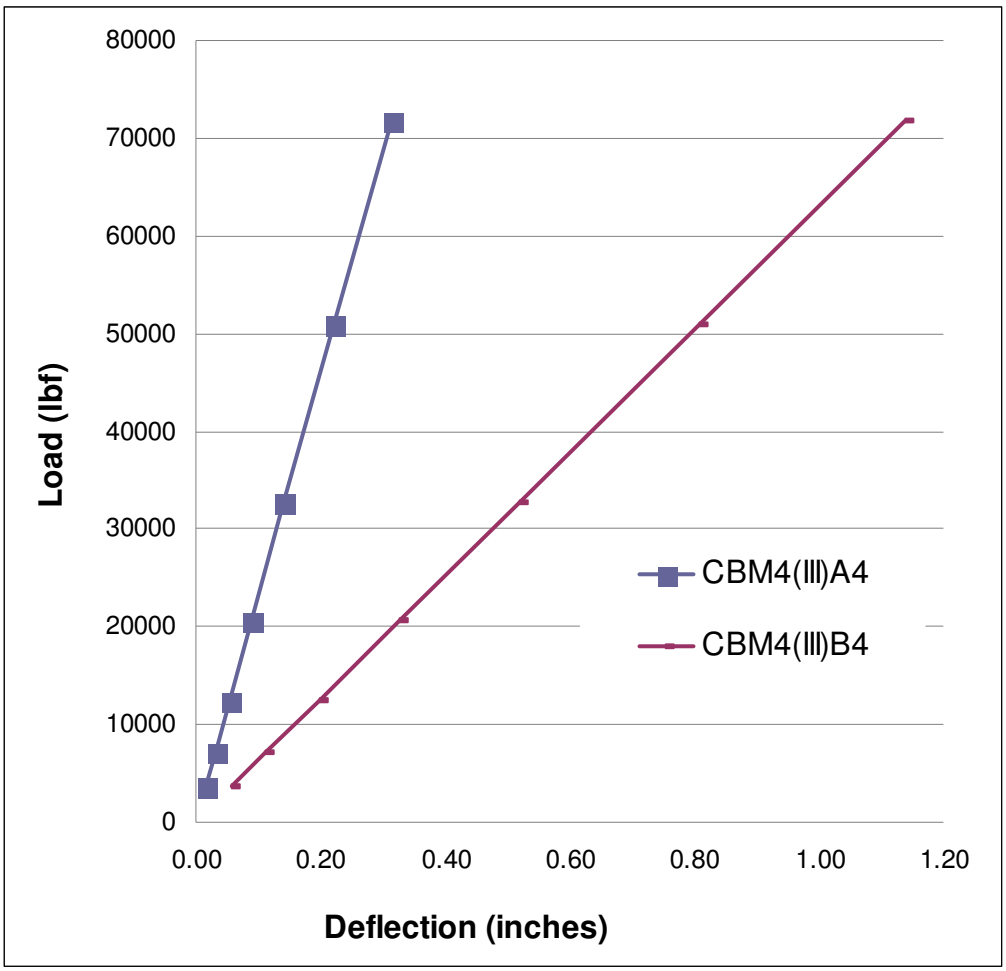

Figure 98 CBM4 Distributed Load, Partially Composite at End Spans, Pinned and Fixed Ends.

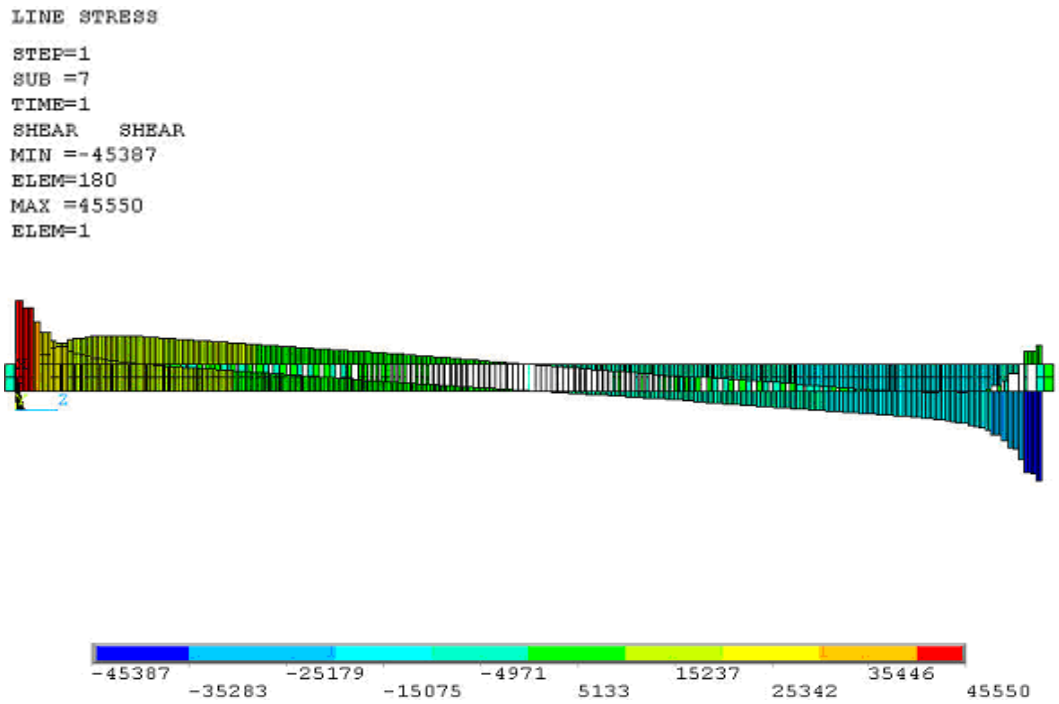

Figure 99 CBM4(III)A4 Shear Diagram

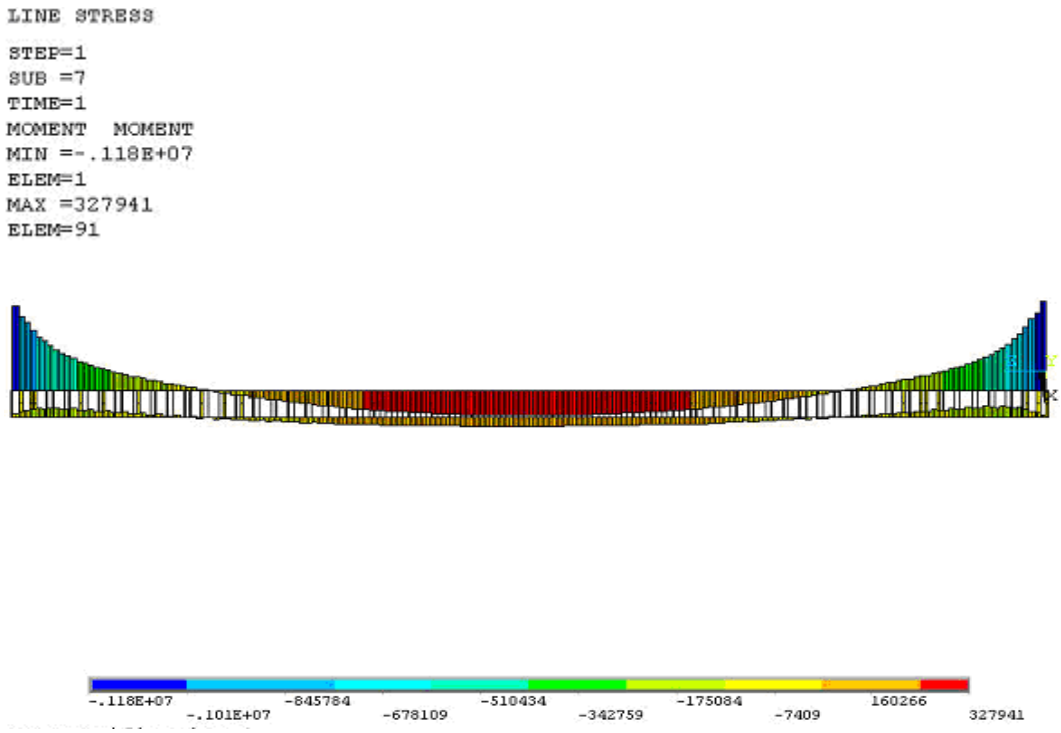

Figure 100 CBM4(III)A4 Moment Diagram

A comparison of the mid span partially composite section and end spans partially composite sections with the fully composite section does not indicate much difference in the amount of deflection (Figure 101). Even though the number of shear connectors was reduced at either the mid span or beam end spans; the remaining shear connectors prevented large deflections.

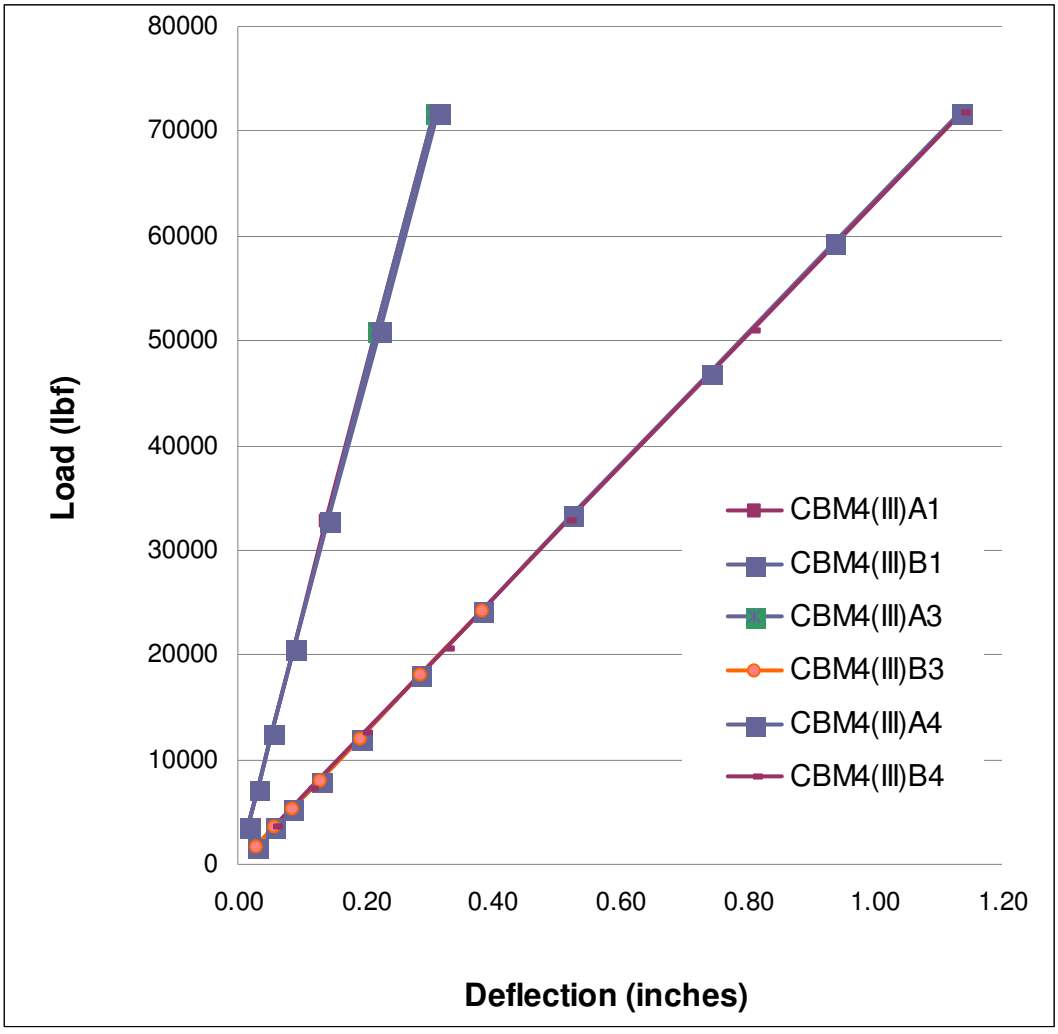

Figure 101 CBM4 Comparison of Fully and Partially Composite Sections

A decrease in the shear area results in a greater amount of deflection (Figure 102).

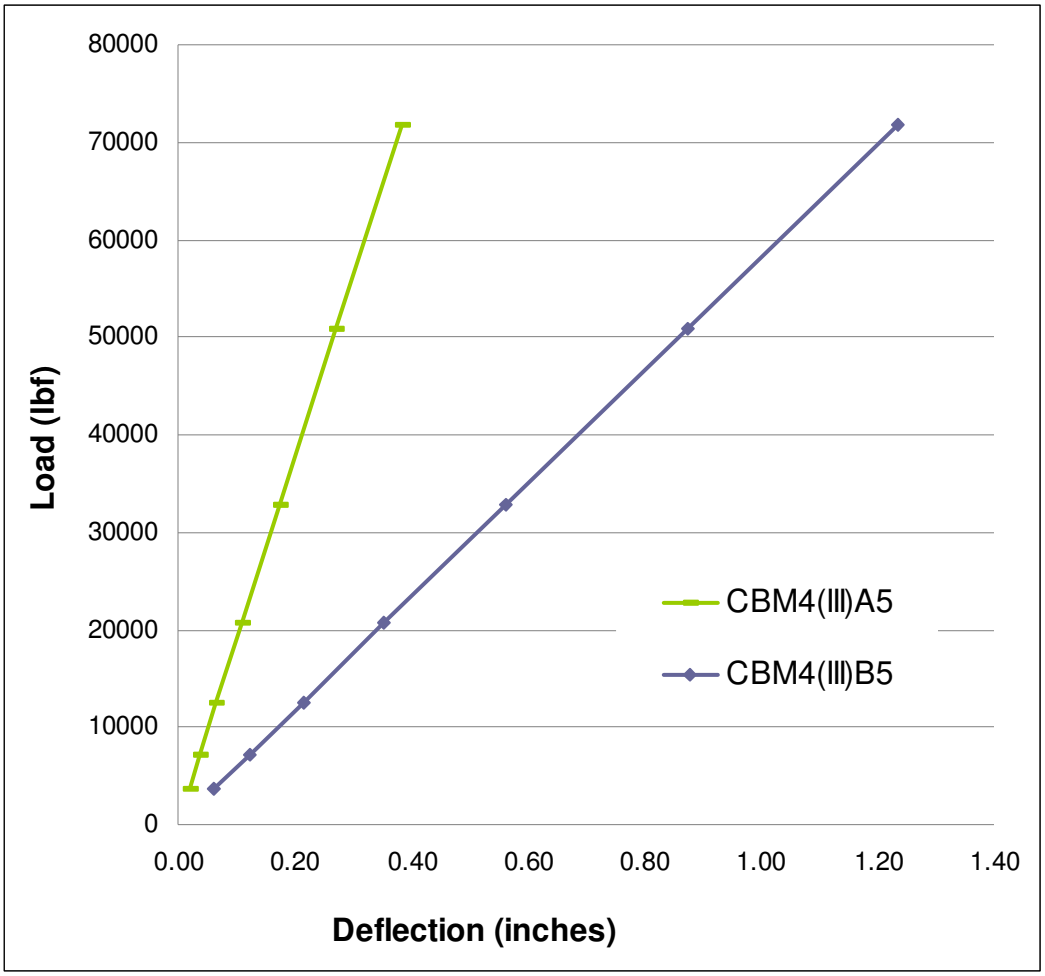

Figure 102 CBM4 Distributed Load, Fully Composite, Reduced Shear Area, Pinned and Fixed Ends.

An increase in the shear area results in less deflection (Figure 103).

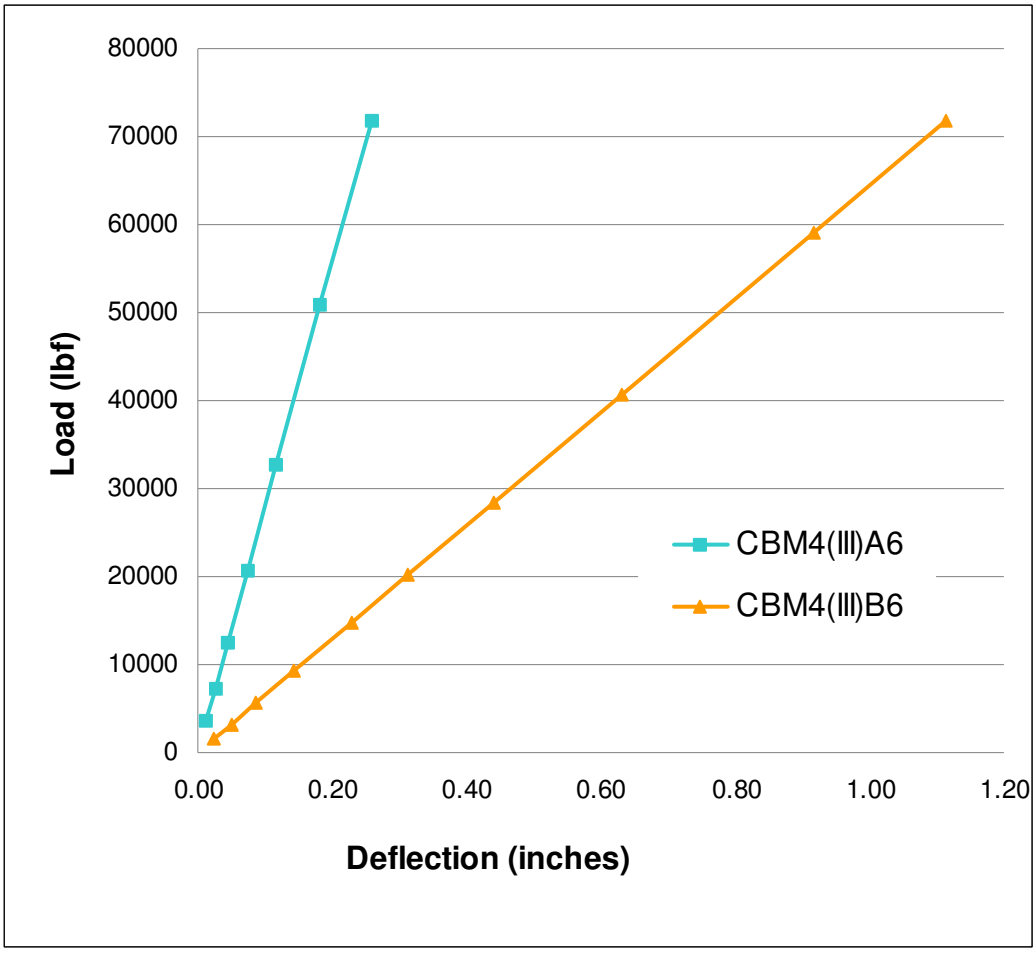

Figure 103 CBM4 Distributed Load, Fully Composite, Increased Shear Area, Pinned and Fixed Ends.

A comparison of the original shear areas with the modified shear areas makes the results more apparent (Figure 104). The results may be summed up: more shear connector area results in less deflection; less shear area results in more deflection. The curves showing the reduced shear connector area is based on the original shear connector area being reduced by 75%. The curve showing the increase shear connector area is base on the original shear connector area being increased by 300%.

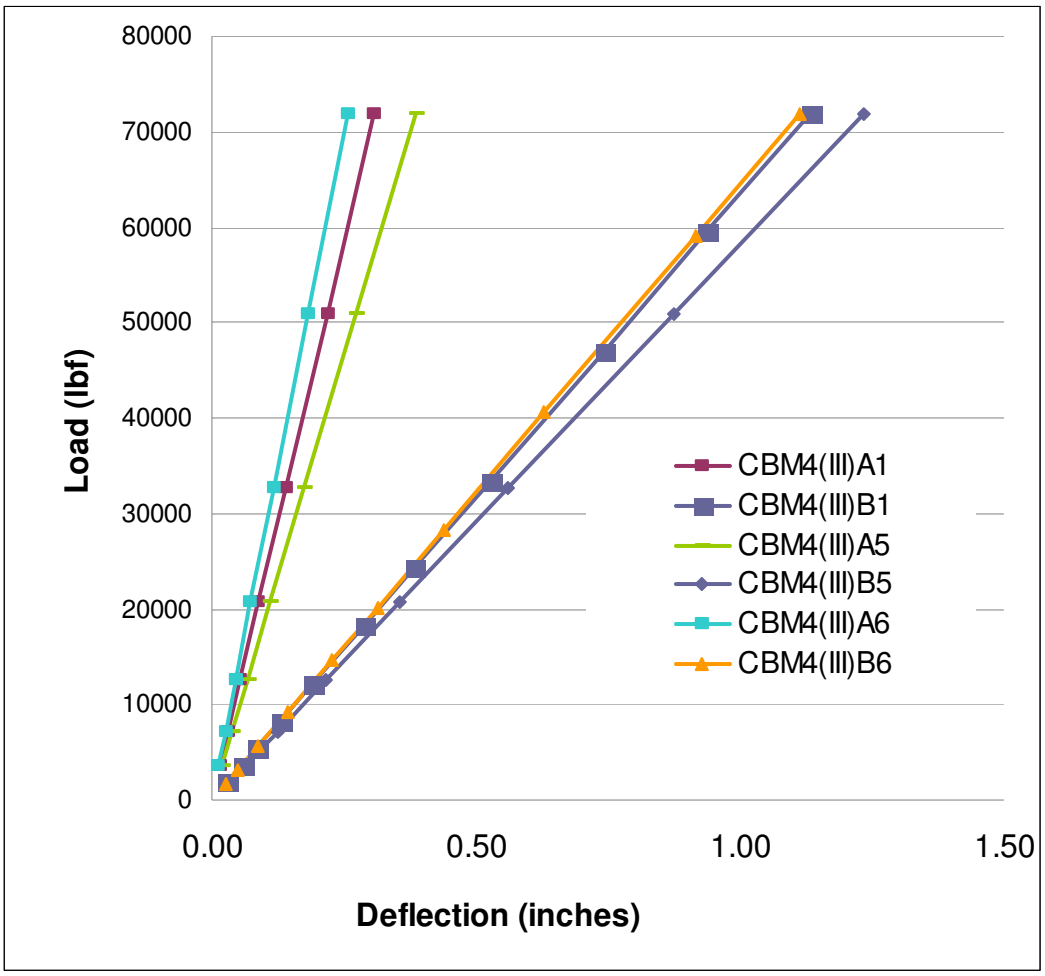

Figure 104 CBM4 Comparison of Shear Connector Areas

Increasing the thickness of the slab results in less deflection (Figure 105).

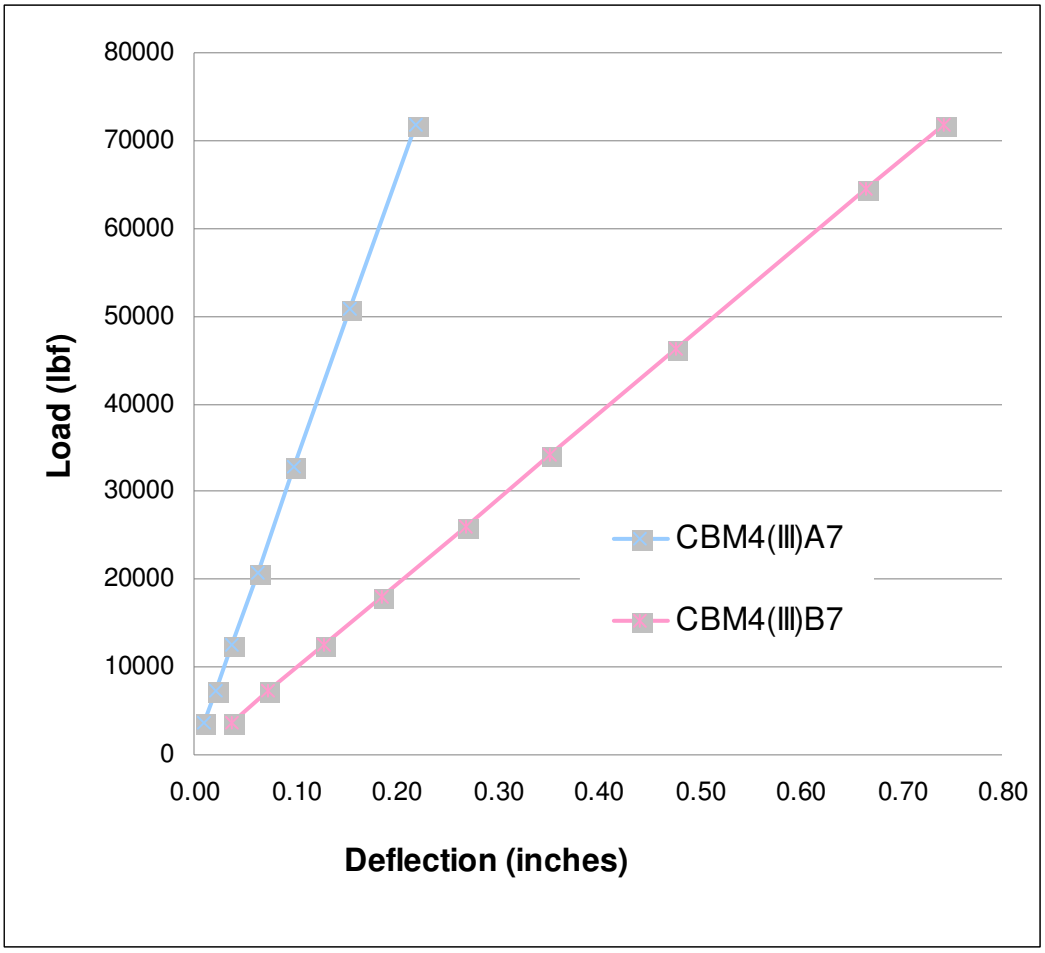

Figure 105 CBM4 Distributed Load, Fully Composite, Increased Slab Thickness Pinned and Fixed Ends

A comparison of the original slab thickness with an increased slab thickness makes the results of a thicker slab more apparent (Figure 106). In both end conditions a thicker slab resulted in less deflection. The curves in the graph indicate and increased slab thickness stiffens the composite section. The slab was thickened by 60% over the original slab thickness in model from which the curves are derived.

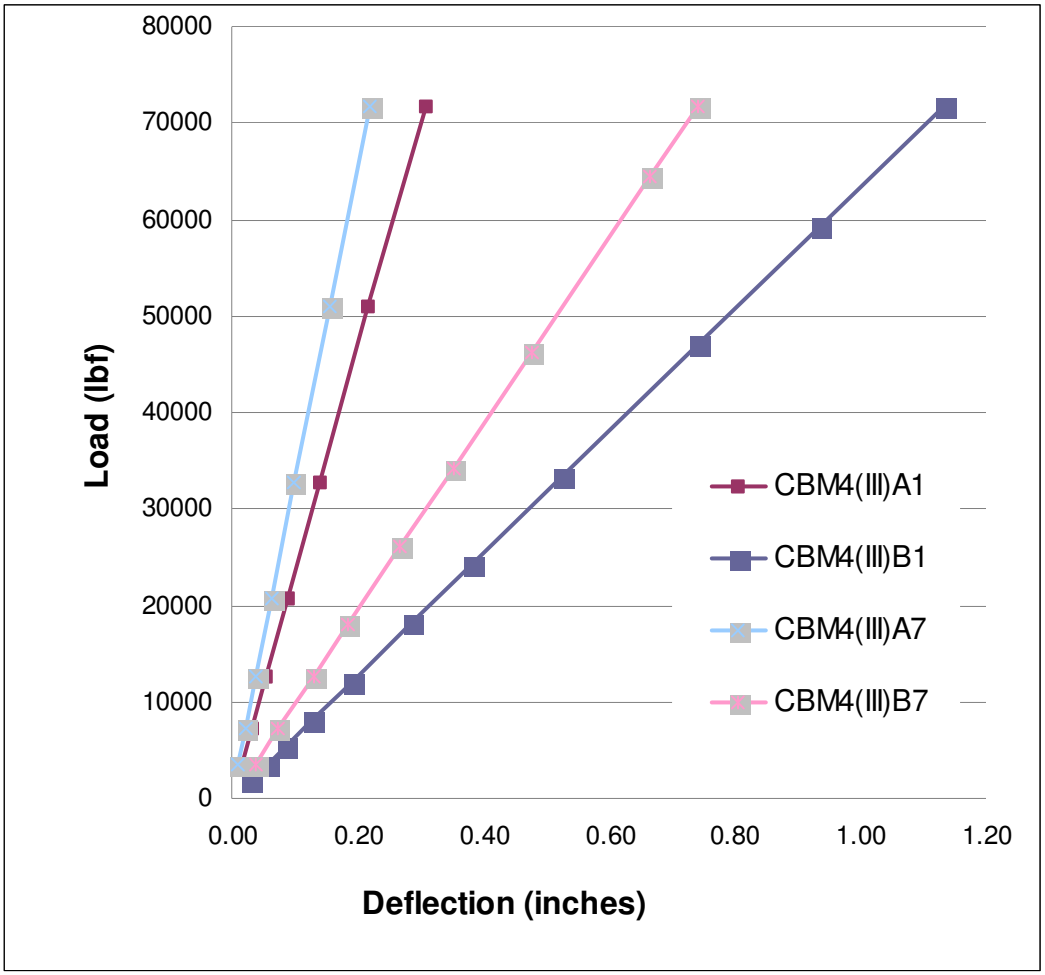

Figure 106 CBM4 Comparison of Slab Thickness

4.6 Parametric Study Results

The focus of this thesis is to help understand how the placement and size of shear connectors, as well as slab thickness influence the ability of composite beams to withstand loads, which create regions of positive and negative moment. The discussion which follows uses load versus deflection comparisons as well as stress comparisons (in regions of negative moment) to help verify standard methods of composite beam design at regions of positive moment, gain an understanding of composite beam behavior at regions of negative moment, and look at the problems of FE modeling of composite beams.

Changes in shear stud location generally yielded minimal changes in the load versus deflection curves. The 1/3 reduction in the number of shear studs over the length of beam made little difference as well. Changes in the shear area had a slightly greater effect. Generally, the change in slab thickness seemed to have the greatest effect (Table 5, Table 6, Table 7, Table 8, Table 9).

Table 5 Deflection Comparisons

Model	Deflection	% Difference
CBM1(II))A1	0.44	
CBM1(II)A2	0.42	4.65
CBM1(III)A1	0.31	
CBM1(III)A2	0.3	3.22
CBM1(II))B1	1.55	
CBM1(II)B2	1.51	2.58
CBM1(III)B1	1.15	
CBM1(III)B2	1.14	0.87

Table 6 Deflection Comparisons

CBM1(II)A1	0.44	
CBM1(II)A3	0.43	2.27
CBM1(II)A4	0.44	0
CBM1(II)B1	1.55	
CBM1(II)B3	1.53	1.3
CBM1(II)B4	1.56	-0.64
CBM1(III)A1	0.31	
CBM1(III)A3	0.3	3.22
CBM1(III)A4	0.3	3.22

CBM1(III)B1	1.15	
CBM1(III)B3	1.14	0.87
CBM1(III)B4	1.14	0.87

CBM1(II)A1	0.44	
CBM1(II)A5	0.44	0
CBM1(II)A6	0.42	4.54
CBM1(III)A1	0.31	
CBM1(III)A5	0.3	3.22
CBM1(III)A6	0.3	3.22
CBM1(II)B1	1.55	
CBM1(II)B5	1.55	0
CBM1(II)B6	1.45	6.45
CBM1(III)B1	1.15	
CBM1(III)B5	1.16	-0.87
CBM1(III)B6	1.12	2.61
CBM1(II))A1	0.44	
CBM1(II)A7	0.35	20.5
CBM1(III)A1	0.31	
CBM1(III)A7	0.24	22.6
CBM1(II))B1	1.55	
CBM1(II)B7	0.98	36.8
CBM1(III)B1	1.15	
CBM1(III)B7	0.72	37.4

The % Difference is between the original condition (an A1 or B1 model) with those directly below it in the tables.

Table 7 Deflection Comparisons

Model	Deflection	% Difference
CBM2(III)A1	0.16	
CBM2(III)A2	0.16	0.00
CBM2(III)A3	0.16	0.00
CBM2(III)A4	0.16	0.00
CBM2(III)A5	0.24	-50.00
CBM2(III)A6	0.11	31.25
CBM2(III)A7	0.12	25
CBM2(III)B1	0.52	
CBM2(III)B2	0.53	-1.90
CBM2(III)B3	0.51	1.94
CBM2(III)B4	0.53	-1.90
CBM2(III)B5	1.08	-107.7
CBM2(III)B6	0.46	11.5
CBM2(III)B7	0.35	32.7

Table 8 Deflection Comparisons

Model	Deflection	% Difference
CBM3(III)A1	0.1	
CBM3(III)A2	0.11	-1.1
CBM3(III)A3	0.1	0.00
CBM3(III)A4	0.11	-1.1
CBM3(III)A5	0.13	-30.0
CBM3(III)A6	0.09	10.0
CBM3(III)A7	0.08	20.0
CBM3(III)B1	0.31	
CBM3(III)B2	0.31	0.00
CBM3(III)B3	0.31	0.00
CBM3(III)B4	0.31	0.00
CBM3(III)B5	0.35	-12.9
CBM3(III)B6	0.3	3.22
CBM3(III)B7	0.21	32.25

Table 9 Deflection Comparisons

Model	Deflection	% Difference
CBM4(III)A1	0.31	
CBM4(III)A2	0.31	0.00
CBM4(III)A3	0.31	0.00
CBM4(III)A4	0.31	0.00
CBM4(III)A5	0.38	-22.6
CBM4(III)A6	0.26	16.1
CBM4(III)A7	0.22	29.0
CBM4(III)B1	1.13	
CBM4(III)B2	1.14	-0.88
CBM4(III)B3	1.13	0.00
CBM4(III)B4	1.14	-0.88
CBM4(III)B5	1.23	-8.84
CBM4(III)B6	1.11	1.76
CBM4(III)B7	0.74	34.5

Although the changes in shear stud placement yielded results showing little change in the beam deflections, it is important to look at the differences in light of the moment diagrams. The diagrams demonstrate how changes in the number of shear connectors in the negative moment region impacted the moment forces on the WF sections. The problem of understanding what is happening in the negative moment regions is one of stress distribution rather than load versus deflection. The values from the moment diagrams provide some insight as to how the reduction in shear connectors influences regions of positive and negative moment (Table 10).

Table 10 Moment Comparisons

Model		Negative End Moments	Positive Mid Span Moments
		(in-lbf)	(in-lbf)
CBM1(III)A1		-687927	301524
CBM1(III)A3		-690173	300011
CBM1(III)A4		-689222	299183
CBM2(III)A1		-42061	117508
CBM2(III)A3		-46003	127397
CBM2(III)A4		-43251	121912
CBM3(III)A1		-310193	88452
CBM3(III)A3		-310203	89932
CBM3(III)A4		-316250	89773
CBM4(III)A1		-327022	120000
CBM4(III)A3		-329112	120000
CBM4(III)A4		-327941	118000

Moment diagrams provided by ANSYS show the moments at the end of the beams to be positive, the moment in the beam centers to be negative; the values have been changed from positive to negative for the end moments and from negative to positive (Table 10) for the mid span moments in an effort to follow standard convention.

The end moments in beam CBM1 are greatest with a reduction in shear connectors at the mid span rather than a reduction in shear connectors at the end spans. However, the end moments for both partially composite conditions are greater than the original, fully composite section (Figure 107). The reason for the negative end moment behavior in model CBM1 has to do with the way the model is created and the way ANSYS works; ANSYS does not combine the line elements to give an overall composite beam moment value; the results of the analysis present moments in the line elements.

Note, the horizontal axis describe the stud conditions in the graphs of the Negative End Moments and Positive Mid Span Moments which follow. The number 1 represents the fully composite condition; number 2 represents a 2/3 reduction in the number of shear connectors at mid span of the beam; number 3 represents a 2/3 reduction at the end 1/3 sections of the beam. In short, number 2 corresponds to stud condition 3, number 3 corresponds to stud condition 4.

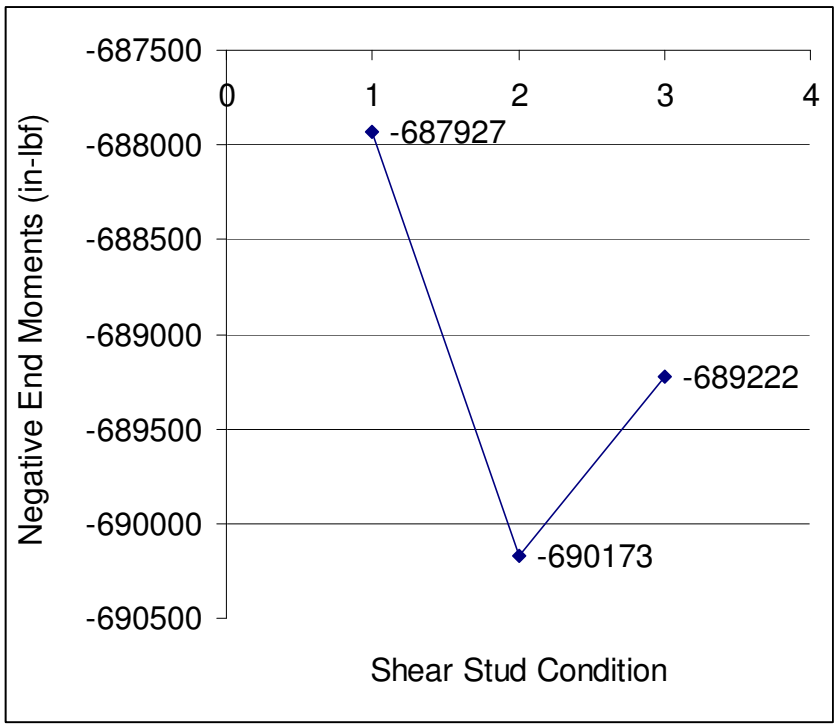

Figure 107 CBM1 Negative End Moments

The bending stresses in the slab and WF sections for CBM1 are presented in Table 11.

Table 11 CBM1 Comparison of Bending Stresses

Fully Composite Bending Stresses	
Slab	6.745 ksi
WF Section	17.28 ksi

Partially Composite Bending Stresses (2/3 Reduction of Shear Connectors Mid Span)	
Slab	6.767 ksi
WF Section	17.34 ksi

Partially Composite Bending Stresses (2/3 Reduction of Shear Connectors @ End Spans)	
Slab	6.758ksi
WF Section	17.32 ksi

With the number of shear connectors reduced at the mid span of the beam there is less shear transfer between the WF beam and slab (at the mid span), which imposes more shear transfer on the shear connectors at the end spans. With more shear transfer at the beam ends the negative moment value increases. With the number of shear connectors reduced at the beam end spans there is less shear transfer into the WF beam reducing the moment value. Due to the large slab, the depth of the stress block, the location of the PNA is well above the beam flange; the large slab area of CBM1 is able to assume more of the tension load in the negative moment region imposing less moment on the beam elements.

The change in the positive moment is interesting. With a reduction in the number of shear connectors the amount of moment in beam elements decreases as more is taken into the slab (Figure 108). The beam elements in the fully composite section take on

more moment (in the regions of positive moment) than they do in the partially composite sections because there is reduction in the number of shear connectors. With a reduction in the number of shear connectors there is less sharing of the moments in the partially composite sections and more of the moment is forced into the slab.

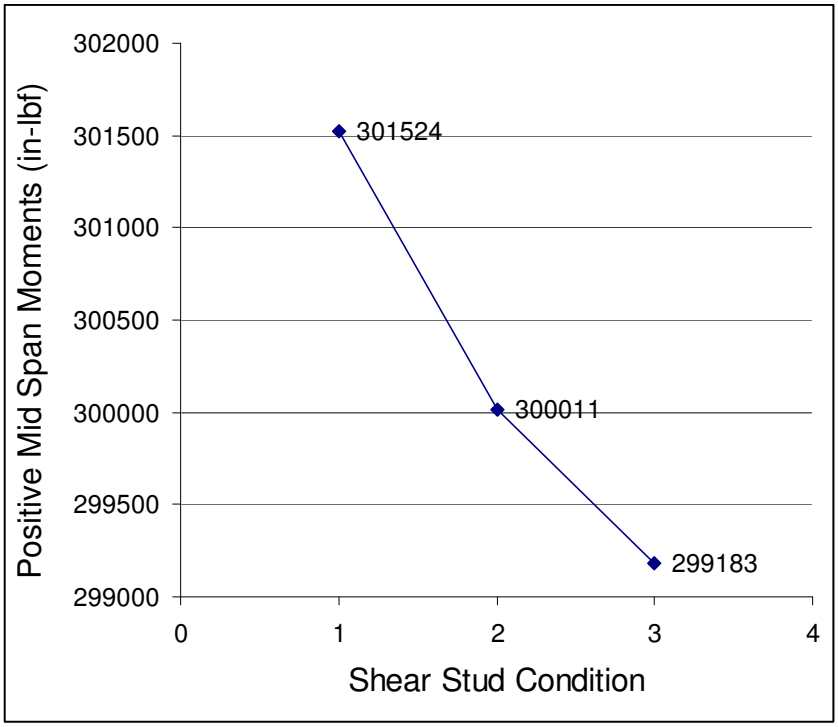

Figure 108 CBM1 Positive Mid Span Moments

Although slight, it is helpful to compare the difference in percentages of the three shear stud conditions (Table 12).

Table 12 Comparison of CBM1 Moments

	% Difference Between CBM1(III)A1 and CBM1(III)A3	% Difference Between CBM1(III)A1 and CBM1(III)A4	% Difference Between CBM1(III)A3and CBM1(III)A4
Negative End Moments	0.33	0.19	0.14
Positive Mid Span Moments	0.50	0.78	0.28

The end moments in beam CBM2 are greatest with a reduction in shear connectors at the mid span rather than a reduction in shear connectors at the end spans. However, the end moments for both partially composite conditions are greater than the original, fully composite section (Figure 109).

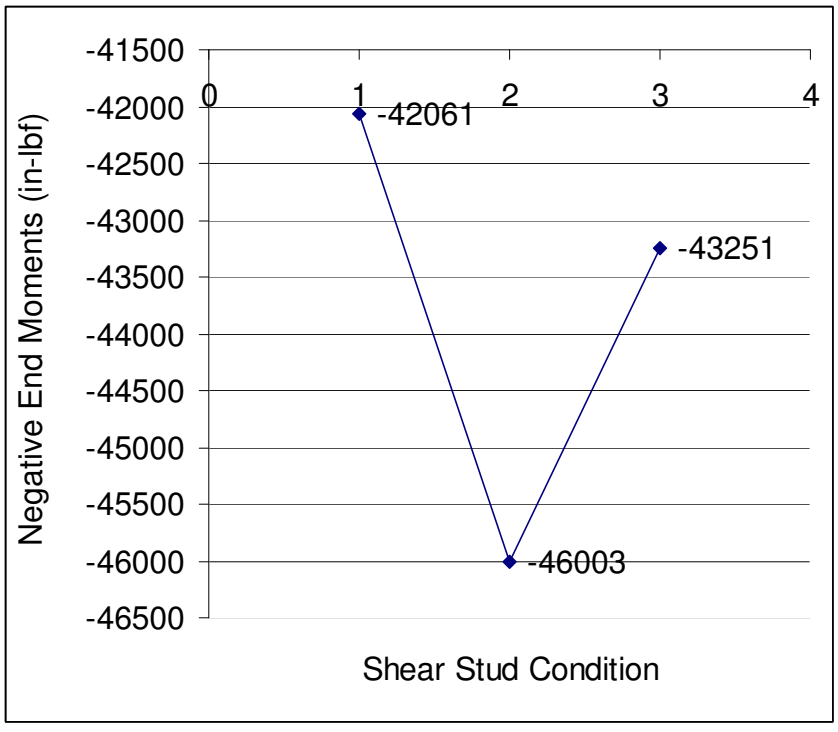

Figure 109 CBM2 Negative End Moments

The bending stresses in the slab and WF sections for CBM2 are presented in Table 13.

Table 13 CBM2 Comparison of Bending Stresses

Fully Composite Bending Stresses	
Slab	.412 ksi
WF Section	1.057 ksi

Partially Composite Bending Stresses (2/3 Reduction of Shear Connectors Mid Span)	
Slab	.451 ksi
WF Section	1.156 ksi

Partially Composite Bending Stresses (2/3 Reduction of Shear Connectors @ End Spans)	
Slab	.424 ksi
WF Section	1.087 ksi

The composite action, or lack thereof, of the model is influencing the negative end moment behavior in model CBM2. Because the model is not acting compositely, there is already little contribution toward the strength of the section by the shear studs at the end spans. A reduction in the number of shear studs at the mid span reduces what little contribution there is by the shear connectors (towards the strength of the section) to even less.

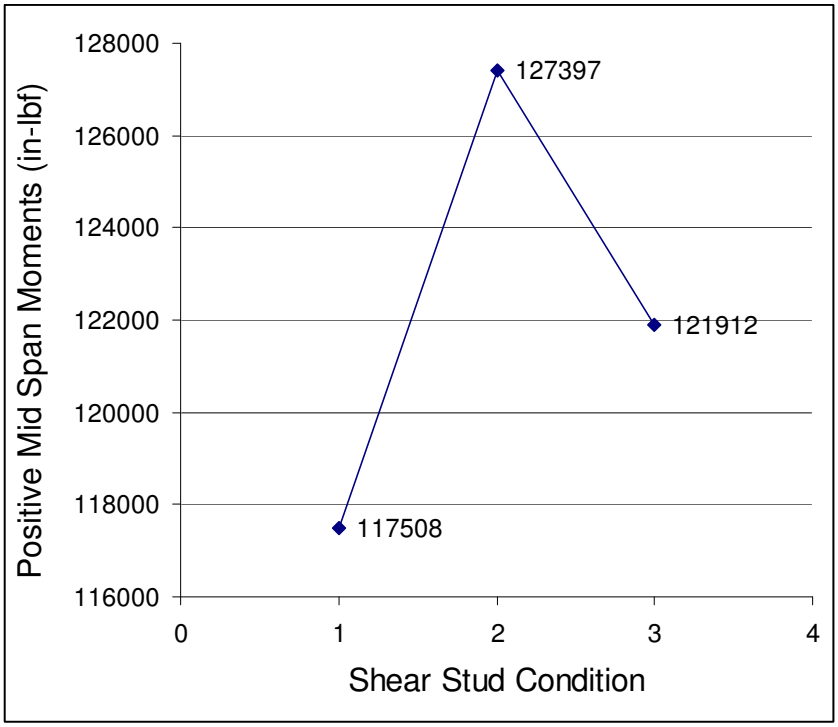

Figure 110 CBM2 Positive Mid Span Moments

If CBM2 were acting compositely the reduction in the number of shear studs at mid span would cause a decrease in the positive moment as less moment is transferred into the beam elements and more into the slab; as is the case with CBM1. Because CBM2 is not acting compositely, the reduction in the number of shear studs causes an increase in the moment for the beam element because there is no mechanism by which the shears (due to moment) may be transferred to slab; the shears are in the WF section (Figure 110).

Although slight, it is helpful to compare the difference in percentages of the three shear stud conditions (Table 14).

Table 14 Comparison of CBM2 Moments

	% Difference Between CBM2(III)A1 and CBM2(III)A3	% Difference Between CBM2(III)A1 and CBM2(III)A4	% Difference Between CBM2(III)A3and CBM2(III)A4
Maximum End Moments	8.57	2.75	6.36
Minimum Mid Moments	7.76	3.61	4.50

The end moments in beam CBM3 are greatest with a reduction in shear connectors at the end spans rather than a reduction in shear connectors at the mid spans. However, the end moments for both partially composite conditions are greater than the original, fully composite section.

With the number of shear connectors reduced at the mid span of the beam there is less shear transfer between the WF beam and slab (at the mid span), which imposes more shear transfer on the shear connectors at the end spans.

With more shear transfer at the beam ends the negative moment value increases. With the number of shear connectors reduced at the beam end spans there is less shear transfer into the WF beam reducing the moment value. (Figure 111). The characteristics of the section with PAN located so close to the beam flange, as well as the length of the beam (given the narrow slab width) contribute to the reduction in the number of shear studs at the end spans of the beam creating greater moments in the composite section.

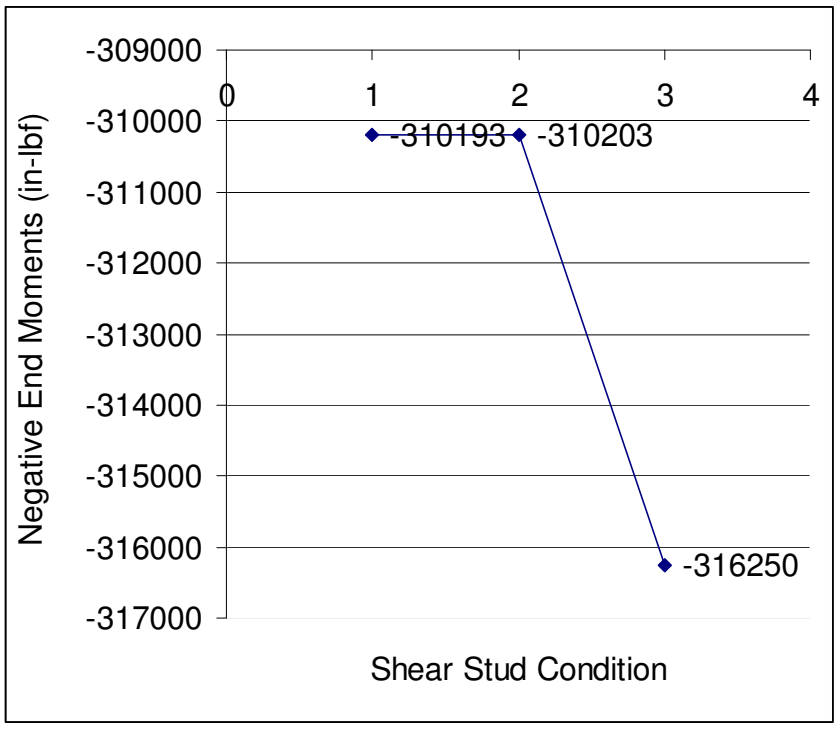

Figure 111 CBM3 Negative End Moments

The bending stresses in the slab and WF sections for CBM2 are presented in Table 13.

Table 15 CBM3 Comparison of Bending Stresses

Fully Composite Bending Stresses	
Slab	4.079 ksi
WF Section	8.301 ksi
Partially Composite Bending Stresses (2/3 Reduction of Shear Connectors Mid Span)	
Slab	4.079 ksi
WF Section	8.301 ksi
Partially Composite Bending Stresses (2/3 Reduction of Shear Connectors @ End Spans)	
Slab	4.158 ksi
WF Section	8.462 ksi

Although CBM3 is acting compositely, the PNA of the section is located so close to the beam flange the positive moment pattern is similar to that of CBM2, which is not acting compositely. As with CBM2, if the PNA were located farther away from the beam flange (and thus acting more compositely) the reduction in the number of shear studs at mid span would cause a decrease in the positive moment as less moment is transferred into the beam elements and more into the slab; as is the case with CBM1. Because CBM3 is barely acting compositely, the reduction in the number of shear studs causes an increase in the moment for the beam element because there is the mechanism by which the shears (due to moment) may be transferred to slab is limited (Figure 110).

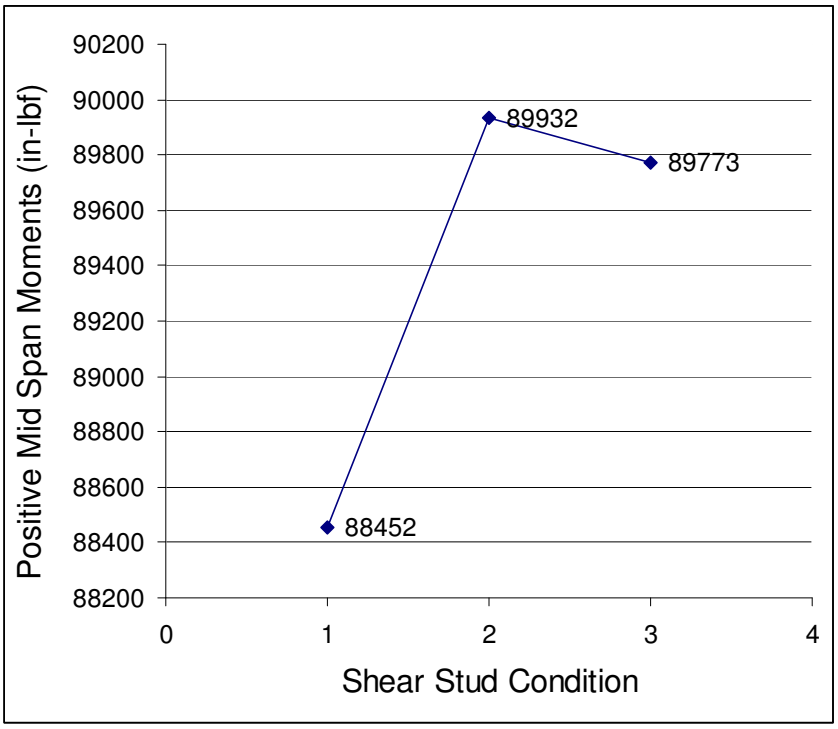

Figure 112 CBM3 Positive Mid Span Moments

Although slight, it is helpful to compare the difference in percentages of the three shear stud conditions (Table 16).

Table 16 Comparison of CBM3 Moments

	% Difference Between CBM3(III)A1 and CBM3(III)A3	% Difference Between CBM3(III)A1 and CBM3(III)A4	% Difference Between CBM3(III)A3and CBM3(III)A4
Maximum End Moments	0.00	1.92	1.91
Minimum Mid Moments	1.65	1.47	0.18

The end moments in beam CBM4 are greatest with a reduction in shear connectors at the mid span rather than a reduction in shear connectors at the end spans. However, the end moments for both partially composite conditions are greater than the original, fully composite section (Figure 113). The behavior of the negative moment in model CBM4 is similar to that of CBM1. The number of shear connectors is reduced at the mid span of the beam leading to less shear transfer between the WF beam and slab (at the mid span), which imposes more shear transfer on the shear connectors at the end spans. With more shear transfer at the beam ends the negative moment value increases. The number of shear connectors reduced at the beam end spans leading to less shear transfer into the WF beam reducing the moment value. Due to the large slab, the depth of the stress block, the location of the PNA is well above the beam flange; the large slab area of CBM4 is able to assume more of the tension load in the negative moment region imposing less moment on the beam elements.

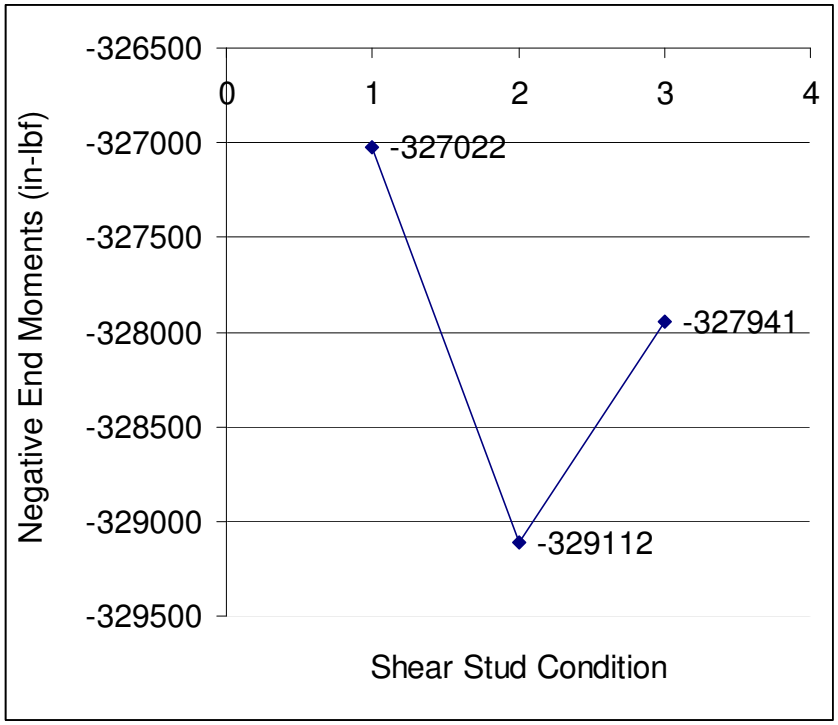

Figure 113 CBM4 Negative End Moments

The bending stresses in the slab and WF sections for CBM4 are presented in Table 17.

Table 17 CBM4 Comparison of Bending Stresses

Fully Composite Bending Stresses	
Slab	.911 ksi
WF Section	4.118 ksi
Partially Composite Bending Stresses (2/3 Reduction of Shear Connectors Mid Span)	
Slab	.917 ksi
WF Section	4.144 ksi
Partially Composite Bending Stresses (2/3 Reduction of Shear Connectors @ End Spans)	
Slab	.914 ksi
WF Section	4.13 ksi

The change in the positive moment is interesting. With a reduction in the number of shear connectors the amount of moment in beam elements decreases as more is taken into the slab (Figure 114). The beam elements in the fully composite section take on more moment (in the regions of positive moment) than they do in the partially composite sections because there is reduction in the number of shear connectors. With a reduction in the number of shear connectors there is less sharing of the moments in the partially composite sections and more of the moment is forced into the slab.

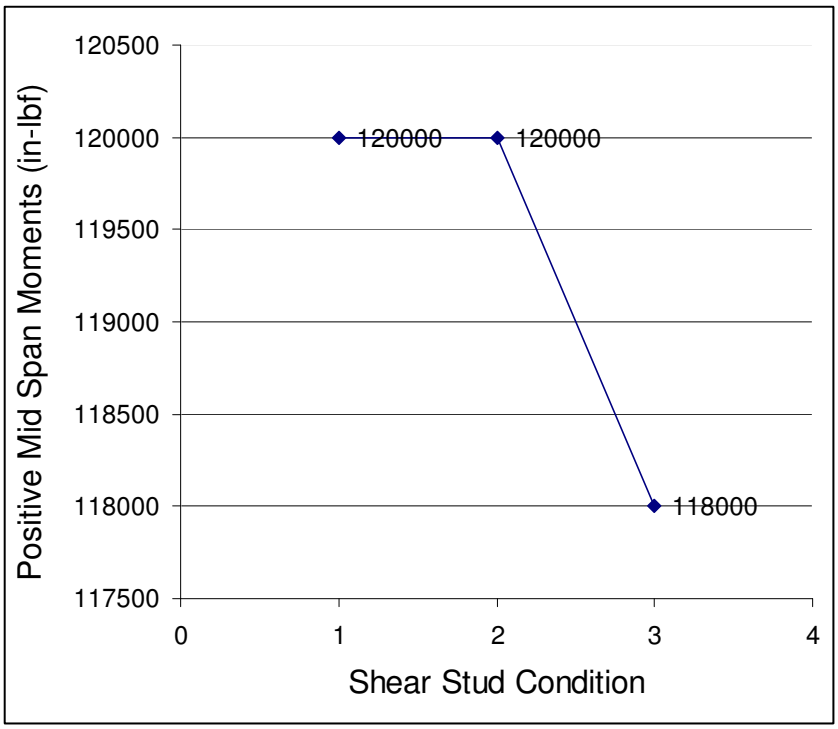

Figure 114 CBM4 Positive Mid Span Moments

Although slight, it is helpful to compare the difference in percentages of the three shear stud conditions (Table 18).

Table 18 Comparison of CBM4 Moments

	% Difference Between CBM4(III)A1 and CBM4(III)A3	% Difference Between CBM4(III)A1 and CBM4(III)A4	% Difference Between CBM4(III)A3and CBM4(III)A4
Maximum End Moments	0.64	0.28	0.36
Minimum Mid Moments	0.00	1.69	1.69

The shear diagrams indicate the shear connectors experience the least load when fully composite, more load with the reduced number of connectors in the middle of the span, and worst-case load with the reduction in the number of shear connectors at each end of the beam span. This corresponds to previous research indicating the shear capacity of beam in negative bending is reduced due to the additional shear imposed on the shear studs (Liang, et al. 2004)

CHAPTER 5
CONCLUSIONS

At the beginning of this thesis, three objectives are listed. They are:

1. Attempt to verify the current methods of composite beam design under positive moment loads.
2. Gain more understanding of composite beams under negative moment loads.
3. Understand the problems associated with FE modeling of composite beams in general.

Addressing the third item first, Finite Element modeling of composite beams is difficult; there are at least three obstacles to obtaining reliable results. The first obstacle is the creation of the FE model. Boundary conditions must be determined and accurately modeled, sections determined, concrete properties modeled. Within ANSYS there are elastic elements, plastic elements, shell elements, solid elements, and beam elements (to name a few) and all contain sub categories of elements, elements with different numbers of nodes. The choice of element has an effect on how efficiently the model calculates; it also has an influence on what sort of information may be derived from the FE model, e.g. a model composed of nothing but beam elements may be a poor choice with which to investigate cracking in the slab.

Another problem with FE modeling is simple inaccuracy. The size of the aggregate in the concrete mix, the size and placement of the reinforcing material, the

gage and orientation of the deck, adhesion between the slab and the deck, adhesion between the deck and beam, cracking in the slab, the action of the concrete crushing around the shear stud, and shear stud bending, these compose a list of items which will influence the strength of a composite section. It is difficult to verify the accuracy of an FE model without some, real life composite beam example with which to compare.

Having "run" the FE model, the modeler is now faced with the problem of understanding the results. The ANSYS models created for this thesis do not provide a single moment value for the combined composite section. Instead, ANSYS provides moment values for the beam elements, slab elements, and shear stud elements. It is up to the researcher to accurately analyze and understand what the FE model is showing. In sum, it may, and probably will, take the researcher numerous attempts and much effort before a satisfactory FE model can be created.

The second objective is to understand better the problem of negative moments in composite beams. The problem with negative moments is cracking in the slab. When the slab cracks there is no composite action. One may overcome the problem of a cracked slab with an increased amount of longitudinal reinforcement or exotic concrete mixes, which may better sustain tension loads. Indeed, there may come a time when commonly used concrete has enough tensile strength to merit designing composite beams with tension forces in the slab; concrete mixes continue to improve.

The fully composite sections in this thesis, fixed at both ends, manifested the least negative moment with shear studs spaced over the entire length of the section. Reducing the number of shear studs at the ends of the beam resulted in less negative moment than reduction in shear connectors at mid span, but both negative moments of the different

partially composite sections were greater than the fully composite condition of shear studs spaced over the length of the beam. Reducing the number of shear connectors at the mid span of the beam resulted in the greatest negative moment load. However, the difference in negative moments, for all three conditions, was not large. In all of the fully composite models created, the difference in the resulting negative moments between fully and partially composite sections was less than 2%. This verifies the thought that shear connectors in regions of negative moment offer little in the way of aiding composite action.

The current practice of welding shear studs over the entire length of a beam section, including regions of hogging moment, should continue. Even though the effect of the shear studs in those regions is nil, there are practical concerns about actual erection procedures. Increasing the complication of shear stud location only increases the possibility of mistakes.

The third objective is to verify current methods of composite beam design under positive moment loads. This thesis provides no reason why the current methods of composite beam design should be changed. The results of the FE modeling yielded results a structural engineer would expect. An increase in slab thickness will increase the stiffness of the composite section. An increase in shear connector area will increase the stiffness of the composite section. A decrease in the shear connector area will reduce the stiffness of the composite. In regions of negative moment, a thicker slab will help resist moment loads. The farther away the stress block is from the WF flange, the better the section will be able to resist negative as well as positive moment loads. Reducing the number of shear connectors in the positive moment region reduces the ability of the

composite section to carry positive moment loads. These results are not surprising and reinforce the design methodology now used for composite beam design, both for positive and negative moment loads.

LIST OF REFERENCES

Allison, Horatio; *Low- and Medium Rise Steel Buildings, Steel Design Guide 5*, American Institute of Steel Construction, Inc. Chicago, Il., 1991.

Aref, Amjad J.; Chiewanichakorn, Methee; Chen, Stuart S; Ahn, Il-Sang; "Effective Slab Width Definition for Negative Moment Regions of Composite Bridges," *Journal of Bridge Engineering*, Vol. 12, No. 3, May 1, 2007, pp. 339-349.

Bujňák, J.; Ondrobiňák, J.; "Crack Control in Concrete Slab of Composite Structure," *Proceedings of the International Conference "Reliability and Diagonostics of Transport Structures and Means,"* University of Pardubice, Czech Republic, September, 2002.

Carlsson, Magnus; Hajjar, Jerome F.; "Fatigue of Stud Shear Connectors in the Negative Moment Region of Steel Girder Bridges," *University of Minnesota Digital Conservancy*, Minnesota, June, 2000.

Chiewanichakorn, Methee; Amjad, J.; Chen, Stuart S.; Ahn, Il-Sang; Carpenter, Jeffrey A.; "Effective Flange Width of Composite Girders in Negative Moment Region," *Transportation Research Board of the National Academies*, Special Volume CD 11-S, June 17, 2008, pp. 203-216.

Civjan, Scott A.; Singh, Prabheet; "Behavior of Shear Studs Subjected to Fully Reversed Cyclic Loading," *Journal of Structural Engineering*, Vol. 129, No. 11, November 1, 2003, pp.1466-1474.

Dekker, N. W.; Kemp, A. R.; Trinchero, P.; "Factors Influencing the Strength of Continuous Composite Beams in Negative Bending," *Journal Constructional Steel Research*, Volume 34, 1995, pp. 161-185.

Dorey, Alfred B.; Cheng, Roger J. J.; "The Behavior of Composite Beams with no Flexural Steel Under Negative Moment," *Annual Conference of the Canadian Society for Civil Engineering*, Sherbrooke, Quebec, May 27-30, 1997.

Easterling, Samuel W.; Gibbings, David R.; Murray, Thomas M.; "Strength of Shear Studs in Steel Deck on Composite Beams and Joists," *Engineering Journal, American Institute of Steel Construction*, Second Quarter, 1993, pp. 44-55.

Fabbrocino, G.; Manfredi, G.; Cosenza, E.; "Analysis of Continuous Composite Beams Including Partial Interaction and Bond," *Journal of Structural Engineering*, Vol. 126, No. 11, November, 2000, pp. 1288- 294.

Gilbert, Ian R.; Bradford, Mark Andrew; "Time Dependent Behavior of Continuous Composite Beams at Service Loads," *Journal of Structural Engineering*, Vol. 121, No. 2, February, 1995, pp. 319-327.

Lääne, Ahti; "Post-Critical Behavior of Composite Bridges Under Negative Moment and Shear," Thèse No. 2889, Ècole Polytechnique Fédérale de Lausanne, 2003.

International Building Code®, 2003, Chapter 10, Composite Steel and Concrete Structure Design Requirements, pp. 175-182.

Lam, Dennis; El-Lobody, Ehab; "Behavior of Headed Stud Shear Connectors in Composite Beam," *Journal of Structural Engineering*, Vol. 131, No. 1, January 1, 2005, pp. 96-107.

Leon, Roberto T.; Hoffman, Jerod J.; Staeger, Tony; *Partially Restrained Composite Connections, Steel Design Guide 8*, American Institute of Steel Construction, Inc., Chicago, IL., 1996.

Liang, Qing Quan; Uy, Brian; Bradford, Mark A.; Hamid, Ronagh R.; "Ultimate Strength of Continuous Composite Beams in Combined Bending and Shear," *Journal of Constructional Steel Research*, Vol. 60, 2004, pp. 1109-1128.

Long, A. E.; Van Dalen, K.; Csagoly, P.; "Fatigue Behavior of Negative Moment Regions of Continuous Composite Beams at Low Temperatures," *Canadian Journal of Civil Engineering*, Vol. 2, No. 1, 1975, pp. 98-115.

Lorenz, Robert F.; "Understanding Composite Beam Design Methods," *Engineering Journal, American Institute of Steel Construction*, First Quarter, 1988, pp. 35-38.

Macorini, L.; Fragiacomo, L.; Amadio, C.; Izzuddin, B.A.; "Long-term Analysis of Steel-Concrete Composite Beams: FE Modeling for Effective Width Evaluation," *Engineering Structures*, Vol. 28, 2006, pp. 110-1121.

Manfredi, Gaetano; Fabbrocino, Giovanni; Cosenza, Edoardo; "Modeling of Steel-Concrete Composite Beams Under Negative Bending," *Journal of Engineering Mechanics*, Vol. 125, No. 6, June, 1999, pp. 654-662.

Moaveni, Saeed; Finite Element Analysis Theory and Application with ANSYS, Third Edition, Pearson Prentice Hall, Upper Saddle River, NJ, 2008

Nie, Jianguo; Fan, Jiansheng; Cai, C.S.; "Stiffness and Deflection of Steel-Concrete Composite Beams Under Negative Bending," *Journal of Structural Engineering*, Vol. 130, No. 11, November 1, 2004, pp.1842-1851.

Nerthercot, D. A.; Composite Construction, Taylor and Francis Group, LLC, 2009.

Raafat, El-Hacha; Ragab, Nora; "Flexural Strengthening of Composite Steel-Concrete Girders Using Advanced Composite Materials, *Third International Conference on FRP Composites in Civil Engineering (CICE 2006)*, Miami, Florida, USA, December 13-15, 2006.

Salmon, Charles G.; Johnson, John E.; Steel Structures Design and Behavior Emphasizing Load and Resistance Factor Design, Third Edition, Harper & Row, New York, 1990.

Šavor, Zlatko; Bleiziffer, Jelena; "From Melan to Arch Bridges of 400 M Spans," *Chinese-Croation Joint Colloquium Long Arch Bridges*, Brijuni Islands, July 10-14, 2008.

Springolo, Mario; Earp, Gerard van; Khennane, Amar; "Design and Analysis of Composite Beam for Infrastructure Application," *International Journal of Materials and Product Technology*, Vol. 25, No. 4, 2006, pp. 297-312.

Steel Construction Institute, www.steelconstruction.org/static/assets/source/114-AdvisoryDeskAD266.pdf, 1988-2002.

Steel Construction Manual, 2nd Edition, American Institute of Steel Construction, Inc., 1998, p. 6-65 through 6-67.

Steel Construction Manual, 13th Edition, American Institute of Steel Construction, Inc., 2005, p. 3-29 through 3-32, 16.1-83 through 16.1-89.

Szabó, Bertalan; "Influence of Shear Connectors on the Elastic Behavior of Composite Girders," *Helsinki University of Technology Publications in Bridge Engineering*, Doctoral Dissertation, Espoo, Finland, December, 2006 .

Tamboli, Akbar; Steel Design Handbook LRFD Method, McGraw-Hill, New York, 1997

Tehami, M.; "Local Buckling in Class 2 Continuous Composite Beams," *Journal of Constructional Steel Research*, Vol. 43, Nos. 1-3, 1997, pp. 141-159.

Thermou, G.; Elnashai, A.S.; Plummier, A.; "Seismic Design and Performance of Composite Frames," *Journal of Constructional Steel Research*, Vol. 60, Issue 1, January 2004, pp. 31-57.

Topkaya, Cem; Yura, Joseph A.; Willamson, Eric B.; "Composite Shear Stud Strength at Early Concrete Ages," *Journal of Structural Engineering*, Vol. 130, No. 6, June1, 2004, pp.952-960.

Veljkovic, Milan; Johansson, Bernt; "Residual Static Resistance of Welded Stud Shear Connectors," Composite Construction in Steel and Concrete V; *Proceedings of the 5th*

International Conference on Composite Construction, Kruger National Park, Berg-en-Dal, July 18-23, 2004.

Viest, Ivan M.; "Development of Design Rules for Composite Construction," *Engineering Journal, American Institute of Steel Construction*, Fourth Quarter, 2003, pp. 181-188.

Viest, Ivan M.; Colaco, Joseph P.; Furlong, Richard W.; Griffis, Lawrence G.; Leon, Roberto T.; Wyllie Jr., Loring A.; Composite Construction Design for Buildings, McGraw-Hill, New York, NY, 1997.

Vinnakota, Sriramulu; Foley, Christopher M.; Vinnakota, Murthy R.; "Design of Partially or Fully Composite Beams. With Ribbed Metal Deck, Using LRFD Specifications," *Engineering Journal, American Institute of Steel Construction*, Second Quarter, 1988, pp. 60-78.

Vulcraft Steel Roof and Floor Deck Catalog, 2001.

Yassin, Airil Y. Mohd; Nethercot, David A.; "Cross Sectional Properties of Complex Composite Beams," *Engineering Structures*, Vol. 29, 2007, pp. 195-212.

Zahn, Mark C.; "The Economies of LRFD in Composite Floor Beams," *Engineering Journal, American Institute of Steel Construction*, Second Quarter, 1987, pp. 87-92.

Zona, A.; Barbato, M.; Conte, J.P.; "The Finite Element Response Sensitivity Analysis of Steel-Concrete Composite Beams with Deformable Shear Connection," *Journal of Engineering Mechanics*, Vol. 131, No. 11, Nov
ember 1, 2005, pp. 1126-1139.

APPENDIX A

CBM1 STRESS BLOCK AND PLASTIC NEUTRAL AXIS CALCULATION

CBM1 PNA Calc

Concrete Weight: $w := 145 pcf$

Compressive Strength: $f'_c := 5000 psi$

Young's Modulus (Steel) $E_s := 29000 ksi$ $F_y := 50 ksi$

$E_c := 33 \cdot \left(\frac{w}{pcf} \right)^{1.5} \cdot \sqrt{\frac{f'_c}{psi}} \cdot psi$ $E_c = 4.074 \times 10^6 \cdot psi$

$n := \frac{E_s}{E_c}$ $n = 7.118$ Use: $n := 7$

$b_E := 51.2 in$ $t_s := 4 in$ $L_{beam} := 177 in$

$b_f := 7.874 in$

$t_f := .394 in$

$t_w := .256 in$

$d_b := 7.48 in$

Reference Steel Structures Design and Behavior

(Salmon and Johnson, 1990) pages 1010-1061 for all equations in Appendix A.

$$I_{bm} := \frac{b_f \cdot d_b^{\,3}}{12} - 2 \cdot \frac{\left(d_b - 2 \cdot t_f\right)^3 \cdot \left(\frac{b_f - t_w}{2}\right)}{12} \qquad I_{bm} = 84.36\,in^4$$

Slab Equivalent Width: $b_{eq} := \frac{b_E}{n}$ $b_{eq} = 7.314\,in$

$A_{tr} := b_{eq} \cdot t_s$ $A_{tr} = 29.257\,in^2$

$I_{slab} := \frac{b_{eq} \cdot t_s^{\,3}}{12}$ $I_{slab} = 39.01\,in^4$

Transformed Areas Moment Arms

Slab: $A_{tr} = 29.257\,in^2$ $d_1 := \frac{d_b + t_s}{2}$ $d_1 = 5.74\,in$

$A_{d1} := d_1 \cdot A_{tr}$ $A_{d1} = 167.936\,in^3$

$A_{d12} := A_{tr} \cdot d_1^{\,2}$ $A_{d12} = 963.953\,in^4$

Total Areas: $A_{total} := A_{tr} + A_s$ $A_{total} = 37.175\,in^2$

Total Moments of Inertia $I_{total} := I_{slab} + I_{bm}$ $I_{total} = 123.37\,in^4$

$I_x := I_{total} + A_{d12}$ $I_x = 1.087 \times 10^3 \cdot in^4$

$y_{bar} := \frac{A_{d1}}{A_{total}}$ $y_{bar} = 4.517\,in$

$y_t := \frac{d_b}{2} - y_{bar} + t_s$ $y_t = 3.223\,in$

$y_b := \frac{d_b}{2} + y_{bar}$ $y_b = 8.257\,in$

$A_s := b_f \cdot t_f \cdot 2 + \left(d_b - 2 \cdot t_f\right) \cdot t_w$ $A_s = 7.918\,in^2$ $d_b = 11.48\,in$

$$I_{tr} := I_x - A_{total} \cdot y_{bar}^2 \qquad I_{tr} = 328.681\,in^4$$

$$S_{top} := \frac{I_{tr}}{y_t} \qquad S_{top} = 101.994\,in^3$$

$$S_{bot} := \frac{I_{tr}}{y_b} \qquad S_{bot} = 39.804\,in^3$$

PNA Calc

Assume Whitney rectangular stress distribution

$$a := \frac{A_s \cdot F_y}{0.85 \cdot f'_c \cdot b_E} \qquad a = 1.819\,in$$ Depth of Stress Block

$$C := .85 \cdot f'_c \cdot a \cdot b_E \qquad C = 3.959 \times 10^5 \cdot lbf$$

$$T := A_s \cdot F_y$$

$$C_c := .85 \cdot f'_c \cdot b_E \cdot t_s \qquad C_s := \frac{A_s \cdot F_y - .85 \cdot f'_c \cdot b_E \cdot t_s}{2}$$

$$M_{n1} := A_s \cdot F_y \cdot \left(\frac{d_b}{2} + t_s - \frac{a}{2} \right) \qquad M_{n1} = 2.704 \times 10^3 \cdot in \cdot kip$$

$$d'_2 := d_b + \frac{t_s}{2} - y_{bar} \qquad d'_2 = 4.963\,in$$

$$d''_2 := d'_2 + \frac{t_s}{2} - \left(t_s + \frac{t_f}{2} \right) \qquad d''_2 = 2.766\,in$$

$$M_{n2} := C_c \cdot d'_2 + C_s \cdot d''_2 \qquad M_{n2} = 3.663 \times 10^3 \cdot in \cdot kip$$

$$M_n := \begin{cases} M_{n1} & \text{if } a < t_s \\ M_{n2} & \text{if } a \geq t_s \end{cases} \qquad M_n = 2.704 \times 10^3 \cdot in \cdot kip$$

$$PNA := \begin{cases} \text{"Located in Slab"} & \text{if } a < t_s \\ \text{"Located in WF Section"} & \text{if } a \geq t_s \end{cases} \qquad PNA = \text{"Located in Slab"}$$

APPENDIX B

CBM2 STRESS BLOCK AND PLASTIC NEUTRAL AXIS CALCULATION

Reference Steel Structures Design and Behavior (Salmon and Johnson, 1990) pages 1010-1061 for all equations in Appendix B.

CBM2 PNA Calc

Concrete Weight: $w := 145 pcf$

Compressive Strength: $f'_c := 5800 psi$

Young's Modulus (Steel) $E_s := 29000 ksi$ $F_y := 50 ksi$

$$E_c := 33 \cdot \left(\frac{w}{pcf} \right)^{1.5} \cdot \sqrt{\frac{f'_c}{psi}} \cdot psi \qquad E_c = 4.388 \times 10^6 \cdot psi$$

$$n := \frac{E_s}{E_c} \qquad n = 6.609$$

$b_E := 17.13 in$ $t_s := 2.2 in$

$b_f := 4 in$

$t_f := .255 in$

$t_w := .23 in$

$d_b := 8 in$

$$A_s := b_f \cdot t_f \cdot 2 + \left(d_b - 2 \cdot t_f \right) \cdot t_w \qquad A_s = 3.763 in^2$$

$$I_{bm} := \frac{b_f \cdot {d_b}^3}{12} - 2 \cdot \frac{\left(d_b - 2 \cdot t_f\right)^3 \cdot \left(\frac{b_f - t_w}{2}\right)}{12} \qquad I_{bm} = 38.657\,in^4$$

Slab Equivalent Width: $b_{eq} := \frac{b_E}{n}$ $\qquad b_{eq} = 2.592\,in$

$$A_{tr} := b_{eq} \cdot t_s \qquad A_{tr} = 5.702\,in^2$$

$$I_{slab} := \frac{b_{eq} \cdot {t_s}^3}{12} \qquad I_{slab} = 2.3 \cdot in^4$$

Transformed Areas Moment Arms

Slab: $A_{tr} = 5.702\,in^2$ $\qquad d_1 := \frac{d_b + t_s}{2}$ $\qquad d_1 = 5.1 \cdot in$

$$A_{d1} := d_1 \cdot A_{tr} \qquad A_{d1} = 29.083\,in^3$$

$$A_{d12} := A_{tr} \cdot {d_1}^2 \qquad A_{d12} = 148.321 \cdot in^4$$

Total Areas: $A_{total} := A_{tr} + A_s$ $\qquad A_{total} = 9.465\,in^2$

Total Moments of Inertia $I_{total} := I_{slab} + I_{bm}$ $\qquad I_{total} = 40.957 \cdot in^4$

$$I_x := I_{total} + A_{d12} \qquad I_x = 189.278\,in^4$$

$$y_{bar} := \frac{A_{d1}}{A_{total}} \qquad y_{bar} = 3.073\,in$$

$$I_{tr} := I_x - A_{total} \cdot {y_{bar}}^2 \qquad I_{tr} = 99.919\,in^4$$

$$y_t := \frac{d_b}{2} - y_{bar} + t_s \qquad y_t = 3.127 \cdot in$$

$$y_b := \frac{d_b}{2} + y_{bar} \qquad y_b = 7.073\,in$$

$$y_t + y_b = 10.2\,in \qquad t_s + d_b = 10.2\,in$$

$$S_{top} := \frac{I_{tr}}{y_t} \qquad S_{top} = 31.95\,in^3$$

$$S_{bot} := \frac{I_{tr}}{y_b} \qquad S_{bot} = 14.128\,in^3$$

PNA Calc

Assume Whitney rectangular stress distribution

$$a := \frac{A_s \cdot F_y}{0.85 \cdot f'_c \cdot b_E} \qquad a = 2.228\,in$$ Depth of Stress Block

$$C := .85 \cdot f'_c \cdot a \cdot b_E \qquad C = 1.881 \times 10^5 \cdot lbf$$

$$T := A_s \cdot F_y$$

$$C_c := .85 \cdot f'_c \cdot b_E \cdot t_s \qquad C_s := \frac{A_s \cdot F_y - .85 \cdot f'_c \cdot b_E \cdot t_s}{2}$$

$$M_{n1} := A_s \cdot F_y \cdot \left(\frac{d_b}{2} + t_s - \frac{a}{2} \right) \qquad M_{n1} = 956.879\,in \cdot kip$$

$$d'_2 := d_b + \frac{t_s}{2} - y_{bar} \qquad d'_2 = 6.027\,in$$

$$d''_2 := d'_2 + \frac{t_s}{2} - \left(t_s + \frac{t_f}{2} \right) \qquad d''_2 = 4.8\,in$$

$$M_{n2} := C_c \cdot d'_2 + C_s \cdot d''_2 \qquad M_{n2} = 1.125 \times 10^3 \cdot in \cdot kip$$

$$M_n := \begin{cases} M_{n1} & \text{if } a < t_s \\ M_{n2} & \text{if } a \geq t_s \end{cases} \qquad M_n = 1.125 \times 10^3 \cdot in \cdot kip$$

$$PNA := \begin{cases} \text{"Located in Slab"} & \text{if } a < t_s \\ \text{"Located in WF Section"} & \text{if } a \geq t_s \end{cases}$$

PNA = "Located in WF Section"

APPENDIX C

CBM3 STRESS BLOCK AND PLASTIC NEUTRAL AXIS CALCULATION

Reference Steel Structures Design and Behavior (Salmon and Johnson, 1990) pages 1010-1061 for all equations in Appendix C.

CBM3 PNA Calc

Concrete Weight: $w := 145 pcf$

Compressive Strength: $f'_c := 4931 psi$

Young's Modulus (Steel) $E_s := 29000 ksi$ $F_y := 58 ksi$

$$E_c := 33 \cdot \left(\frac{w}{pcf} \right)^{1.5} \cdot \sqrt{\frac{f'_c}{psi}} \cdot psi \qquad E_c = 4.046 \times 10^6 \cdot psi$$

$$n := \frac{E_s}{E_c} \qquad n = 7.167$$

$b_E := 31.5 in$ $t_s := 4 in$

$b_f := 7.874 in$

$t_f := .394 in$

$t_w := .256 in$

$d_b := 7.48 in$

$$A_s := b_f \cdot t_f \cdot 2 + \left(d_b - 2 \cdot t_f \right) \cdot t_w \qquad A_s = 7.918 in^2$$

$$I_{bm} := \frac{b_f \cdot {d_b}^3}{12} - 2 \cdot \frac{\left(d_b - 2 \cdot t_f\right)^3 \cdot \left(\frac{b_f - t_w}{2}\right)}{12} \qquad I_{bm} = 84.36\,in^4$$

Slab Equivalent Width: $b_{eq} := \frac{b_E}{n}$ $\qquad b_{eq} = 4.395\,in$

$$A_{tr} := b_{eq} \cdot t_s \qquad A_{tr} = 17.579\,in^2$$

$$I_{slab} := \frac{b_{eq} \cdot {t_s}^3}{12} \qquad I_{slab} = 23.439\,in^4$$

Transformed Areas Moment Arms

Slab: $A_{tr} = 17.579\,in^2$ $\qquad d_1 := \frac{d_b + t_s}{2}$ $\qquad d_1 = 5.74\,in$

$$A_{d1} := d_1 \cdot A_{tr} \qquad A_{d1} = 100.906\,in^3$$

$$A_{d12} := A_{tr} \cdot {d_1}^2 \qquad A_{d12} = 579.202\,in^4$$

Total Areas: $A_{total} := A_{tr} + A_s$ $\qquad A_{total} = 25.497\,in^2$

Total Moments of Inertia $I_{total} := I_{slab} + I_{bm}$ $\qquad I_{total} = 107.8\,in^4$

$$I_x := I_{total} + A_{d12} \qquad I_x = 687.001\,in^4$$

$$y_{bar} := \frac{A_{d1}}{A_{total}} \qquad y_{bar} = 3.958\,in$$

$$I_{tr} := I_x - A_{total} \cdot {y_{bar}}^2$$

$$I_{tr} = 287.663\,in^4$$

$y_t := \frac{d_b}{2} - y_{bar} + t_s$ $y_t = 3.782\,in$

$y_b := \frac{d_b}{2} + y_{bar}$ $y_b = 7.698\,in$

$y_t + y_b = 11.48\,in$ $t_s + d_b = 11.48\,in$ $L_{beam} := 177\,in$

$S_{top} := \frac{I_{tr}}{y_t}$ $S_{top} = 76.051\,in^3$ $S_{bot} := \frac{I_{tr}}{y_b}$ $S_{bot} = 37.371\,in^3$

PNA Calc

Assume Whitney rectangular stress distribution

$a := \frac{A_s \cdot F_y}{0.85 f'_c \cdot b_E}$

$C := .85 f'_c \cdot a \cdot b_E$ $C = 4.592 \times 10^5 \cdot lbf$

$T := A_s \cdot F_y$

$a = 3.478\,in$ Depth of Stress Block

$C_c := .85 f'_c \cdot b_E \cdot t_s$ $C_s := \frac{A_s \cdot F_y - .85 f'_c \cdot b_E \cdot t_s}{2}$

$M_{n1} := A_s \cdot F_y \cdot \left(\frac{d_b}{2} + t_s - \frac{a}{2} \right)$ $M_{n1} = 2.756 \times 10^3 \cdot in \cdot kip$

$d'_2 := d_b + \frac{t_s}{2} - y_{bar}$ $d'_2 = 5.522\,in$

$d''_2 := d'_2 + \frac{t_s}{2} - \left(t_s + \frac{t_f}{2} \right)$ $d''_2 = 3.325\,in$

$M_{n2} := C_c \cdot d'_2 + C_s \cdot d''_2$ $M_{n2} = 2.802 \times 10^3 \cdot in \cdot kip$

$$M_n := \begin{cases} M_{n1} & \text{if } a < t_s \\ M_{n2} & \text{if } a \geq t_s \end{cases} \qquad M_n = 2.756 \times 10^3 \cdot in \cdot kip$$

$$PNA := \begin{cases} \text{"Located in Slab"} & \text{if } a < t_s \\ \text{"Located in WF Section"} & \text{if } a \geq t_s \end{cases} \qquad PNA = \text{"Located in Slab"}$$

APPENDIX D

CBM4 STRESS BLOCK AND PLASTIC NEUTRAL AXIS CALCULATION

Reference Steel Structures Design and Behavior (Salmon and Johnson, 1990) pages 1010-1061 for all equations in Appendix D.

CBM4 PNA Calc

Concrete Weight: $w := 145 pcf$

Compressive Strength: $f'_c := 5000 psi$

Young's Modulus (Steel) $E_s := 29000 ksi$ $F_y := 50 ksi$

$$E_c := 33 \cdot \left(\frac{w}{pcf} \right)^{1.5} \cdot \sqrt{\frac{f'_c}{psi}} \cdot psi \qquad E_c = 4.074 \times 10^6 \cdot psi$$

$$n := \frac{E_s}{E_c} \qquad n = 7.118 \qquad n := 7$$

$b_E := 90 in$ $t_s := 5 in$

$b_f := 5.525 in$

$t_f := .440 in$

$t_w := .275 in$

$d_b := 15.85 in$

$$A_s := b_f \cdot t_f \cdot 2 + \left(d_b - 2 \cdot t_f \right) \cdot t_w \qquad A_s = 8.979 in^2$$

$$I_{bm} := \frac{b_f \cdot {d_b}^3}{12} - 2 \cdot \frac{\left(d_b - 2 \cdot t_f\right)^3 \cdot \left(\frac{b_f - t_w}{2}\right)}{12} \qquad I_{bm} = 365.602 in^4$$

Slab Equivalent Width: $b_{eq} := \frac{b_E}{n}$ $\qquad b_{eq} = 12.857 in$

$A_{tr} := b_{eq} \cdot t_s$ $\qquad A_{tr} = 64.286 in^2$

$$I_{slab} := \frac{b_{eq} \cdot {t_s}^3}{12} \qquad I_{slab} = 133.929 in^4$$

Transformed Areas Moment Arms

Slab: $A_{tr} = 64.286 in^2$ $\qquad d_1 := \frac{d_b + t_s}{2}$ $\qquad d_1 = 10.425 in$

$A_{d1} := d_1 \cdot A_{tr}$ $\qquad A_{d1} = 670.179 in^3$

${A_{d12} := A_{tr} \cdot {d_1}^2}$ $\qquad A_{d12} = 6.987 \times 10^3 \cdot in^4$

Total Areas: $A_{total} := A_{tr} + A_s$ $\qquad A_{total} = 73.264 in^2$

Total Moments of Inertia $I_{total} := I_{slab} + I_{bm}$ $\qquad I_{total} = 499.53 in^4$

$I_x := I_{total} + A_{d12}$ $\qquad I_x = 7.486 \times 10^3 \cdot in^4$

$y_{bar} := \frac{A_{d1}}{A_{total}}$ $\qquad y_{bar} = 9.147 in$

$I_{tr} := I_x - A_{total} \cdot {y_{bar}}^2$

$I_{tr} = 1.356 \times 10^3 \cdot in^4$

$y_t := \frac{d_b}{2} - y_{bar} + t_s$ $y_t = 3.778\,in$

$y_b := \frac{d_b}{2} + y_{bar}$ $y_b = 17.072\,in$

$y_t + y_b = 20.85\,in$ $t_s + d_b = 20.85\,in$ $L_{beam} := 177in$

$S_{top} := \frac{I_{tr}}{y_t}$ $S_{top} = 358.893in^3$ $S_{bot} := \frac{I_{tr}}{y_b}$ $S_{bot} = 79.412in^3$

PNA Calc

Assume Whitney rectangular stress distribution

$a := t_s$ $a = 5 \cdot in$

$C := .85 f'_c \cdot a \cdot b_E$ $C = 1.913 \times 10^6 \cdot lbf$

$T := A_s \cdot F_y$

$a := \frac{A_s \cdot F_y}{0.85 f'_c \cdot b_E}$ $a = 1.174\,in$ Depth of Stress Block

$C_c := .85 f'_c \cdot b_E \cdot t_s$ $C_s := \frac{A_s \cdot F_y - .85 f'_c \cdot b_E \cdot t_s}{2}$

$M_{n1} := A_s \cdot F_y \cdot \left(\frac{d_b}{2} + t_s - \frac{a}{2} \right)$ $M_{n1} = 5.539 \times 10^3 \cdot in \cdot kip$

$d'_2 := d_b + \frac{t_s}{2} - y_{bar}$ $d'_2 = 9.203\,in$

$d''_2 := d'_2 + \frac{t_s}{2} - \left(t_s + \frac{t_f}{2} \right)$ $d''_2 = 6.483\,in$

$M_{n2} := C_c \cdot d'_2 + C_s \cdot d''_2$ $\quad M_{n2} = 1.286 \times 10^4 \cdot in \cdot kip$

$$M_n := \begin{cases} M_{n1} & \text{if } a < t_s \\ M_{n2} & \text{if } a \geq t_s \end{cases} \qquad M_n = 5.539 \times 10^3 \cdot in \cdot kip$$

$$PNA := \begin{cases} \text{"Located in Slab"} & \text{if } a < t_s \\ \text{"Located in WF Section"} & \text{if } a \geq t_s \end{cases} \qquad PNA = \text{"Located in Slab"}$$

APPENDIX E

BENDING STRESS CALCULATIONS

CBM1 Stress Calculations, Negative Moments

$I_{tr} := 328.681 in^4$ (all equations by author)

$S_{conc} := 101.99 in^3$ $S_{tr} := 39.804 in^3$

$M_1 := 687927 in \cdot lbf$ $M_3 := 690173 in \cdot lbf$ $M_4 := 689222 in \cdot lbf$

$f_{b1conc} := \frac{M_1}{S_{conc}}$ $f_{b1conc} = 6.745\, ksi$ (Concrete Bending Stress)

$f_{b1tr} := \frac{M_1}{S_{tr}}$ $f_{b1tr} = 17.283\, ksi$ (WF Beam Bending Stress)

$f_{b3conc} := \frac{M_3}{S_{conc}}$ $f_{b3conc} = 6.767\, ksi$ (Concrete Bending Stress)

$f_{b3tr} := \frac{M_3}{S_{tr}}$ $f_{b3tr} = 17.339\, ksi$ (WF Beam Bending Stress)

$f_{b4conc} := \frac{M_4}{S_{conc}}$ $f_{b4conc} = 6.758\, ksi$ (Concrete Bending Stress)

$f_{b4tr} := \frac{M_4}{S_{tr}}$ $f_{b4tr} = 17.315\, ksi$ (WF Beam Bending Stress)

CBM2 Stress Calculations, Negative Moments (all equations by author)

$I_{tr} := 328.681in^4$

$S_{conc} := 101.99in^3$ $S_{tr} := 39.804in^3$

$M_1 := 42061in \cdot lbf$ $M_3 := 46003in \cdot lbf$ $M_4 := 43251in \cdot lbf$

$f_{b1conc} := \frac{M_1}{S_{conc}}$ $f_{b1conc} = 0.412ksi$ (Concrete Bending Stress)

$f_{b1tr} := \frac{M_1}{S_{tr}}$ $f_{b1tr} = 1.057ksi$ (WF Beam Bending Stress)

$f_{b3conc} := \frac{M_3}{S_{conc}}$ $f_{b3conc} = 0.451ksi$ (Concrete Bending Stress)

$f_{b3tr} := \frac{M_3}{S_{tr}}$ $f_{b3tr} = 1.156ksi$ (WF Beam Bending Stress)

$f_{b4conc} := \frac{M_4}{S_{conc}}$ $f_{b4conc} = 0.424ksi$ (Concrete Bending Stress)

$f_{b4tr} := \frac{M_4}{S_{tr}}$ $f_{b4tr} = 1.087ksi$ (WF Beam Bending Stress)

CBM3 Stress Calculations, Negative Moments (all equations by author)

$I_{tr} := 287.663in^4$

$S_{conc} := 76.051in^3$ $S_{tr} := 37.371in^3$

$M_1 := 310193in \cdot lbf$ $M_3 := 310203in \cdot lbf$ $M_4 := 316250in \cdot lbf$

$f_{b1conc} := \frac{M_1}{S_{conc}}$ $f_{b1conc} = 4.079ksi$ (Concrete Bending Stress)

$$f_{b1tr} := \frac{M_1}{S_{tr}} \qquad f_{b1tr} = 8.3\,ksi$$ (WF Beam Bending Stress)

$$f_{b3conc} := \frac{M_3}{S_{conc}} \qquad f_{b3conc} = 4.079\,ksi$$ (Concrete Bending Stress)

$$f_{b3tr} := \frac{M_3}{S_{tr}} \qquad f_{b3tr} = 8.301\,ksi$$ (WF Beam Bending Stress)

$$f_{b4conc} := \frac{M_4}{S_{conc}} \qquad f_{b4conc} = 4.158\,ksi$$ (Concrete Bending Stress)

$$f_{b4tr} := \frac{M_4}{S_{tr}} \qquad f_{b4tr} = 8.462\,ksi$$ (WF Beam Bending Stress)

CBM4 Stress Calculations, Negative Moments (all equations by author)

$$I_{tr} := 1356in^4$$

$$S_{conc} := 358.893in^3 \qquad S_{tr} := 79.412in^3$$

$$M_1 := 327022in{\cdot}lbf \qquad M_3 := 329112in{\cdot}lbf \qquad M_4 := 327941in{\cdot}lbf$$

$$f_{b1conc} := \frac{M_1}{S_{conc}} \qquad f_{b1conc} = 0.911\,ksi$$ (Concrete Bending Stress)

$$f_{b1tr} := \frac{M_1}{S_{tr}} \qquad f_{b1tr} = 4.118\,ksi$$ (WF Beam Bending Stress)

$$f_{b3conc} := \frac{M_3}{S_{conc}} \qquad f_{b3conc} = 0.917\,ksi$$ (Concrete Bending Stress)

$$f_{b3tr} := \frac{M_3}{S_{tr}} \qquad f_{b3tr} = 4.144\,ksi$$ (WF Beam Bending Stress)

$$f_{b4conc} := \frac{M_4}{S_{conc}} \qquad f_{b4conc} = 0.914\,ksi$$ (Concrete Bending Stress)

$$f_{b4tr} := \frac{M_4}{S_{tr}} \qquad f_{b4tr} = 4.13\,ksi$$ (WF Beam Bending Stress)